# Immunopathological analysis of immune diseases as Th1/Th2 unbalanced diseases

## Th1/Th2 病としての免疫疾患の免疫病理学的解析

The United Graduate School of Veterinary Science

Yamaguchi University

Tomomi Nakashima

中嶋 朋美

March 2014

# Contents

# 1. General introduction

## 1.1 Background of the PhD thesis

The complexities of various abnormalities in humoral and cellular immune response under the influence with predisposing genetic, sex hormonal and environmental factors have been reported in immune diseases in humans and animal models [Koffler 1974; Klinman & Steinberg 1995; Hayashi 2010; Holloway *et al.* 2010] (Fig. 1). Immune diseases are divided into autoimmune diseases and allergic diseases. Autoimmune diseases are essentially helper T (Th) 1 diseases, whereas allergic diseases are essentially Th2 diseases (Fig. 2). The hygiene hypothesis postulates the increasing prevalence of asthma and atopy due to decreased pathogen exposure [Strachan 1989]. It has been reported that the level of environmental exposure to endotoxin and other bacterial wall components is an important protective determinant for the development of allergic asthma and atopic diseases in childhood [von Mutius *et al.* 2000; Liu 2002]. The notion initially put forth that infections exclusively protect against allergic diseases through stimulation of Th1 cells.

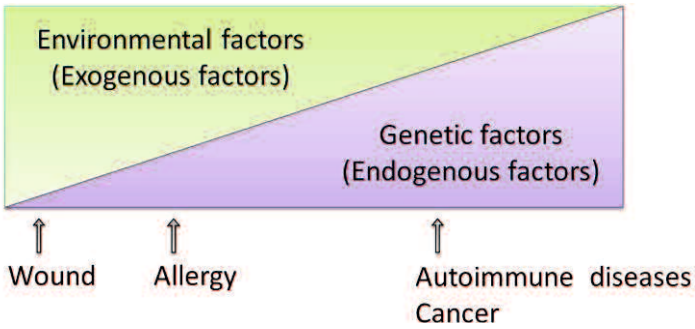


**Fig. 1**: Factors affecting on diseases.

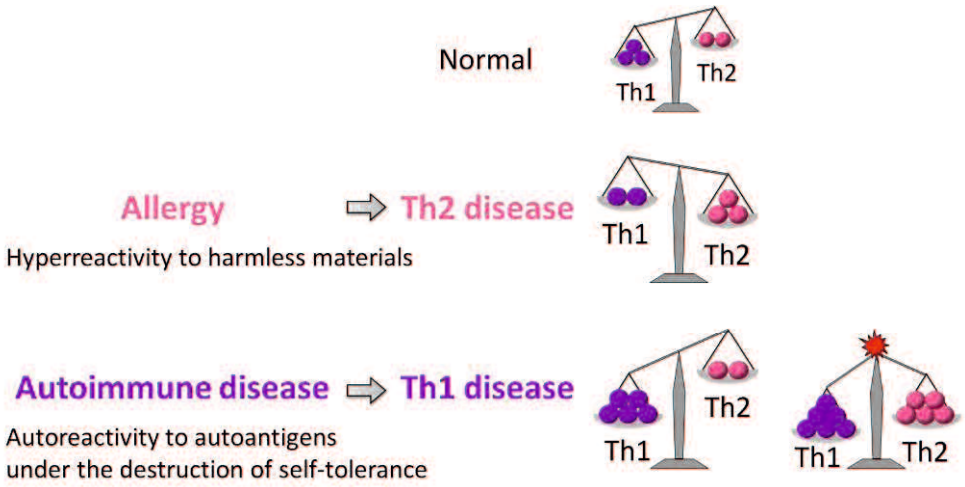


Fig. 2: Th1/Th2 balance shift in immune diseases.

## 1.2 Autoimmune diseases

Autoimmune diseases are a disorder of immunoregulation under the breakdown of self-tolerance, characterized by the aberrant autoreactivity against the body own proteins (self-antigens). This is divided into two major types: organ specific diseases (e.g. Type 1 diabetes: T1D) and systemic diseases (e.g. systemic lupus erythematosus: SLE or lupus). Several cytokines and chemokines are involved in the autoimmune pathogenesis, especially Th1 cytokine interferon (IFN)-γ, including IFN-γ inducible interleukin (IL) -12 and IL-18, play important roles in autoimmune diseases such as SLE [Hayashi 2010], T1D [Hayashi *et al.* 1998, 2001], multiple sclerosis [Karni *et al.* 2002] and Crohn's disease [Pizarro *et al.* 1999]. In general, the treatment of autoimmune diseases is typically with immunosuppressants (e.g., prednisolone, cyclophosphamide and tacrolimus) which decrease the immune response.

## 1.3 Allergic diseases

There are several allergic diseases such as allergic asthma, which develop under the hyperreactivity to non-harmful materials. For example, allergic asthma of the

human nasal mucosa can be divided into two phases: an immediate- and a late-phase reaction, and some of the patients develop a late-phase reaction after a symptom-free interval [Bachert 1990]. The inflammatory response in the nasal mucosa in subjects with allergic rhinitis challenged intranasally with an allergen includes an immediate IgE-mediated increased mast cell response as well as a late-phase response characterized by recruitment of eosinophils, basophils, and Th2 cells producing cytokines including IL-4, a switch factor for IgE synthesis, and IL-5, an eosinophil growth factor [Mosmann & Coffman 1989; Hatzivlassiou *et al.* 2010]. Th2 cells play a fundamental role in both immediate and late reactions, whereas late reaction may be independent of IgE/mast cells [Hatzivlassiou *et al.* 2010]. These cells release pro-inflammatory mediators, including cysteinyl leukotrienes, eosinophil cationic proteins (ECP), eosinophil peroxidase (EPO), and a major basic protein (MBP) which participate in inflammation through the airway or systemic pathways [Knol & Olszewski 2011]. Preclinical studies show an important role for epithelial-derived cytokines (thymic stromal lymphopoietin: TSLP, IL-18, IL-25, and IL-33) in regulating Th2 responses at mucosal surfaces, and for $H_4$-histamine receptors in mediating itching [Liu 2001; Broide 2010; Smith 2010].

## 1.4 Hygiene hypothesis

According to the hygiene hypothesis initially formulated for allergic diseases, exposure to some pathogens (e.g. bacteria, endotoxins, viruses) in infantile period protects the development of allergic rhinitis through stimulation of Th1 cells [Strachan 1989, 2000]. This is evidenced by the reports that the environmental factors such as lactate dehydrogenase-elevating virus infection and bacterial CpG-DNA, reduce the

development of allergic rhinitis in experimental animal models [Sasaki *et al.* 2007; Hayashi *et al.* 2008].

The hygiene hypothesis has also been implicated in the increasing incidence of autoimmune diseases and infectious agents can also suppress not only allergic diseases but also autoimmune disorders [Bach 2002]. Aberrant function of the gut immune system may be involved in the development of autoimmune disease [Vaarala 1999; Westerholm-Ormio *et al.* 2003]. Wen L *et al.* [2008] have indicated that interaction of the intestinal microbes with the innate immune system is a critical epigenetic factor modifying T1D predisposition. It is conceivable that a decreased microbial load in early life may have a major impact on the programming of the immune system especially gut-associated lymphoid tissue (GALT) [Vaarala 1999]. Experiments in Biobreeding (BB) rats and non-obese diabetic (NOD) mice, both are models of T1D, have clearly demonstrated that progression of the disease was ameliorated by targeting the gut immune system with bacterial immunostimulants such as oral administration of lipopolysaccharide (LPS) or the *Escherichia coli* extract OM-89, leading to a shift toward Th2 from Th1 responses, which is associated with "destructive" insulitis [Bellmann *et al.* 1997]. The colonizing microbiota not only provides colonization resistance to potentially pathogenic bacteria, but also has a major role in the development of the intestinal immune system, both in terms of GALT development and mucosal immunity, and the induction of oral tolerance [Bauer *et al.* 2006].

Alternatively, a number of investigators have suggested that allergic diseases could protect against autoimmune diseases such as T1D and that there are lower rates of atopic diseases among T1D patients [Meerwaldt *et al.* 2002; Rosenbauer *et al.* 2003; Tirosh *et al.* 2006], and these incidents may be due to the mutual Th1/Th2 inhibitory

effects [Mosmann & Coffman 1989; Meerwaldt *et al.* 2002]. The reduced risk of T1D in children living with siblings, sharing a bedroom and moving house more often could reflect the protection afforded by exposure to infections in early life and consequently may provide support for the hygiene hypothesis [Cardwell *et al.* 2008]. On the other hand, the meta-analysis revealed that there was a small but significant reduction in the prevalence of asthma in children with T1D, but the findings for the other atopic diseases were less conclusive [Cardwell *et al.* 2003]. It has also been reported that T1D may not seem to downregulate the development of allergic sensitization to aeroallergens, but may decrease the frequency and/or the severity of its clinical manifestations at respiratory level [Tosca *et al.* 2009]. In addition, Stene & Nafstad [2001] reported a strong positive association between the occurrence of T1D and symptoms of asthma at the population level in Europe and elsewhere by using published data on disease occurrence in different countries. There is a tendency toward increased incidence of concomitant occurrence of allergic and autoimmune diseases in single individuals, and Th1 and Th2 diseases can coexist, indicating a common environmental denominator behind the disease processes [Kero *et al.* 2001]. Moreover, Cookson [2002] identified genetic basis share linkages between asthma and some autoimmune diseases (e.g., ankylosing spondylitis, T1D, inflammatory bowel disease and rheumatoid arthritis).

## 1.5 Th1/Th2 balance shift

Needless to say, autoimmune and allergic diseases are associated with the Th1/Th2 unbalanced immune systems. Depending on the notion of mutual inhibitory mechanisms, it has been reported that autoimmune diseases (lupus and virus-induced insulitis model) and allergic disease (allergic rhinitis model) were exacerbated and

ameliorated by Th2 cytokine and Th1 cytokine, respectively [Hasegawa & Hayashi 2003; Hayashi *et al.* 2003b, 2007, 2008a]. Normalization of homeostasis in individuals by Th1/Th2 balance shift is another way to prevent the diseases. This idea has advantageous, because it is suggested that this therapy may preserve host immune system normally, leading to not only the therapeutic effects but also the resistance of infections and tumors (Fig. 3).

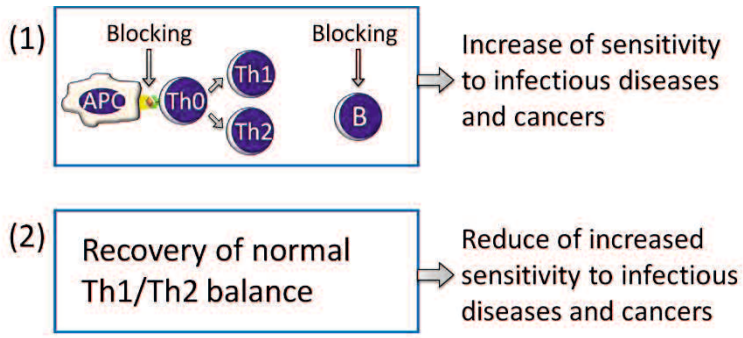


**Fig. 3**: Two major stream of prevention and therapy.
(1) Targeting immune cells and molecules
(2) Recovery of homeostasis

Depending on the concept of Th1/Th2 balance shift, there are three strategies for prevention and therapy of immune diseases as follows: [I] alteration of the balance between Th1 (IFN-γ) and Th2 cell (IL-4) activity [Mosmann & Coffman 1989; Theofilopoulos *et al.* 2001] (Fig. 2), [II] shift pro-inflammatory versus immunosuppressive cytokine profiles (IL-1, IL-6, IL-10, TNF-α) and [III] shift from immunogenic (IFN-α/β) to tolerogenic (tumor necrosis factor: TNF-α) dendritic cells (DCs) (Fig. 4). Compared to the treatment of [II] and [III], [I] has advantage as follows. [II] may have effectiveness without host normal responses to foreign matters, but it is very difficult to monitor, since they located the downstream of Th1/Th2 reaction. [III] may have the risk of inducing abnormal immune responses to endogenous and

exogenous agents. Although [I] has the clinical implications including usefulness and unfavorable side effects this treatment may cover those weak points of [II] and [III].

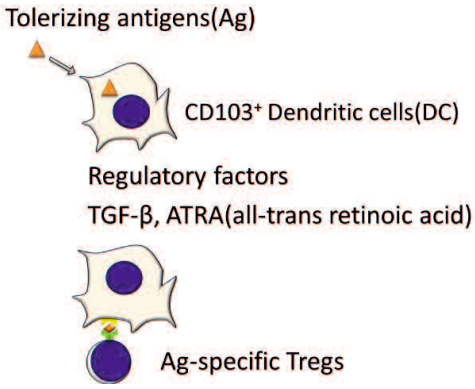


**Fig. 4**: Dendritic cell.

Bacterial immunostimulants may induce $CD4^+CD25^+Foxp3^+$ regulatory T (Treg) cells, which maintain peripheral tolerance [Sakaguchi 2000; Shevach 2002; Sakaguchi *et al.* 2006; Toda & Piccirillo 2006]. If this event does not work in early life, both allergic and autoimmune diseases might develop. The majority of these cells constitutively express the IL-2R-chain (CD25) and represent 1–10% of thymic or peripheral $CD4^+$ T cells in mice and man [Sakaguchi *et al.* 1995]. $CD4^+$ naturally occurring Treg (nTreg) cells, most of which are produced by the normal thymus, have emerged as the predominant regulatory population mediating peripheral self-tolerance [Sakaguchi *et al.* 2006; Toda & Piccirillo 2006]. Targeted deletions or natural mutations of the *foxp3* gene leads to a deficiency of nTreg cells and provokes the development of severe autoimmunity in scurfy mice and immune dysregulation, polyendocrinopathy, enteropathy, and X-linked inheritance (IPEX) syndrome [Gambineri *et al.* 2003; Fontenot *et al.* 2005]. It has been reported that multiple immunoregulatory Treg cell defects underlie islet cell autoimmunity leading to T1D in humans [Kukreja *et al.* 2002]. Patients with T1D were markedly defective in $CD4^+$ $CD25^+$ or $CD4^+$ $CD25^{(+Bright)}$ T-cell ability to suppress the

proliferation of autologous effector T-cells in vitro [Brusko *et al.* 2005], and foxp3-deficient NOD mice display a significantly increased incidence and earlier onset of T1D compared with normal NOD mice, strongly implying a role for $Foxp3^+$ nTreg cells in the control of type 1 diabetes pathogenesis [Chen *et al.* 2005]. Disruption of the B7/CD28 pathway in NOD mice has been shown to decrease $CD4^+CD25^+$ nTreg cell frequency, leading to an accelerated T1D onset [Salomon *et al.* 2000; Tang *et al.* 2003]. Ott *et al.* [2005] have demonstrated that islet cell antigens (ICA)-reactive T cells occur in both diabetes resistant non-obese resistant (NOR) and diabetes susceptible NOD mice, suggesting uninhibited thymic and post-thymic maturation of islet reactive T cells in both mouse strains. However, in the NOR mouse, $CD4^+CD25^+$ regulatory cells are capable of abrogating effector functions of primed ICA-specific T cells in the target organ. Thus they concluded that $CD4^+CD25^+$ Treg cells control the progression from periinsulitis to destructive insulitis in murine autoimmune diabetes. Tritt *et al.* [2008] have demonstrated that foxp3-expressing nTreg cells in NOD mice regulate diabetogenesis, but temporal alterations in nTreg cell function promote immune dysregulation and the onset of spontaneous autoimmunity. Furthermore, it has been reported previously that elimination of Tregs exacerbated the development of autoimmune diseases such as sialoadenitis and lupus nephritis in lupus prone NZBxNZWF1 mice including Reo-2-triggered TID in DBA/1J mice [Hayashi *et al.* 2005a, 2006, 2009]. Also, oral tolerance may be induced by Th3 $CD4^+$ regulatory cells, which primarily secrete transforming growth factor (TGF)-β, provide a help for IgA and have suppressive properties for both Th1 and Th2 cells [Weiner 2001]. So-called thymic-derived nTregs and/or IL-10-producing T regulatory (Tr)-1 cells are capable of suppressing Th2 responses to allergens [Akdis *et al.* 2004; Wu *et al.* 2007]. In this context, both cell-cell

contact-dependent (either through membrane bound TGF-β or via suppressive molecules such as CLTA-4 and soluble cytokine-(TGF-β and IL-10)-dependent mechanisms have been shown to contribute to the function of Tregs [Suri-Payer *et al.* 1998; Takahashi *et al.* 2000; Akdis *et al.* 2004; Nakamura *et al.* 2004]. A clinical improvement seen after allergen immunotherapy for allergic diseases such as rhinitis and asthma is associated with the induction of IL-10 and TGF-β producing Tr-1 cells as well as foxp3 expressing IL-10 T cells, resulting in suppression of the Th2 cytokine milieu [Akdis *et al.* 1998, 2004; Jutel *et al.* 2003; Wu *et al.* 2007; Nouri-Aria & Durham 2008]. In addition, it has been reported that peripheral $CD4^+CD25^-$ naïve T cells to $CD4^+CD25^+$ Treg cells can be converted by TGF-β induction of transcription on factor Foxp3 [Chen *et al.* 2003] and that activation and expansion of antigen-specific $CD4^+CD25^+$ Tregs in vivo using adjuvants or pharmacological agents such as low dose steroids or vitamin D3 could represent novel approaches to induce antigen-specific tolerance in human diseases including allergic asthma, autoimmune disease and the rejection of transplanted organs [Nouri-Aria & Durham 2008]. Moreover, several studies have implicated nTreg cells in prevention of allergic and autoimmune diseases [Elkord 2008; Toubi 2008]. Although $CD4^+CD25^+$ Tregs-mediated regulation has a possibility to suppress the diabetogenic process and control the onset of T1D, it is unclear whether these $CD4^+CD25^+$ Treg cells are thymus-derived nTreg or inflammation-induced Treg cells [Piccirillo *et al.* 2005]. Alternatively, Kim *et al.* [2006] have reported natural killer T (NKT) cells play a critical role in oral tolerance induction. At least, functional deficiency of Treg cells including NKT cells may be underlying in permission of the development of both Th1 and Th2 diseases. Although some questions remain (e.g., How and where do nTreg cells mediate immune tolerance and disease protection ? Also, does the spontaneous onset

of immune diseases reflect developmental or functional deficiencies in nTreg cells?), $CD4^+CD25^+$ therapy for allergy and autoimmune disease may support the idea as mentioned by Jiang & Lechler [2006].

It should be taken into consideration that all patients with autoimmune disease including T1D may not permit the development of allergic disease. For example, it has been reported that in children with T1D, the presence of allergic symptoms was not associated with the development of T1D in human [Karavanaki *et al.* 2008]. Thus, at present, there still remain numerous questions concerning the hygiene hypothesis in allergic and autoimmune diseases regarding the nature of protective infectious agents, the timing of their involvement and, most importantly, the mechanisms of protection [Bach 2002].

## 1.6 IL-17/IL-23 axis

IL-23 is a heterodimeric cytokine composed of a unique p19 subunit and a common p40 subunit shared with IL-12, which is produced by activated DCs [Oppmann *et al.* 2000]. Compared to IL-12, IL-23 does not promote the development of IFN-γ-producing Th1 cells, but play a crucial role for the proliferation and maintenance of IL-17 producing $CD4^+$ T cell subset (Th17) [Aggarwal *et al.* 2003]. In addition, IL-6 and TGF-β are responsible for differentiating naïve T cells into Th17 cells [Korn *et al.* 2009] (Fig. 5). IL-17 is a pro-inflammatory cytokine that stimulates epithelial, endothelial, and fibroblastic cells to produce other inflammatory cytokines and chemokines including IL-1β, IL-6, IL-8, TNF-α, granulocyte-colony stimulating factor (G-CSF), and monocyte chemoattractant protein (MCP)-1, especially acts as chemoattractant for neutrophils [Aggarwal *et al.* 2003]. The importance of IL-17/IL-23

axis in autoimmune [Stockinger & Veldhoen 2007; Wong *et al.* 2008; Kunz & Ibrahim 2009] and allergic [Cosmi *et al.* 2011] diseases in human and animal models is pointed out and the possibility of IL-17 targeted therapy is recently proposed [Wong *et al.* 2008].

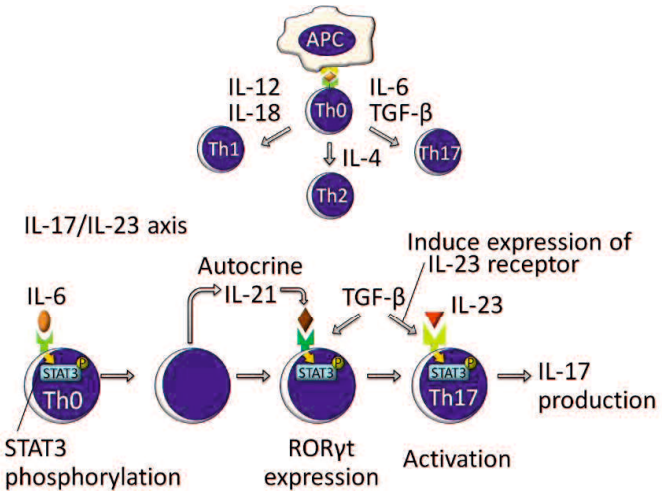


**Fig. 5**: Differentiation of helper T cells.

## 1.7 Therapies for immune diseases

Immune regulation forming cytokine/chemokine networks including intracellular signaling of cytokines is highly complex and the mechanisms of regulation is not as yet fully understood in pathogenesis of immune diseases [Hayashi 2010, 2012a]. It suggests that therapy focusing on one cytokine (or combination of several cytokines) or one immunocompetent cell including the concept of IL-23/IL-17 axis seems to be difficult (Fig. 6). Concerning IL-23/IL-17 complexity, one reason is those axis may exist downstream after Th1 and Th2 differentiation. Same reasons in Tregs like IL-23/IL-17 may be due to their complexity including unsolved mechanisms. From these reasons, the importance of concept of Th1/Th2 balance shift in immune diseases is pointed out again recently [Meloni *et al.* 2009; Hayashi 2010].

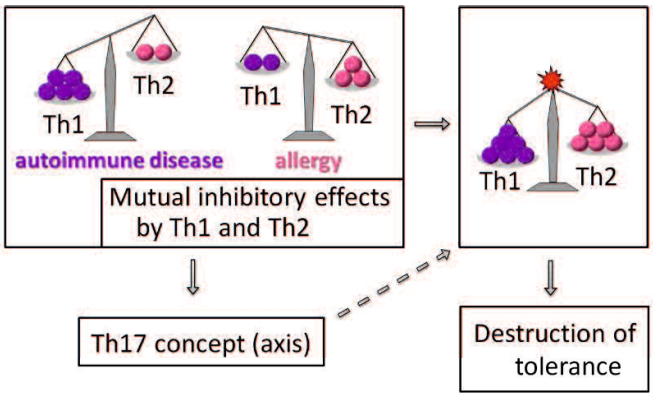


Fig. 6: The development of acquired immunity in immune diseases.

In general, patients with overt disease will be treated with immunosuppressants (e.g., prednisolone, cyclophosphamide, and tacrolimus) or NSAIDs (nonsteroidal anti-inflammatory drugs). Those immunosuppressive drugs are strongly effective in prevention of the development of allergic and autoimmune diseases due to reducing the host immune responses (Fig. 7). Cytokines are protein messengers responsible for cellular communication with great therapeutic potential to control inflammatory and immune disorders such as allergic asthma, rheumatoid arthritis and SLE [Berry *et al.* 2006; Díaz-Jouanen *et al.* 2009; Hayashi 2010]. Amoura *et al.* [2008] have recently reviewed new biotherapies that new approaches in human SLE are based on a better understanding of the autoimmune response as follows: (1) "B lymphocyte (BL)" inhibitors such as anti-CD20 monoclonal antibody (mAb), anti-CD22 mAb, B lymphocyte stimulator (BlyS) antagonists, tolerogenic peptide such as human complementary-determining region 1 (hCDR1: Edratide) which is based on the sequence of the CDR1 of a human anti-DNA mAb that bears the major idiotype designated 16/6Id [Sthoeger *et al.* 2009], and LJP 394 (abetimus sodium) which selectively reduces antibodies to dsDNA and their parent B cells via antigen-specific tolerance [Klinman & Steinberg 1995; Alarcón-Segovia *et al.* 2003]; (2) "Inhibitors of the co-stimulation" between antigen presenting cells and T lymphocyte like monoclonal anti-CD40 ligand

antibody or cytotoxic T-lymphocyte-associated antigen (CTLA)-4-Ig (abatacept); (3) "Cytokine antagonists" inhibiting key cytokines of SLE: IL-10 [Llorente *et al.* 2000], IFN-α [Mathian *et al.* 2005], IL-6 [Finck *et al.* 1994] and TNF-α [Prud'homme *et al.* 2001]. Although effectiveness is reported by the treatment of anti-IL-10 mAb [Llorente *et al.* 2000], LJP 394 [Alarcón-Segovia *et al.* 2003], Edratide [Sthoeger *et al.* 2009], inhibition of T cell co-stimulation with anti-CD154 [Kalunian *et al.* 2002] and anti-IFN α/β [Yao Y. *et al.* 2009] in human lupus, many cytokine-related therapies have failed to establish clinical utility. If this method can not get an advantage in effectiveness over cortisone, it is not suitable for therapy, even though it is less toxic. Less toxic approaches to avoid severe adverse events (infections, infertility, amenorrhea, and metabolic abnormalities) are required [Doria & Briani 2008; van Raalte *et al.* 2009]. Thus, there are a lot of trials focusing on improved therapy compared to classic immunosuppressive drugs in experimental basis [Monneaux & Muller 2009]. The purpose of the PhD thesis is to clarify the immune diseases from the point of views for better understandings for future prevention and therapy for immune diseases.

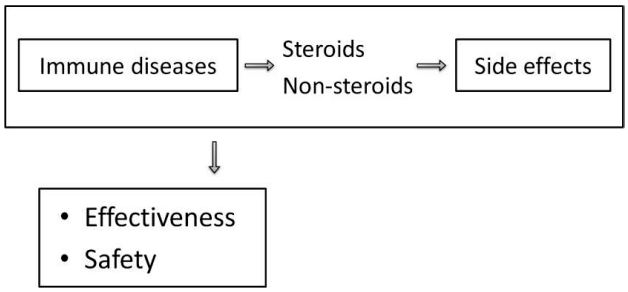


**Fig. 7**: Treatment of immune diseases.

This PhD thesis analyzes immune diseases such as allergy and autoimmune diseases depending on the notion of Th1/Th2 balance shift including the role of endogenous and exogenous environmental factors. The thesis consists of 3 chapters as follows.

# 2. Chapter 1.

## Regulate the development of asthmatic inflammation by *in situ* $CD4^{+}Foxp3^{+}$ T cells in a mouse model of late allergic asthma

## Introduction

Allergic asthma is a chronic inflammatory airway disease characterized by variable airflow obstruction, bronchial eosinophil infiltration, airway hyper-responsiveness and mucus overproduction [Aikawa *et al.* 1992]. It has been widely accepted the idea that allergic asthma is associated with an imbalance from Th1 cells to Th2 cells, and Th2 cells orchestrate the recruitment and activation of mast cells and IgE in immediate type, and eosinophils and Th2 cells in late type of airway allergic reactions by releasing cytokines such as IL-4, IL-5 and IL-13 from Th2 cells in both type [Kaur & Brightling 2012]. In addition, late type of allergic asthma was eosinophils/Th2 cells dependent [Minai-Fleminger & Levi-Schaffer 2009] and IgE/mast cells independent [Hatzivlassiou *et al.* 2010].

Peripheral $CD4^+$ $CD25^+Foxp3^+$ regulatory T-cells (Tregs) have been shown to be critical in the maintenance of peripheral immune responses [Sakaguchi *et al.* 1995, 1996, 2009; Caramalho *et al.* 2003; Tarbell *et al.* 2004]. Tregs producing immunosuppressive cytokines such as TGF-β, IL-10 and IL-35 have been shown to be responsible for the protection of immune reactions following exposure to allergens such as aero-allergens or food allergens [Weiner 2001; Kearley *et al.* 2005; Robinson 2009]. In this regard, cell-cell contact through membrane bound TGF-β1 via suppressive molecules such as CTLA-4 or released soluble immunosuppressive cytokines from Tregs have been shown to contribute to the maintenance of self-tolerance in peripheral tissues [Sakaguchi *et al.* 1996; Cronin & Penninger 2007]. Besides immunosuppressive cytokine production by Tregs, those cells are known to exert suppressive function in a number of ways, including release of perforin [Grossman *et al.* 2004] and granzyme B [Shevach 2009], and possibly through the release of cAMP [Bopp *et al.* 2007]. Moreover, Tregs are

capable of suppressing Th2 responses to allergens in health and attenuate allergic conditions [Strickland & Holt 2011]. Transfer of antigen-specific Tregs inhibited the development of asthma in mice [Kearley *et al.* 2005], and the treatment with glucocorticosteroids in asthmatics might increase this Foxp3 protein expression within Tregs in human [Provoost *et al.* 2009] and fluorescence activated cell sorter (FACS) analysis revealed decreased Tregs obtained from lung tissues in a model of asthma [Melgert *et al.* 2005].

Asthmatic patients had lower Tregs ratio and Foxp3 mRNA expression with the decrease of Tregs ratio, and those functions in peripheral blood mononuclear cells may be associated with pathogenesis of asthma in human [Xue *et al.* 2007]. Also, asthmatic patients have decreased circulating Foxp3 protein expression in Tregs in patients with stable asthma [Provoost *et al.* 2009]. The decreased number of peripheral blood Tregs in atopic patients to intrabronchial allergen provocation has been reported [Moniuszko *et al.* 2008]. These suggest regulatory effects of Tregs in the development of asthmatic inflammation, but local (*in situ*) cell-cell interaction of Tregs such as at inflamed bronchi and regional lymph nodes (LNs) in human patients with asthma and animal models remains largely unclear.

The aim of the present study is to analyze the relationship between locally accumulated Tregs and the development of asthmatic inflammation in a mouse model of late allergic asthma.

## Materials and methods

### Animals

Specific pathogen-free, 8 week-old female BALB/c mice (Japan Charles River Co., Kanagawa, Japan) were used (total number of mice: *n*=15). The number of mice used in each experiment was shown in parenthesis below. They were kept at 24 ± 2 °C room temperature, 45 ± 10 % humidity, and at 12 h light dark cycle (lightening time 08:00-20:00) in metal cages covered with woodchips sterilized by dry heating (180 °C, 30 min). Animals were fed with commercial pellets (CE-2; CLEA Japan, Tokyo, Japan) and supplied water ad libitum sterilized by heating at 121 °C for 20 min. The number of mice used in each experimental group is given in parenthesis of experimental protocol. The animal experiments were approved by the Research Ethics Board of the Faculty of the Agriculture, Yamaguchi University.

### Experimental protocols and sampling

A model of late allergic asthma was induced by a simple modification of our previous reports [Hayashi *et al.* 2002a, 2003a; Bui *et al.* 2011; Nakashima *et al.* 2012]. As shown in Fig. 1, mice were divided into two groups as follows: sensitization and challenge with ovalbumin (OVA) (asthma group; *n*=9), and neither sensitization nor challenge with OVA (control group; *n*=6). Mice were sensitized by intraperitoneal injection (i.p.) of 10 μg of OVA (Grade V; Sigma-Aldrich Co., St. Louis, MO, USA) in 1.2 mg aluminum hydroxide gel (Alum; SERVA, Heidelberg, Germany) adjuvant (OVA/Alum), which was suspended in 100 μl of phosphate-buffered saline (PBS; pH 7.4), on day 0 and boosted on day 10. On days 14, 15, 16 and 17, the mice were challenged intranasally (i.n.) with 200 μg of OVA in 50 μl of PBS (both right and left nasal cavities by a micropipette alternately) under anesthesia by injection with 0.5 ml mixture of ketamin

and xylazine i.p. The control group was treated as the same manner of the asthma group with PBS instead of OVA. 24 h after the last challenge (on day 18), blood, lungs, spleens, pulmonary LNs (pLNs) and thymi were obtained. For flow cytometry, peripheral blood leukocytes were obtained just before the time of sensitization (on day 0) and the challenge (on day 14) or the sampling (on day 18), respectively.

The number of $Foxp3^+$ cells in pLNs and thymi (*n*=3 in each group) in immunohistochemically stained section was counted using an eyepiece micrometer (high view: ×400, 0.25×0.25 $mm^2$) morphologically 2-10 different fields of view at random in each section. Then the number of Tregs / $mm^2$ was expressed in each mouse. Each result was averaged and totaled in each mouse, and thereafter the mean ± standard error of the mean (SEM) was calculated.

Also, the number of Tregs in bronchial-bronchiolar mucosa (the asthma group: *n*=7; the control group: *n*=3) was counted using an eyepiece micrometer (high view: ×400, 0.1×0.25 to 0.25×0.25 $mm^2$) morphologically 3-6 different fields of view at random in each section. Number of Tregs per each bronchus-bronchioles was expressed (/$\mu m^2$), and then examined the relationship between the severity of asthmatic lesions (score index: S.I.; we will describe later) and accumulation of Tregs per one mouse.

### Leukocyte number in blood

Peripheral venous blood samples were obtained from orbital sinus under ether anesthesia on days 0 (just before the sensitization), 14 (just before the challenge), and 18 (asthma group: *n*=6; control group: *n*=3), and the absolute number of leukocytes (/μl) was counted. Percentage (%) of eosinophils, neutrophils, lymphocytes and monocytes was calculated after blood smear stained with May-Grünwald-Giemsa. Then, the total

number of each leukocyte was determined, and thereafter the mean ± SEM of each group was calculated.

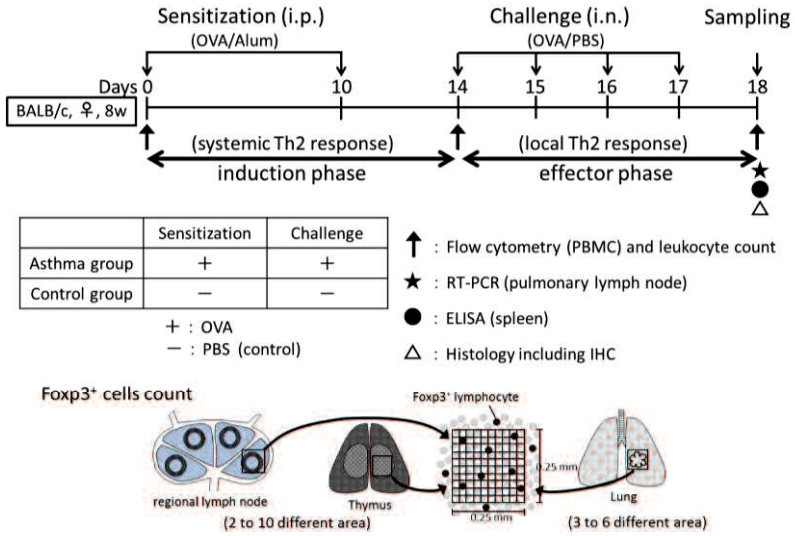


**Fig. 1**: Experimental protocol in a model of late allergic asthma.

## Histological evaluation of lung lesions

Lung samples (asthma group: *n*=6; control group: *n*=3) were fixed in 10% of neutral-buffered formalin solution (pH 7.0), and embedded in paraffin wax. Four µm sections were stained with hematoxylin and eosin (H&E), methylgreen pyronin for plasma cells, Periodic Acid Schiff's (PAS), alcian blue (pH 2.5) for goblet cells and connective tissue type mast cell, and methylene blue for mucosal type mast cell [Bui *et al.* 2011]. The severity of lesions in each transversely sectioned bronchus-bronchiole was evaluated by light microscopy and scored as follows [Hayashi *et al.* 2003a]: no lesions, 0; mucus or desquamated epithelial cells in the lumen, 1; a few goblet cells in the epithelial layer, 1; many such cells, 2; thickened basement membrane, 1; mild infiltration of eosinophils and lymphocytes in mucosa, 1; severe infiltration of those cells in the mucosa, 2; hypertrophy of smooth muscle cells in mucosa, 1. In each mouse the S.I. was calculated by dividing the total number of bronchi-bronchioles examined. The

average of S.I. was then determined for each group. The number of eosinophils, lymphocytes, neutrophils, macrophages, plasma cells and mast cells in the bronchial-bronchiolar mucosa was counted using an eyepiece micrometer morphologically on five different bronchi-bronchioles at random in each left lung of H&E sections by two different observers. Each result was averaged and totaled in each mouse, and thereafter the mean ± SEM (/ $mm^2$) was calculated.

### Immunohistochemistry (IHC)

Deparaffinized sections of the lungs, pLNs and thymi were treated with autoclaving in Dako Target Retrieval Solution (pH 6; Dako Japan, Tokyo, Japan) at 120 °C for 5 min (Foxp3; the asthma group: *n*=7; the control group: *n*=3, iNOS, arginase-1 and CD4; *n*=3 in each group) or Dako Target Retrieval Solution (pH 9) at 121 °C for 1 min (CD3, CD20 and Iba1; *n*=3 in each group). Endogenous peroxidase activity was inactivated in 3% hydrogen peroxide in distilled water for 10 min. Then, sections were treated with Protein Block Serum-Free (Dako Japan) for 30 min to block non-specific binding of antibody. Sections were treated with primary antibodies at 4 °C overnight as follows: rat anti-mouse Foxp3 mAb (Cross-reactivity of anti-mouse Foxp3 mAb to other proteins has not been reported. Constitutive high expression of foxP3 mRNA has been shown in $CD4^+/CD25^+$ Regulatory T cells.) (eBioscience, San Diego, CA, USA) diluted in 1/20, rabbit anti-iNOS polyclonal antibody (pAb) (Abcam Japan, Tokyo, Japan) diluted in 1/1000, rabbit anti-arginaze-1 pAb (Fitzgerald, Acton, MA, USA) diluted in 1/1000, rabbit anti-human CD3 pAb (Dako Japan) diluted in 1/400, mouse anti-human CD4 mAb (Abcam Japan) diluted in 1/10, rabbit anti-human CD20 pAb (Lab Vision Co., Fremont, CA, USA) diluted in 1/400 and rabbit anti-human Iba1 pAb (Wako, Osaka, Japan) diluted in 1/4000. Cross-reactivity with mouse is reported of anti-human CD3 pAb,

anti-human CD4 mAb and anti-human Iba1 pAb, but not anti-human CD20 pAb. Thereafter, sections were treated with secondary antibodies, undiluted peroxidase-labeled goat anti-rabbit IgG pAb (Nichirei Bioscience, Tokyo, Japan), undiluted peroxidase-labeled goat anti-mouse IgG pAb (Nichirei Bioscience) or undiluted peroxidase-labeled goat anti-rat IgG pAb (Nichirei Bioscience) for 30 min depending on the immunized animals of primary antibodies. Positive reactions were visualized with 3'3-diaminobenzidine tetrahydrochloride (Roch Diagnostic, GmbH, Penzberg, Germany) for 5 min and sections were counterstained with Mayer's hematoxylin for 1 min. All incubations were done at room temperature except for those of primary antibodies (4 °C). Between each step, sections were washed three times with PBS. The reaction without primary antibody served as negative control.

### Isolation of splenocytes

Spleens (asthma group: *n*=6; control group: *n*=3) were aseptically removed and placed in phosphate buffered-balanced salt solution (PBBS; pH 7.4) on day 18. Single cell suspensions were made by teasing spleens apart with scissors and passing through a disposable syringe with a 23G needle (Terumo Co., Tokyo, Japan) as described previously [Hayashi & Fujii 2008; Nakashima *et al.* 2012]. Cell suspensions were collected in sterile conical tubes (Fisher Sci., Pittsburgh, PA, USA), and thereafter red blood cells were hemolysed by Tris-buffered $NH_4Cl$ solution, and washed in PBBS followed by centrifugation at 500 *g* for 10 min at 4 °C. The total number of splenocytes was counted using a hemocytometer and diluted in Minimum Essential Medium (MEM; Nissui, Tokyo, Japan) to a density of $1 \times 10^6$ cells/ml. Viability of cells was more than 98% by trypan blue dye exclusion test. Splenocytes ($2 \times 10^5$/200 µl MEM with 5% heat-inactivated fetal calf serum; Gibco, Grand Island, NY, USA) were cultured for 48h at

37 °C under 5% $CO_2$ in the presence of 5.5 μg/ml of concanavalin A (Con A; ICN Biomedical Inc., Aurora, OH, USA) using 96 well-plates (Coster, Cambridge, MA, USA) and supernatants were obtained and stored at -80 °C until use.

## Flow cytometry

Peripheral blood leukocytes were collected from blood and centrifuged at 1000 *g* for 30 min at 4 °C on days 0, 14 and 18 (asthma group: *n*=9; control group: *n*=6) in each time point. After that lymphocytes from mice were separated by Ficoll-Hypaque density-gradient centrifugation for isolation of mouse lymphocytes (Lymphocyte M; Cedarlane, Hornby, Ontario, Canada) and washed with FACS buffer (PBS containing 2% fetal calf serum and 0.1% $NaN_3$). After incubation with fluorescein isothiocyanate (FITC)-conjugated anti-mouse CD4 antibody (clone: RM4-5; Beckton Dickinson, Tokyo, Japan) on ice for 30 min, the cells were washed with FACS buffer, followed by the intracellular staining of Foxp3 according to manufacturer's instruction. In brief, the fixed and permeabilized cells were stained with PE-conjugated anti-mouse Foxp3 antibody (clone: FJK016s; eBioscience) and stored at 4°C until analysis. Appropriate isotype controls (rat IgG2a-PE antibody; eBioscience) were used for each sample. Flow cytometry analysis was performed on EPIX-XL (Beckman Coulter, Tokyo, Japan), and the results obtained were analyzed using the FlowJo software (Treestar, Inc., San Carlos, CA, USA).

After determining the percent of $CD4^+Foxp3^+$ cells in total $CD4^+$ cells (% of $Foxp3^+/CD4^+$) on day 0 given as point 1, ratio of $Foxp3^+/CD4^+$ (decrease in the number of Tregs) on days 14 or 18 was calculated based on that on day 0 in each individual; (% of $Foxp3^+/CD4^+$ on days 14 or 18) / (% of $Foxp3^+/CD4^+$ on day 0).

## Production of OVA-specific IgE in plasma and IL-4, TGF-β1, IL-10 or IFN-γ in supernatants of cultured splenocytes by ELISA

Values for OVA-specific IgE (DS pharmacia Biomedical Co., Ltd, Suita, Osaka, Japan) in plasma and concentrations of IL-4 (Bender MedSystems GmbH, Vienna, Austria), TGF-β1 (R&D system, Inc.), IL-10 (GEN-PROBE, Inc., San Diego, CA, USA) (asthma group; *n*=6, control group; *n*=3) or IFN-γ (Bender MedSystems) (asthma group; *n*=5, control group; *n*=3) respectively in supernatants from cultured splenocytes were measured by mouse ELISA kits according to the manufacturer's instructions. Detectable amounts of OVA-specific IgE, IL-4, TGF-β1, IL-10 and IFN-γ are 2.7 ng/ml, 2.0 pg/ml, 1.7-15.4 pg/ml, 20 pg/ml and 5.3 pg/ml respectively. In case of antibodies or cytokines could not be detected, their concentration was considered as below of sensibility.

## mRNAs expression for IL-4, TGF-β1, IL-10 and IFN-γ in pLNs by real-time PCR

Total RNAs used for real-time PCR analysis were isolated from the frozen pLNs (*n*=3 in each group except for IFN-γ; *n*=2) with TRI reagent (Molecular Research Center, Cincinnati, OH, USA) according to the manufacturer's instructions. One μg of total RNA was treated with Turbo DNA-free (Applied Biosystems Japan, Tokyo, Japan), and transcribed into cDNA using Superscript III (Invitrogen, Tokyo, Japan) according to the manufacturer's instructions. Oligo dT primers were used to prime the first-strand synthesis for each reaction. After single-strand cDNA was generated from each sample, it was subjected to real-time PCR amplification with a QuantiTect SYBR Green PCR Kit (Qiagen, Valencia, CA, USA) according to the manufacturer's protocol. The primers used for assaying IL-4 [Miyake *et al.* 2008], TGF-β1 [Mu *et al.* 2005], IL-10 [Koga *et al.* 2009], IFN-γ [Menon *et al.* 2007] and glyceraldehyde-3-phosphate dehydrogenase

(GAPDH) [Wen Y. *et al.* 2008] are as follows; IL-4: forward, 5'-ACAGGAGAAGGGACGCCAT-3', and reverse, 5'-GAAGCCCTACAGACGAGCTCA-3', TGF-β1: forward, 5'-ACCGGGTGGCAGGCGAGAG-3', and reverse, 5'-CGGGACAGCAATGGGGGTTCT-3', IL-10: forward, 5'-GGACAACATACTGCTAACCG-3', and reverse, 5'-TTCATGGCCTTGTAGACACC-3', IFN-γ: forward, 5'-TCAAGTGGCATAGATGTGGAAGAA-3', and reverse, 5'-TGGCTCTGCAGGATTTTCATG-3' and GAPDH: forward, 5'-TCACCACCATGGAGAAGGC-3', and reverse, 5'-GCTAAGCAGTTGGTGGTGCA-3' respectively. Each assay was performed in duplicate. Predenaturation at 95 °C for 15 min was followed by 45 cycles of PCR amplification consisting of denaturation at 94 °C for 15 sec, annealing at 60 °C for 30 sec, and extension at 72 °C for 30 sec. PCR and fluorescence intensity detection were performed with the StepOne PCR system (Perkin–Elmer, Waltham, MA, USA). The data were analyzed using StepOne software v.2.0. Briefly, the PCR cycle number at the threshold was represented as $C_T$. The difference between $C_T$ values for the target and internal control, i.e., $\Delta C_T$, was calculated. The value of $2\Delta C_T$ was considered representative of the amount of target mRNA relative to the amount of internal control.

### Statistical analysis

The means ± SEM were calculated and analyzed by *F*-test and then by Student's *t*-test (one-tailed or two-tailed). Correlation and regression analysis were performed using Microsoft Excel 2007 (Microsoft Corp., Redmond, Washington, USA). The accepted level of significance was $P<0.05$.

## Results

### Number of leukocyte in blood

The number of total leukocytes, neutrophils, lymphocytes and monocytes in the asthma group increased on days 14 and 18 compared to the control group (Fig. 2A, C-E: $P<0.05$ and $P<0.01$, two-tailed *t*-test). On day 18, but not on day 0, there was a significant increase in the number of eosinophils ($P<0.05$, two-tailed *t*-test) in the asthma group compared to the control group (Fig. 2B). The number of eosinophils on day 14 in the asthma group was increased when compared to that in the control group ($P<0.01$, two-tailed *t*-test).

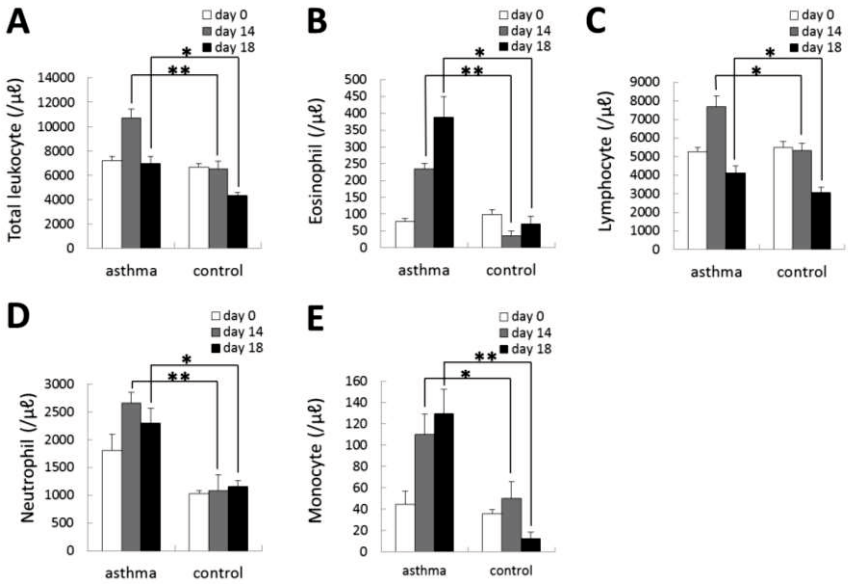


Fig. 2: Number of each leukocyte (A-E) in blood (/μl) on days 0, 14 and 18. Each value represents the mean ± SEM. *$P<0.05$, ** $P<0.01$.

### Asthmatic inflammation and characterization of inflammatory cell

The asthma group developed asthmatic inflammation (Fig. 3A-C, J) and infiltrated cells were summarized in Fig. 3K. There were goblet cell metaplasia and/or hyperplasia with mucous hypersecretion in the asthma group (Fig. 3B, C), although

those changes varied within the same lung and among mice. There was severe infiltration of eosinophils with degranulation and lymphocytes including some neutrophils, macrophages and plasma cells, but not mast cells (Fig. 3I). At the site of asthmatic inflammation edematous lamina propria was recognized, and in some cases destructed and desquamated epithelial cells into the bronchial-bronchiolar lumen and hypertrophic smooth muscle cells were observed. There were no asthmatic inflammation in the control group (Fig. 3D, J). In addition, eosinophilic vasculitis in venules and small sized arterioles was often observed throughout the lung tissue.

The number of total cells in the asthma group increased when compared to that in the controls (asthma group: 3622.1 ± 263.4 /$\mu m^2$; control group: 0 /$\mu m^2$). Inflammatory cell consisted of lymphocytes expressing $CD3^+$ (Fig. 3E), $CD4^+$ (Fig. 3F), and $CD20^+$ (Fig. 3G), including $Iba1^+$ macrophages (Fig. 3H) and mucosal type, but not connective tissue type, mast cells (Fig. 3I). Compared to other inflammatory cells, mast cell infiltration was few (Fig. 3K).

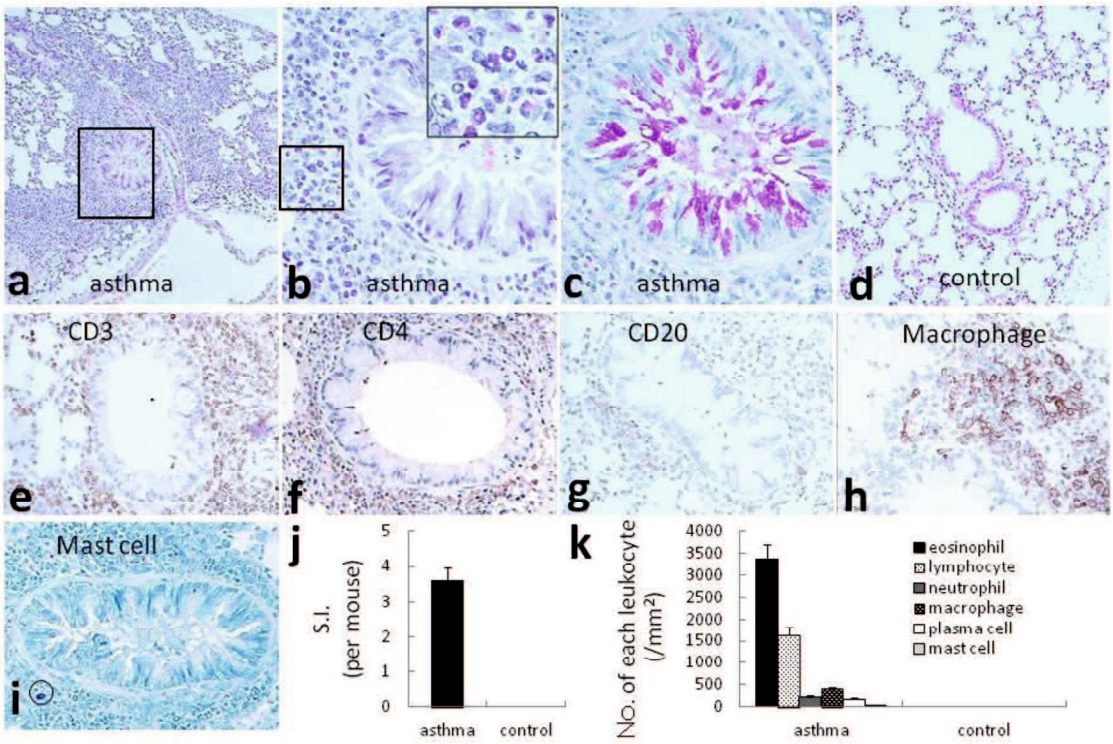


**Fig. 3.** Histopathology of asthmatic inflammation on day 18. Severe bronchial-bronchiolar lesions with desquamated epithelial cells in the bronchial lumen and hypertrophic smooth muscle cells are seen in the asthma group (**A**, and **B**; enlargement of rectangle in **A**). Densely infiltrated eosinophils and lymphocytes (**B**, and insert: enlargement of rectangle in **B**) and metaplasia and hyperplasia of goblet cells (**C**) with mucous hypersecretion are visible. There are no those changes in the control group (**D**). Characterization of infiltrated cells. $CD3^+$ (**E**), $CD4^+$ (**F**) and $CD20^+$ (**G**) lymphocytes, $Iba1^+$ (**H**) macrophages and mast cells (**I**; circle indicates mast cell). S.I. (severity of lesions) of asthmatic inflammation per one mouse (**J**). Number of inflammatory cells (/$mm^2$) at the site of bronchi-bronchioles is shown (**K**). Each value represents the mean ± SEM. Asthma group (**A**-**C**, **E**-**I**) and control group (**D**). (**A**, **B**) and (**D**): H&E; (**C**): PAS; (**E**-**H**): IHC (brown color: positive cells), and counterstained with Mayer's hematoxylin; and (**I**): methylene blue. (**A**): ×100, (**D**): ×200, (**E**-**I**): ×400, (**B**, **C**): ×600 and insert of (**B**): ×1200.

### Relationship between severity of asthmatic inflammation (S.I.) and number of Tregs

S.I. of each bronchus varied within the same lung in the asthma group. In the control, there were no or a few Tregs at bronchial walls (0 to $9.6 \times 10^{-5}$ /μm$^2$) (Fig. 4B). On the other hand, there were mild-to-moderate infiltrations of Tregs at bronchial walls (Fig. 4C, D). The number of Tregs was inversely correlated with S.I. per each bronchus-bronchiole in one mouse of the asthma group (regression analysis) (Fig. 4A).

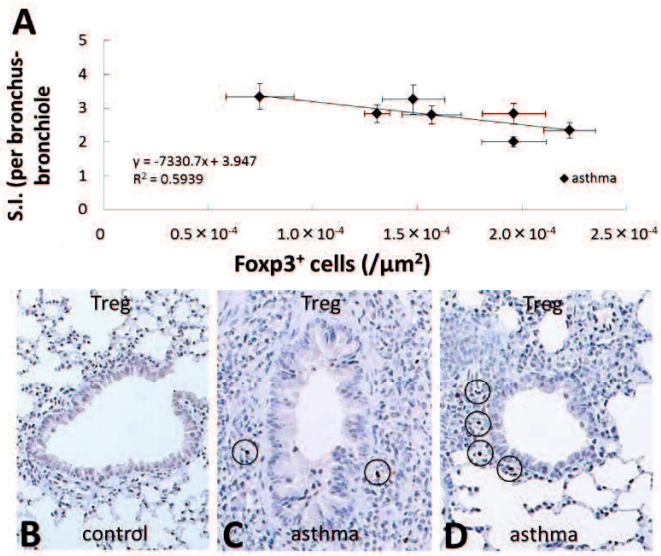


**Fig. 4.** Relationship between Tregs number and S.I. of asthmatic inflammation per each bronchus-bronchiole in each mouse (**A**). The control shows no Tregs (**B**). High S.I. with no increase of Tregs (**C**) and low S.I. with increased Tregs (**D**) can be recognizable. IHC (Foxp3; brown color: positive cells including circles). Counterstained with Mayer's hematoxylin. Number of Tregs per each bronchus-bronchiole is expressed per 1 μm$^2$. ×200.

## M1/M2 macrophages in bronchi-bronchioles lesions

Compared to the control, there were severe infiltrations of arginase-$1^+$ macrophages (alternative activated M2 macrophages) at the site of asthmatic inflammation in the asthma group (Fig. 5A). On the other hand, $iNOS^+$ macrophages (classically activated M1 macrophages) were very few at the same site of asthmatic inflammation in the asthma group (Fig. 5B).

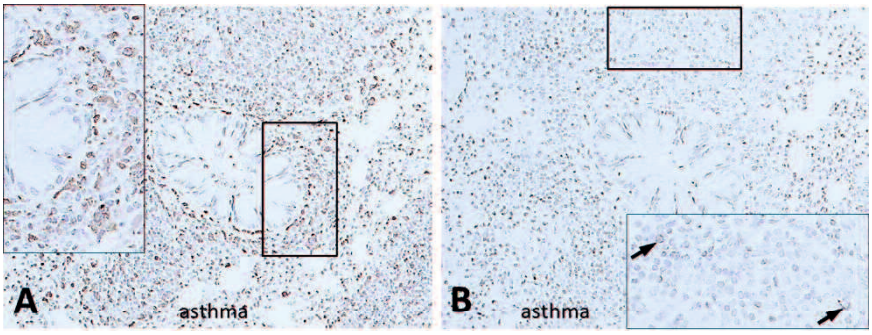


**Fig. 5.** M1/M2 macrophages in bronchi-bronchioles lesions. Compared to the control, numerous arginase-$1^+$ macrophages (M2 macrophages) is observed at asthmatic inflammation in the asthma group (**A**, and insert: enlargement of rectangle in **A**). There are very few $iNOS^+$ macrophages (M1 macrophages, arrows) in the asthma and control groups (**B**, and insert: enlargement of rectangle in **B**; the asthma group). Representative IHC (brown color: positive cells), and counterstained with Mayer's hematoxylin. (**A**, **B**): ×200, insert of (**A**, **B**): ×400.

## Tregs in regional LNs and thymi

Tregs distributed in cortex and medulla of pLNs (Fig. 6A) and thymus medulla (Fig. 6B) in the asthma group and control group (Fig. 6C, D). Tregs at pLN and thimi in the asthma group decreased compared to the control group (Fig. 6E, F: $P<0.01$, two-tailed *t*-test).

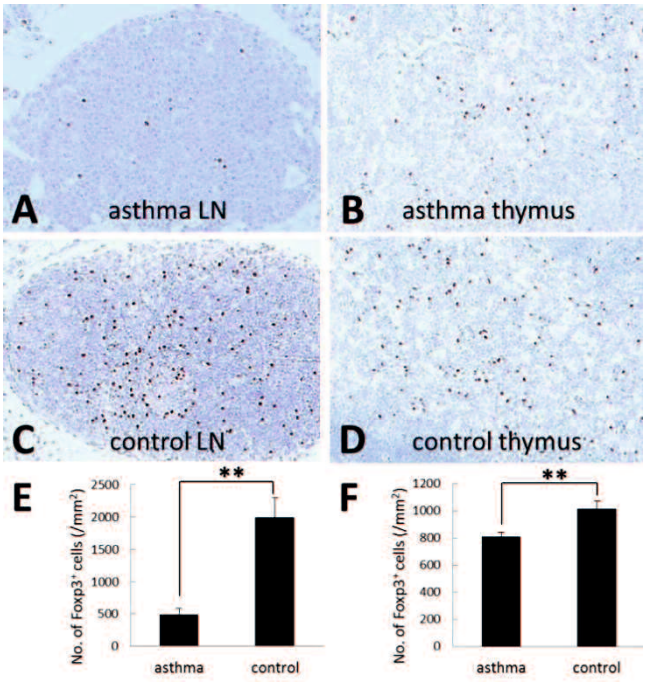


**Fig. 6.** Tregs in pLNs and thymi. Asthma group: (**A**) and (**B**), and control group: (**C**) and (**D**). IHC (Foxp3; brown color: positive cells). Counterstained with Mayer's hematoxylin. ×200. The presence of Tregs in pLN (**E**) and thymus (**F**) in the asthma and control groups. Numbers of Tregs per each bronchus are expressed per 1 $mm^2$. Each value represents the mean ± SEM. ** $P$<0.01.

## Proportion of Tregs in PBMCs

To clarify the Tregs change in the asthma group, quantitative analysis was performed with the flow cytometry (Fig. 7A). On day 18 there was a significant difference in the percent of $Foxp3^+/CD4^+$ and the ratio of $Foxp3^+/CD4^+$ between the asthma and control groups (Fig. 7B, C: $P$<0.05, two-tailed $t$-test). In addition, on day 18 compared to on day 14, the ratio of $Foxp3^+/CD4^+$ at the effector phase, but not the induction phase, was significantly decreased in the asthma group, but not the control group (Fig. 7C: $P$<0.05, two-tailed $t$-test). Moreover, the percent of $Foxp3^+/CD4^+$ and the ratio of $Foxp3^+/CD4^+$ on day 18 compared to on day 0 significantly increased in the control group (Fig. 7B, C: $P$<0.01, two-tailed $t$-test). The proportion of Tregs was inversely correlated with S.I. in each mouse (regression analysis) (Fig. 7D, E).

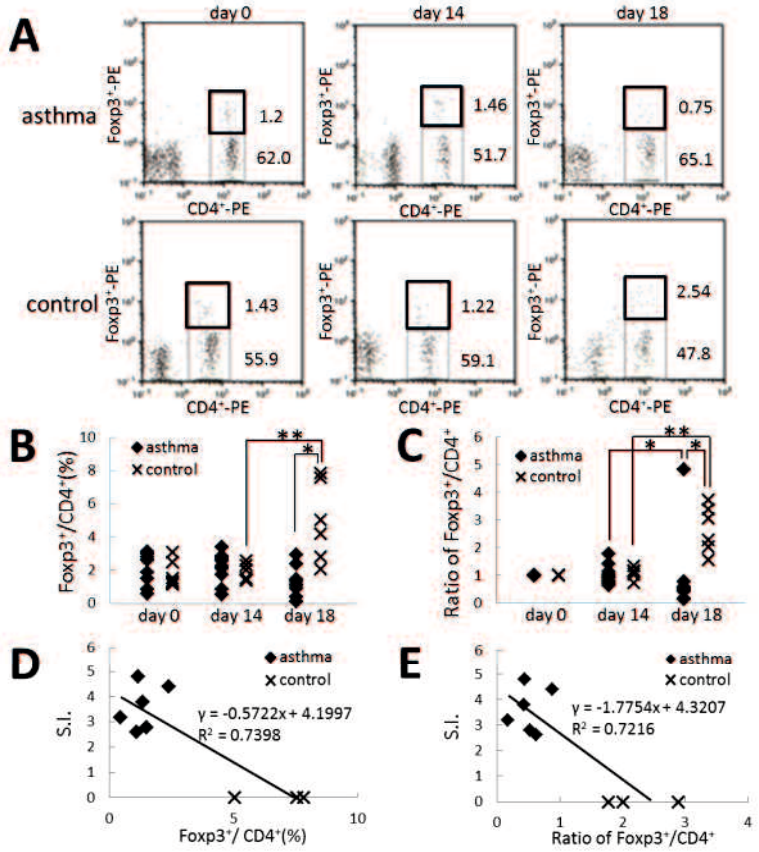


**Fig. 7.** Representative FACS analysis of Tregs in the asthma and control groups on day 0, 14 and 18, respectively (**A**). Percent of $Foxp3^+/CD4^+$ (**B**) and ratio of $Foxp3^+/CD4^+$ (**C**) based on those on day 0 given as the point 1 by flow cytometry analysis. Correlation analysis between (**D**) percent of $Foxp3^+/CD4^+$and (**E**) ratio of $Foxp3^+/CD4^+$ and S.I. of asthmatic inflammation per one mouse. Trendline and correlation coefficient were shown. **P*<0.05; ***P*<0.01.

## Systemic production of OVA-specific IgE in plasma, IL-4, TGF-β1, IL-10 and IFN-γ from supernatants of cultured splenocytes with concanavalin A and local mRNA expression for IL-4, TGF-β1, IL-10 and IFN-γ in pulmonary LNs

OVA-specific IgE (Fig. 8A), and production of IL-4 (Fig. 8B), but not IFN-γ (Fig. 8E), of the asthma group increased statistically (*P*<0.05, two-tailed *t*-test) compared to the control group. In addition, there was no significant difference in TGF-β1 (Fig. 8C) and IL-10 (Fig. 8D) values between the asthma and control groups.

IL-4 mRNA expression of the asthma group increased statistically ($P$<0.05, two-tailed $t$-test) compared to the control group (Fig. 8F). In the asthma group, mRNAs expression of TGF-β1 (Fig. 8G: $P$<0.05, one-tailed $t$-test) and IL-10 (Fig. 8H: $P$<0.05, one-tailed $t$-test) decreased compared to the control group. There was no difference in mRNA expression for IFN-γ between the asthma and control groups (Fig. 8I).

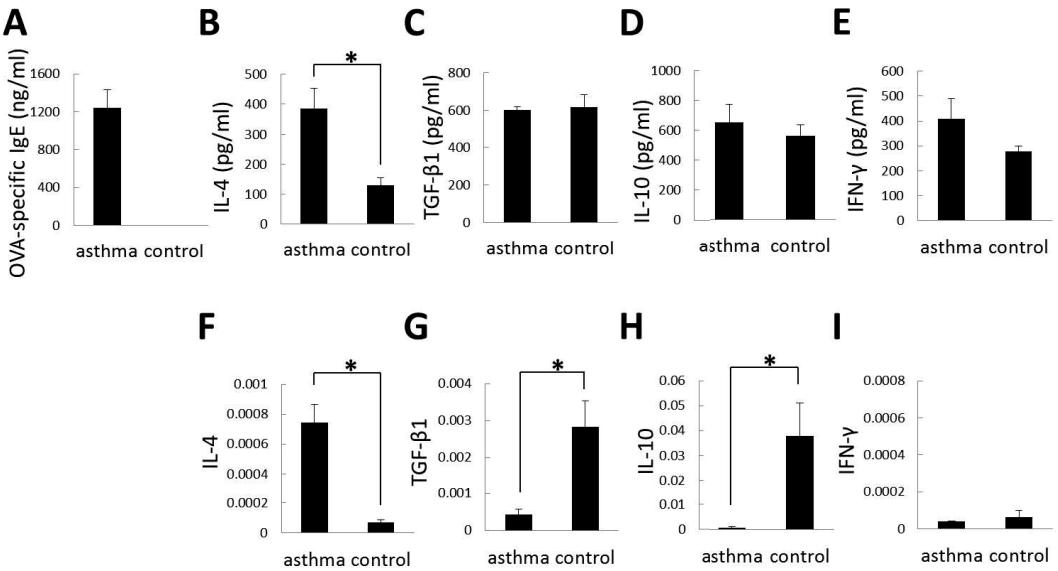


**Fig. 8.** Concentration of OVA-specific IgE in plasma (**A**) and values of IL-4 (**B**), TGF-β1 (**C**), IL-10 (**D**) and IFN-γ (**E**) in supernatants of cultured splenocytes cells stimulated with Con A detected by ELISAs. IL-4 (**F**), TGF-β1 (**G**), IL-10 (**H**) and IFN-γ (**I**) mRNAs expression in pLNs detected by real-time PCR. Each value represents the mean ± SEM. *$P$<0.05.

## Relationship between production and mRNA expression of cytokines and Tregs number, or relationship between those of cytokines and S.I.

As shown in Fig. 9A-D, there was no relationship between cytokines production and Tregs number in blood. There was no relationship between S.I. per each mouse and IL-4, but not IFN-γ, including TGF-β1 and IL-10 production (Fig. 9E-H).

There was relationship between mRNAs expressions for TGF-β1, but not for IL-4

and IFN-γ, and Tregs number in blood (Fig. 9I-L). mRNAs expression of IL-4, TGF-β1 and IL-10, but not IFN-γ, were related with the degree of S.I. per each mouse (Fig. 9M-P).

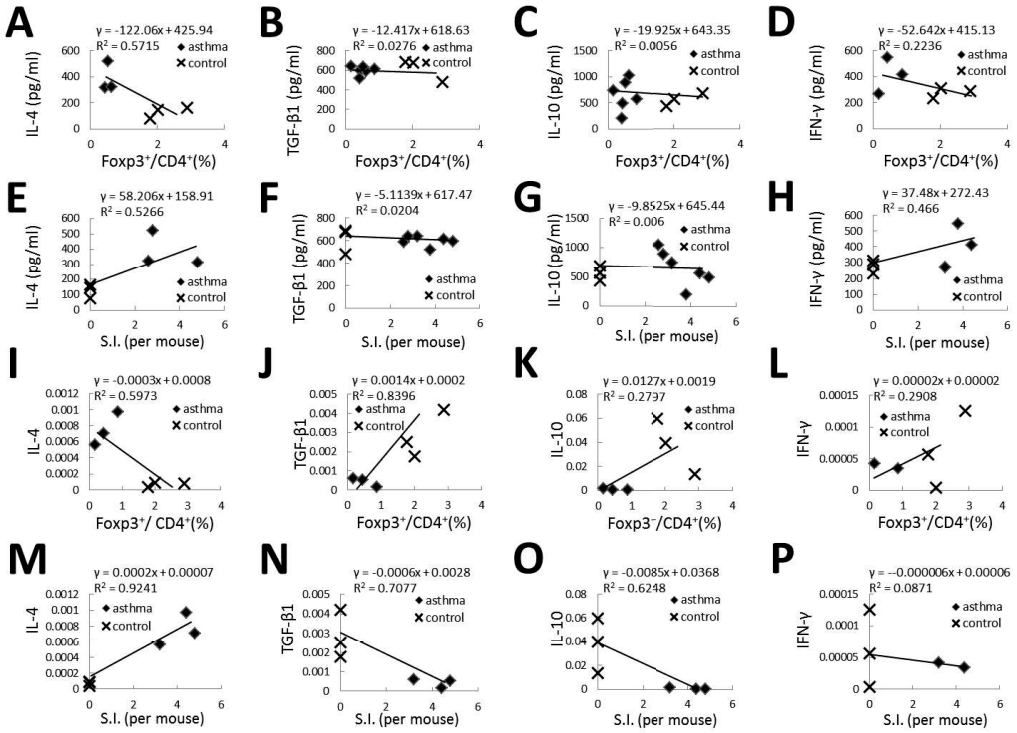


**Fig. 9.** Correlation analysis between systemic cytokines production, and ratio of $Foxp3^+/CD4^+$ (**A**-**D**) and S.I. of asthmatic inflammation (**E**-**H**) and between local (pulmonary LNs) mRNAs expression, and ratio of $Foxp3^+/CD4^+$ (**I**-**L**) and S.I. (**M**-**P**) per one mouse. Trendlines and correlation coefficients are shown in each graph.

## Discussion

The present study clearly demonstrated the evidence that the development of Th2-dominant late allergic asthmatic inflammation [Melgert *et al.* 2005] with decreased Tregs at the site of asthmatic inflammation with systemic reduction of circulating Tregs during the effector phase, but not the induction phase. These suggest that the systemic sensitization and the following exposure of OVA may evoke the reduction of Tregs at the inflamed site, resulting in the promotion of asthmatic inflammation. The

parallel association of the reduced Tregs in circulation and *in situ* accumulation of Tregs seems likely, since bronchial allergen inhalation in sensitized human patients (predominantly in those who did not develop significant bronchoconstriction) was associated with the decreased proportion of Tregs in the circulation [Moniuszko *et al.* 2008]. In addition, exposure to allergen (house dust mite) in sensitized patients led to the decrease in circulating Tregs in an early response (6 h) in immediate reaction [Moniuszko *et al.* 2008].

In each bronchus showed a different relationship between S.I. of asthmatic inflammation and Tregs number within the same lung, although the development of asthmatic lesions and decrease in peripheral Tregs was inversely correlated. The less accumulation of Tregs led to severe asthmatic inflammation (Fig.4C), whereas increased Tregs reduced the severity of asthmatic inflammation (Fig.4D), suggesting the idea that Tregs may determine the outcome of the development of asthmatic inflammation by their cell-to-cell contact suppression with productions of immunosuppressive cytokines locally and systemically. Induction of inducible Tregs (iTreg) and naturally occurring Tregs (nTregs) [McGee & Agrawal 2009; Lowder & Kunz 2011], including allergen-specific Tregs [Taylor *et al.* 2004] in animal models and human patients with allergic asthma have been reported. Also, Tregs suppress allergen-specific Th1 and Th2 cell responses playing an important role in the physiological immune response to allergens [Braga *et al.* 2011]. Moreover, it has been reported recently that suppressor of cytokine signaling (SOCS) proteins especially SOCS2 expressed in both nTregs and iTregs, and SOCS2 inhibited the development of Th2 cells and local allergic immune responses in vivo and in vitro by flow cytometry analysis [Knosp *et al.* 2013].

The process of diseases may be determined by other suppressive mechanisms

other than Tregs. For example, the pathogenesis of allergic asthma is orchestrated by a complex interplay of several cells such as immature dendritic cells, which maintain tolerance [Hayashi 2012b], suggesting that the direction of the development of asthmatic inflammation may be determined by cooperation of different mechanisms. Taken together, dynamic changes may occur within each bronchus in terms of the development of asthmatic inflammation. Further study is needed to clarify those points.

Decreased local mRNAs expression, but not systemic production, of immunosuppressive cytokines such as TGF-β1 and IL-10 [Weiner 2001; Kearley *et al.* 2005; Robinson 2009] was associated with the reduced number of Tregs, suggesting that decreased mRNAs expression of those cytokines may be due to the decreased number of Tregs [Borish *et al.* 1996; Koning *et al.* 1997; Hellings *et al.* 2002]. Also, decrease in Tregs, at least in part, may reflect the decrease in circulating Tregs with impairment of quality and quantity of Tregs function. Alternatively, decreased local IL-10 mRNAs expression may decrease Tregs number, since it has been reported that IL-10 may differentiate from naïve Th0 to Tregs [Maldonado *et al.* 2010; Kay 2004], and that IL-10 mRNA expression was decreased in pLNs. In addition, another possibility is that the appearance of M2 macrophages may induce Tregs [Hamzaoui *et al.* 2010; Egawa *et al.* 2013]. If so, there are some contradictions since there were many M2 macrophages at the site of asthmatic inflammation. Further study is needed to clarify the relation between the role of M2 macrophages and the decrease in Tregs. Alternatively, the dissociation between systemic productions and local mRNAs expression in TGF-β1 and IL-10 was found, whereas the systemic productions of Th2 cytokines (e.g., IL-4 and IL-5) were paralleled with those local mRNAs expression in our

mouse model of late allergic asthma [Hayashi *et al.* 2002a, 2003a; Morimoto *et al.* 2002]. On the other hand, systemic TGF-β1 and IL-10 responses do not mean local response. It seems likely, since TGF-β1 or IL-10 will be produced by several cells (e.g. fibroblasts, endothelial cells and Th3 cells other than Tregs [Weiner 2001].

We reported previously that the expression of vascular cell adhesion molecule (VCAM)-1 on endothelium and very late antigen (VLA)-4 on lymphocytes and eosinophils may contribute to the accumulation and infiltration of those cells at the site of asthmatic inflammation in a model of late allergic asthma [Nakashima *et al.* 2012]. On the other hand, accumulation and/or recruitment of Tregs were impaired at the site of severe lesions, but not less severe lesions, nevertheless those adhesion molecules were expressed in this model. It has been reported that tumor cells and microenvironmental macrophages in human produce the C-C chemokine ligand (CCL)-22, which mediate trafficking of Tregs to the tumor [Curiel *et al.* 2004]. Normal blood Tregs express C-C chemokine receptor (CCR) 4 and CCR8, and migrate in response to CCL1, CCL17 or CCL22 on the basis of *in vitro* assay [Iellem *et al.* 2001], suggesting that recruitment of Tregs, and Th2 cells and eosinophils may use different adhesion molecules. Moreover, relatively many Tregs accumulated at the site of severe asthmatic inflammation. These suggest the accumulation of Tregs may be determined by not only adhesion molecules and other unknown factors.

In conclusion, the present study demonstrated the local presence of Tregs and suggests that *in situ* decreased Tregs may, at least in part, enhance the development of asthmatic inflammation by cell-to-cell interaction and cytokine-mediated suppression.

## Summary

$CD4^+Foxp3^+$T cells (Tregs) mediate homeostatic peripheral tolerance by suppressing helper T2 cells in allergy. However, regulation of asthmatic inflammation by local (*in situ*) Tregs in asthma remains unclear. BALB/c mice sensitized and challenged with ovalbumin (OVA) (asthma group) developed asthmatic inflammation with eosinophils and lymphocytes, but not mast cells. The number of Tregs in the circulation, pulmonary lymph nodes (pLNs) and thymi significantly decreased in the asthma group compared to the control group without OVA-sensitization and -challenge in the effector phase. The development of asthmatic inflammation is inversely related to decreased Tregs with reduced mRNAs expression such as interleukin (IL)-4, transforming growth factor-β1 and IL-10, but not interferon-γ, in pLNs. Moreover, M2 macrophages increased in the local site. The present study suggests that decreased Tregs, at least in part, may enhance the development of asthmatic inflammation by cell-cell contact and cytokine-mediated suppression.

# 3. Chapter 2.

## Reovirus type-2-triggered autoimmune cholangitis in extrahepatic bile ducts of weanling DBA/1J mice

## Introduction

Biliary atresia is the most common cause of neonatal cholestasis and is characterized by progressive sclerosing cholangitis of the extrahepatic biliary tree [Sokol & Mack 2001; Mack 2007]. Although the etiology of biliary atresia is not completely understood, several factors have been proposed [Sokol & Mack 2001; Bezerra 2006; Mack 2007]. These include viral infection of the primary perinatal hepatobiliary epithelium and autoimmune-mediated bile duct injury [Mack 2007]. Two *Reoviridae* virusues, group C rotavirus and reovirus type (Reo)-3, have been implicated as causative agents of biliary atresia [Sokol & Mack 2001]. Importantly, the anatomical and inflammatory profiles associated with rotavirus-induced biliary atresia in mice share striking similarities those of human biliary atresia [Shivakumar *et al.* 2004; Bezerra 2006].

Reovirus is a ubiquitous, nonenveloped, cytoplasmically replicating virus isolated from a wide variety of mammalian species, including humans [Schiff *et al.* 2007; Onodera & Hayashi 2013]. Reovirus consists of three serotypes and is considered an "orphan virus" because no definitive links to disease have been established. However, several reports suggest that reovirus may be associated with diarrheal illnesses, upper respiratory infections, and hepatobiliary diseases, including biliary atresia and rare infections of the central nervous system [Clarke *et al.* 2005; Schiff *et al.* 2007]. For instance, animals infected either naturally or experimentally with Reo-3 develop various diseases [Schiff *et al.* 2007]. In addition, Reo-3 replicates in the cytoplasm of extrahepatic biliary epithelia and causes acute, transient or segmental cholangitis in weanling mice [Papadimitriou 1968; Bangaru *et al.* 1980; Wilson *et al.* 1994]. High levels of Reo-3 were found in the serum of a 6-week-old female rhesus monkey with

jaundice and conjugated hyperbilirubinemia [Rosenberg *et al.* 1983]. Reo-3 antigens and virus-like particles were found in the bile duct of a patient with biliary atresia [Morecki *et al.* 1984], and in patients with extrahepatic biliary atresia or choledochal cysts [Tyler *et al.* 1998].

We previously reported that Reo-2 infection in weanling DBA/1J mice induces transient Th1 dominant autoimmune insulitis with impaired glucose tolerance (IGT) within 24 h after birth [Onodera & Hayashi 2013]. In addition, the autoimmune disease susceptibility locus (first chromosome *VAS1* gene) in DBA/1J mice is involved with development of insulitis [Holmdahl *et al.* 1990]. Thymic atrophy in conjunction with the production of autoantibodies suggests that autoimmune response may be formed in Reo-2-infected weanling mice [Onodera & Hayashi 2013]. Thus, we propose that cholangiotropic Reo-2 infection and subsequent autoimmune-induced bile duct injury may potentiate the development of infantile biliary atresia. To address this, we studied the mechanism of Reo-2 infection and its effects on immune-mediated injury to extrahepatic bile ducts in a mouse model.

## Materials and methods

### Virus isolation

The BN-77 Reo-2 strain, isolated from bovine diarrheal matter, was grown on HmLu-1 cells as described previously [Nakashima *et al.* 2012]. One-day-old mice were infected with $5\times10^5$ plaque-forming unit (pfu.)/0.05 ml with Dulbecco's modified Eagle's medium (DMEM; Nissui) (i.p.; designated as day 0).

### Infection of mice

One-day-old DBA/1J mice of both sexes (Seac Yoshitomi, Fukuoka, Japan) were

divided into Reo-2 infected and age-matched uninfected control groups. Mice were sacrificed as in Fig. 1A (infected group: *n*=5; control group: *n*=4 at each time point unless otherwise stated). They were kept at 24 ± 2 °C in dry-heat-sterilized metal cages. Mother mice were fed with autoclaved commercial pellet (CE-2; CLEA Japan) and were freely supplied sterilized water. The Animal Research Ethics Board of the Faculty of Agriculture at Yamaguchi University approved the animal experiments.

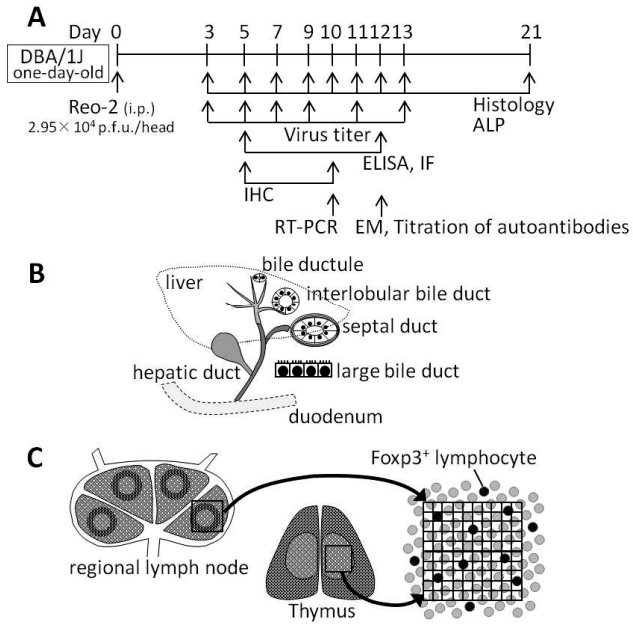


**Fig. 1**: Experimental protocol (**A**), scheme of counting bile duct cells (**B**) and Foxp3$^+$ cells (**C**). See **Materials and methods** for details. ALP: alkaline phosphatase; EM: electron microscope; IF: immunofluorescence; IHC: immunohistochemistry; pfu: plaque-forming unit; RT-PCR: real-time PCR.

## Virus titration in liver

Whole blood was obtained while exogenous viral contamination was carefully avoided. Subsequently, 20 mg of liver was resected from the left side of 5 Reo-2 infected mice and pooled (100 mg total). Liver samples were then homogenized in 1 ml of DMEM and centrifuged at 3,000 *g* for 10 min. The titers, performed in duplicate, were determined by inoculating a monolayer of HmLu-1 cells in 35 mm dishes (Sumitomo, Tokyo, Japan) with 0.2 ml of 10-fold diluted supernatants. After adsorption for 2 h at 37 °C, the monolayeres were overlaid with DMEM-20%

heat-inactivated fetal calf serum and 0.8% agar, incubated at 37 °C for 6 days and overlayed with DMEM-20% heat-inactivated fetal calf serum, 0.8% agar, and 1% neutral red. Plaques were counted, and the viral titers (pfu./ml) were presented in $\log_{10}$ units.

### Alkaline phosphatase (ALP) value in serum

Serum ALP concentrations were measured to assess the degree of biliary injury. ALP values were determined using Fuji Dry-chem 5500s (Fuji Film, Tokyo, Japan) and expressed as IU/l.

### Histopathology of bile duct epithelium

Bile ducts were examined based on the anatomical location illustrated by Nakamura *et al.* [2001] (Fig. 1B). Liver tissues were fixed in 10% neutral buffered formalin, embedded in paraffin, sectioned at 6 μm-thickness and stained with hematoxylin and eosin (H&E) and Masson's trichrome. Histopathological examination and grading were performed as described previously [Orth *et al.* 2000] with simple modifications. In brief, epithelial cell damage, infiltration (inflammation) of the bile duct, epithelium proliferation, and fibrosis were graded as follows: 0=none; 1=minimal; 2=mild; 3=moderate; 4=severe. S.I. of each bile duct is calculated as $[(n0\times0)+(n1\times1)+(n2\times2)+(n3\times3)+(n4\times4)]/\Sigma n$. S.I. and standard deviation (SD) were calculated from four different parts of extrahepatic bile ducts randomly and blindly selected from each liver section by two investigators.

### Detection of viral antigens in biliary epithelia

Paraffin sections of Reo-2 infected mice at 5 and 12 days post infection (dpi) ($n$=3 for each time point) were probed with rabbit anti-Reo-2 antibody, followed by incubation with FITC-labeled goat anti-rabbit secondary antibody (Leinco, Manchester, UK). Uninfected mice were used as a control ($n$=2).

### Titration of autoantibodies against cholangiocytes and nuclei

Autoantibodies against cholangiocytes and nuclei in sera at 12 dpi (infected: *n*=13, control: *n*=5) were assayed by indirect immunofluorescence (IF). Frozen sections of liver and pancreas from a healthy adult female DBA/1J mouse were blocked with goat serum, and then incubated with goat FITC-labeled anti-mouse IgG/M/A (Serotec, Oxford, UK). The IF titers were expressed as the reciprocal of the lowest dilutions that had a positive response and were transformed to $\log_2$ scale. To confirm the specificity of the reaction, IF-positive sera were subjected to absorption test with liver extract from normal weanling DBA/1J mouse. The titer from sera of infected mice over $\log_2$ 4 that of control mice was considered as the lower limit of positive value.

### IF and IHC

For IF, the liver samples at 12 dpi (infected: *n*=3, control: *n*=2) were frozen in chilled *n*-hexane, sectioned at 4 μm-thickness by cryostat, and fixed in acetone. Sections were treated with primary antibodies as follows: rat anti-mouse major histocompatibility complex (MHC)-class I mAb (clone: ERMP42, Abcam Japan), FITC-conjugated rat anti-mouse IFN-γ mAb (clone: 05-142, Upstate Biotechnology, Lake Placid, NY, USA), FITC-conjugated rat anti-mouse CD4 (L3/T4) mAb (clone: YTS 191.1, Cedarlane, Westbury, NY, USA), FITC-conjugated rat anti-mouse CD8 mAb (clone: SE-A1006, Sumitomo Electric, Osaka, Japan), and FITC-conjugated rat anti-mouse macrophage (clone: MCA519, Serotec). The sections that reacted with anti-MHC class I antibody were incubated with FITC-conjugated goat anti-rat immunoglobulin secondary antibody (Biosource, Camarillo, CA, USA).

The paraffin sections of the livers, regional (hepatic) lymph nodes and thymi at 5 dpi or 10 dpi were autoclaved in Dako Target Retrieval Solution (pH 6, Dako Japan) at

120 °C for 5 min or Dako Target Retrieval Solution (pH 9) at 121 °C for 1 min. Endogenous peroxidase activity was inactivated with 3% aqueous hydrogen peroxide for 10 min. Then, sections were treated with Protein Block Serum-Free (Dako Japan) for 30 min to block non-specific binding of antibodies. Sections were treated with primary antibodies overnight as follows: rabbit anti-human CD3 pAb (Dako Japan), rat anti-mouse Foxp3 mAb (clone: NRRF-30, eBioscience), rabbit anti-mouse FAS pAb (Santa Cruz Biotechnology Inc., Santa Cruz, CA, USA), rabbit anti-human FASL pAb (Abcam Japan), and rabbit anti-mouse TNF-α pAb (Abcam Japan). Thereafter, sections were incubated with the Histofine Simple Stain MAX-PO (R) or (Rat) (Nichirei Bioscience). Positive reactions were visualized with 3'3-diaminobenzidine tetrahydrochloride (Roch Diagnostic), and sections were counterstained with Mayer's hematoxylin.

All incubations were done at room temperature except for those of primary antibodies (4 °C). To test the specificity, the reaction without the primary antibodies served as a negative control.

### Electron microscopy (EM)

At 12 dpi, a part of the liver (infected: *n*=3; control: *n*=2) was fixed in 1% osmium tetroxide and embedded in Epon 812. The orientation of the blocks was achieved by examining 1 μm-thickness sections stained with toluidine blue (TB). Ultra-thin sections were stained with uranyl acetate and lead nitrate, and observed by electron microscopy (H-7600; Hitachi, Ibaraki, Japan) at 80 kV.

### Detection of apoptosis of cholangiocyte and infiltrated lymphocyte by TUNEL staining

DNA fragmentation of apoptotic cells at 5 and 12 dpi was visualized by enzymatic reaction in paraffin sections (*n*=3 in each group at each time point) using the *in situ* cell detection kit (Enzo, Penzberg, Germany). In brief, deparaffinized sections were

incubated in 20 μg/ml of proteinase K to strip proteins from nuclei and then in 0.3% $H_2O_2$-methanol to abolish endogenous peroxidase activity. Subsequently, TdT buffer solution containing TdT and fluorescein-labeled dUTP was added. The sections were reacted with peroxidase-conjugated anti-fluorescein antibody. The reaction products were visualized by a benzidine reaction, and sections were counterstained with Mayer's Hematoxylin.

### ELISA for serum levels of IFN-γ, IL-4, IL-17A and TGF-β1

The concentrations of IFN-γ, IL-4, IL-17A and TGF-β1 at 5 and 12 dpi were measured with ELISA kit for mouse IFN-γ (Genzyme Techne, Minneapolis, MN, USA), IL-4 (American Research Products, Cambridge, MA, USA), IL-17A (eBioscience) and TGF-β1 (Genzyme Techne). Detectable amounts of IFN-γ, IL-4, IL-17A and TGF-β1 are 2.0, 1.6, 4 and 1.6 pg/ml, respectively. In cases where cytokines were not detected, their concentration was assigned a value of 0 pg/ml.

### Detection of mRNA expression of IL-4, IFN-γ and IL-17A in spleen

Total RNA was isolated from frozen spleen samples (*n*=3 in each group) at 10 dpi with TRI reagent (Molecular Research Center). One μg of total RNA was treated with Turbo DNA-free (Applied Biosystems Japan), and transcribed into cDNA using Superscript III (Invitrogen). Oligo dT primers were used to prime the first-strand synthesis for each reaction. After single-strand cDNA was generated, it was subjected to real-time PCR amplification with a QuantiTect SYBR Green PCR Kit (Qiagen). The primers used for amplification of IFN-γ [Menon *et al.* 2007], IL-4 [Miyake *et al.* 2008], IL-17A [Hattori *et al.* 2010] and glyceraldehyde-3-phosphate dehydrogenase (GAPDH) [Peter *et al.* 2008] are as follows:

IFN-γ: forward, 5'-TCAAGTGGCATAGATGTGGAAGAA-3', and reverse,

5’-TGGCTCTGCAGGATTTTCATG-3’, IL-4: forward, 5’-ACAGGAGAAGGGACGCCAT-3’, and reverse, 5’-GAAGCCCTACAGACGAGCTCA-3’, IL-17A: forward, 5’-TCCAGAAGGCCCTCAGACTA-3’, and reverse, 5’-AGCATCTTCTCGACCCTGAA-3’ and GAPDH: forward, 5’-TCACCACCATGGAGAAGGC-3’, and reverse, 5’-GCTAAGCAGTTGGTGGTGCA-3’

Each assay was performed in duplicate. Predenaturation at 95 °C for 15 min was followed by 45 cycles of PCR amplification consisting of denaturation at 94 °C for 15 sec, annealing at 60 °C for 30 sec, and extension at 72 °C for 30 sec. PCR and fluorescence intensity detection were performed with the StepOne PCR system (Perkin-Elmer). The data were analyzed using StepOne software v.2.0. Briefly, the PCR cycle number at the threshold was represented as $C_T$. The difference between $C_T$ values for the target and internal control, i.e., $\Delta C_T$, was calculated. The value of $2\Delta C_T$ was considered representative of the amount of target mRNA relative to the amount of internal control.

### Measurement of Tregs in ducts, regional lymph nodes and thymi

The number of $Foxp3^+$ cells in hepatic lymph nodes (lymphoid nodules) and thymi at 5 and 10 dpi (*n*=3 in each group at each time point) was counted using an eyepiece micrometer (Fig. 1C). This method was favored over FACS analysis of peripheral blood leukocytes because it is very difficult to get adequate amounts of blood from weanling mice. Results were averaged from each group and represented as the mean ± SEM.

### Statistical analysis

The means ± SEM or ± SD were calculated and analyzed by *F*-test and then by Student’s *t*-test (one-tailed or two-tailed). The accepted level of significance was $P<0.05$.

## Results

### Virus replication in the liver and serum ALP levels

Isolation of virus at 3 and 5 dpi yielded $2.5\times10^2$ and $1.25\times10^3$ pfu./g, respectively. Virus was undetectable at 7-13 dpi (Fig. 2A). Serum ALP levels increased significantly at 7, 13 and 21 dpi in infected mice, when compared to uninfected controls (Fig. 2B; $P<0.05$).

### Extrahepatic bile duct lesion (S.I.)

Upon Reo-2 infection, inflammation developed in the extrahepatic septal bile ducts (Fig. 2C). We observed two events of epithelial destruction at 5 and 11 dpi. Infiltration of mononuclear cells and proliferation of epithelia began at 7 dpi and peaked at 12 dpi. Those lesions persisted to 21 dpi, but inflammation reduced.

### Production of IFN-γ and TGF-β1 in serum, and mRNA expression of IFN-γ, IL-4 and IL-17A in splenocytes

At 5 and 12 dpi, the infected mice had significantly increased serum IFN-γ values, and no production of IL-4 and IL-17A, whereas there was no production of any of these three cytokines in the control mice (Fig. 2D). TGF-β1 levels decreased in the infected mice compared with the control mice. Increased IFN-γ mRNA expression was detected in splenocytes in the infected mice at 10 dpi (Fig. 2E). There was no mRNAs expression of IL-4 and IL-17 in both groups (Fig. 2E).

### Production of autoantibodies against cholangiocytes

Autoantibodies against cholangiocyte-specific nuclear and cytoplasmic factors were detected in sera of the infected mice. Specifically, autoantibodies were detected at 12 dpi (Fig. 2F). The titer of cholangiocyte-specific anti-cytoplasmic antibodies was higher than that of anti-nuclear antibodies.

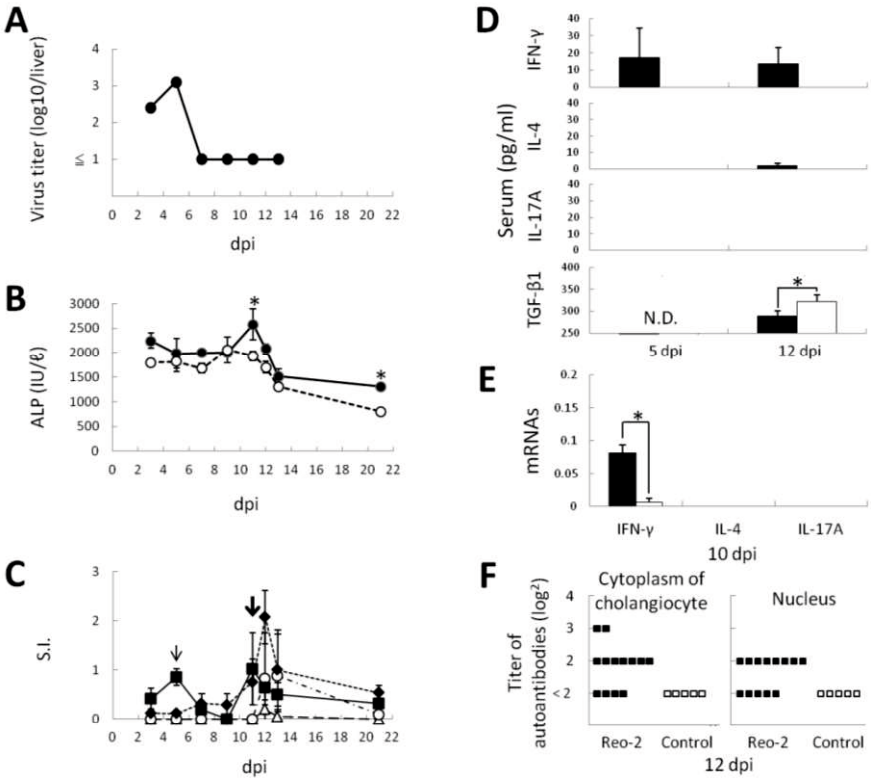


**Fig. 2**: Virus titer in livers (**A**, black circles: Reo-2 infected); ALP values in sera (**B**; black circles: Reo-2 infected and white circles: control); S.I. (**C**; black squares: bile ductal damage; black rhombuses: inflammation; white circles: proliferation of biliary epithelium; white triangles: fibrosis in extrahepatic septal ducts; and thin and bold arrows: peaks of epithelial destruction at 5 and 11 dpi, respectively); values in serum (**D**) or mRNAs expression from splenocytes of IFN-γ, IL-4, TGF-β1 and/or IL-17A (**E**); and titer of autoantibodies against cytoplasm of cholangiocytes (ductal epithelium) in liver and nucleus of hepatocytes (**F**) (black squares: Reo-2 infected and white squares: control). Data are presented as mean ± SEM except for **C** (mean ± SD). **P*<0.05, compared with control. dpi: days post infection; N.D.: not done.

## Nonsuppurative inflammation after Reo-2 clearance in intra and extrahepatic bile ducts

Extramedullary hematopoiesis (EMH) containing erythrocytes and leukocytes was observed in the intrahepatic portal and parenchymal tissue of infected and control mice at 3-12 dpi. Although limited EMH was observed in extrahepatic bile ducts, it decreased gradually from 13 to 21 dpi. Minor lesions formed in the interlobular ducts and large bile ducts. These lesions were less severe than those of the extrahepatic septal ducts. In addition, several focal necroses formed in the parenchyma at 3 and 5 dpi but were no longer detectable after 5 dpi.

At 3 and 5 dpi, some cholangiocytes and inflammatory cells were necrotic and apoptotic (data no shown). They were also structurally irregular and were located in slightly damaged ducts (Fig. 3A). Notably, viral antigens were detected in these cholangiocytes and hepatocytes (Fig. 3B). Accordingly, slight-to-mild infiltration of mononuclear cells was detected at 7-9 dpi (Fig. 3C). At this stage, viral antigens were no longer detectable in the extrahepatic bile ducts or in the hepatic lesions. At 11-13 dpi, slight-to-severe infiltration of mononuclear cells and damage to the epithelia (Fig. 3D) were observed. This was followed by the formation of necrotic and apoptotic cells (Fig. 3E). There were slight-to-severe stenosis, bile ductal loss or ductopenia with mild fibrosis (Fig. 3F). At this phase proliferation of bile ductules was recognized (Fig. 3G). At 21 dpi, bile duct obstruction with a slight fibrosis around ducts was seen (Fig. 3H).

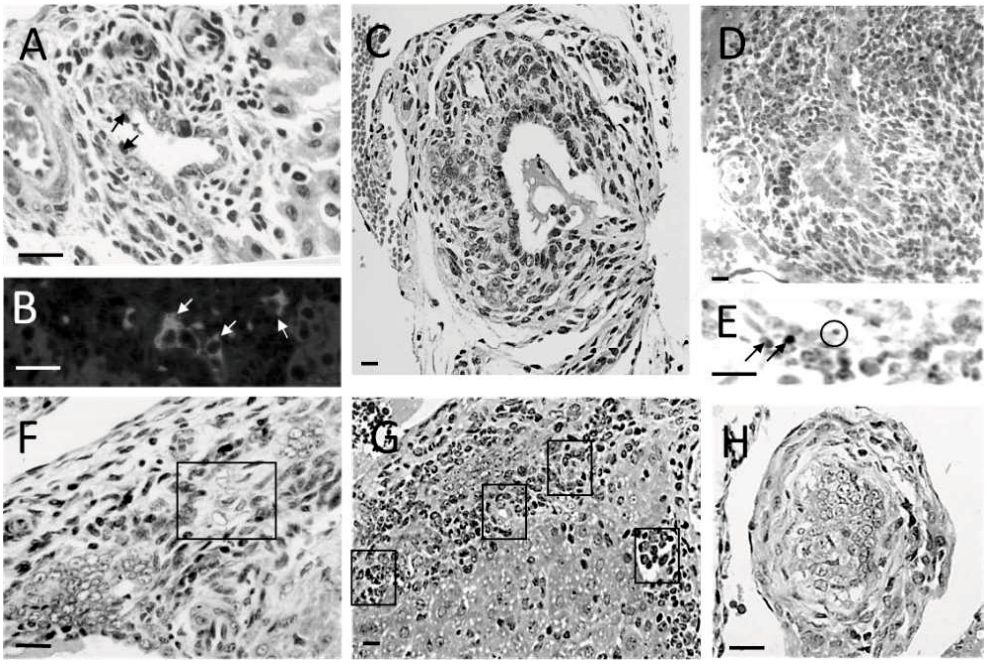


**Fig. 3.** Histology of the cholangiocytes in the septal bile duct and bile ductule. Shrunken cholangiocytes with pyknotic nuclei (arrows: suggestive of apoptosis), degeneration of epithelial cells with few inflammatory cells, and EMH are visible (**A**). Viral antigens in cholangiocytes (arrows) are detected at 5 dpi (**B**). Irregular shaped ducts with partial destruction of cholangiocytes and infiltrating mononuclear cells (lymphocytes and macrophages) around bile ducts at 7 dpi are shown (**C**). The cholangiocytes show swelling and disordered polarity induced by severe infiltration of mononuclear cells, leading to stenosis and destruction of bile ducts at 12 dpi (**D**). In those lesions, apoptosis of cholangiocytes (arrows) and some infiltrating lymphocytes (a circle in **E**) can be seen. Moreover, ductopenia due to fibrosis (a rectangle in **F** indicate the process of loss of bile ducts) including proliferation of bile ductules (rectangles in **G**) are visible. Obstruction of bile ducts with proliferated and degenerated cholangiocytes by slight fibrosis (onion skin appearance) is seen at 21 dpi (**H**). **A**, **C**, **F**, **G**, **H**: HE; **B**: IF; **D**: TB (semi-thin section); and **E**: TUNEL. **A**, **B**, **E**: x950; **C**, **D**, **G**: x350; and **F**, **H**: x750 (original magnification). Bar=50 μm.

## Ultrastructure changes of extrahepatic bile ducts

At 12 dpi, no virus particles were observed in septal bile ducts. Bile ducts were relatively intact in case of lacking of inflammatory cell infiltration into epithelial layers despite irregular structure and damage of basement membranes (Fig. 4A). Epithelia

were infiltrated with macrophages and small- to mid-sized lymphocytes, containing little cytoplasm and few organelles (Fig. 4B, C). Thereafter, those leukocytes had fully infiltrated the epithelium and were docked on cholangiocytes (Fig. 4D). At this stage, cholangiocytes were highly apoptotic and necrotic (Fig. 4E). Moreover, macrophage-engulfed apoptotic lymphocytes and abnormal basement membrane structure (e.g., discontinuous, irregular or lytic) were routinely detected. In addition, dendritic cells (DCs) having fewer phagocytic vacuoles, lysosomes, phagosomes and phagolysosomes were recognized in the inflamed epithelial layers.

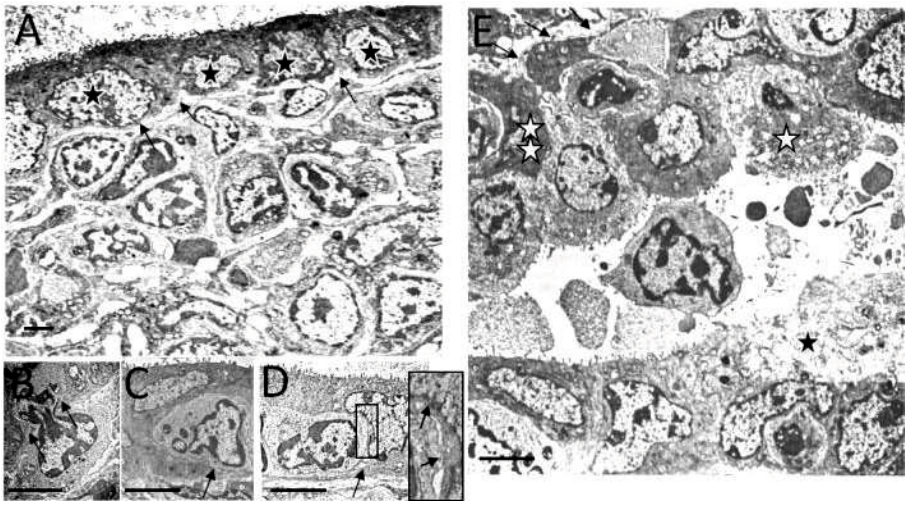


**Fig. 4**: Ultrastructure of the cholangiocytes in septal bile ducts. Cholangiocytes (black stars) are relatively intact due to a lack of lymphocyte and macrophage invasion (**A**). Intraepithelial migration (**B**) and infiltration of lymphocytes are visible (**C**). Attachment of lymphocytes to cholangiocytes and intrusion of cytoplasmic process of lymphocytes into cholangiocytes (**D**, and arrows in insert: enlargement of rectangle in **D**) lead to degeneration (a black star) and apoptosis (a white star) of cholangiocytes (**E**). Among them, dendritic cells (double white stars) can be seen. Long arrows of **A**-**D** indicate basement membranes. **A**: x4,000; **B**-**E**: x7,500; and insert of **D**: x14,000 (original magnification). 12 dpi. Bar=5 µm.

## Detection of autoantigens, and protein expression in cholangiocytes and infiltrated mononuclear cells

Sera from the infected mice recognized cytoplasm of cholangiocyte but not that of hepatocytes, pancreatic duct cells, and acinar cells (Fig. 5A). Moreover, sera from the infected mice recognized nuclear factors of cholangiocyte, hepatocytes, acinar cells, and pancreatic ductal cells (Fig. 5B). At the inflamed site, MHC-class I antigens were strongly expressed on cholangiocytes (Fig. 5C) and weakly expressed on mononuclear cells. Infiltrated mononuclear cells consisted of macrophages (Fig. 5D) and lymphocytes that were $CD3^+$ (Fig. 5E), IFN-$\gamma^+$ (Fig. 5F), $CD4^+$ or $CD8^+$. $FAS^+$ cholangiocytes were strongly associated with $FASL^+$ infiltrating mononuclear cells (Fig. 5G). Moreover, weak expression of $FAS^+$ lymphocytes and moderate expression of $FASL^+$ cholangiocytes were observed (Fig. 5H). Moreover, TNF-$\alpha^+$ mononuclear cells were strongly associated with ducts. The degrees of expression of these antigens and cytokines in cholangiocytes and inflammatory cells at 12 dpi were summarized in Table 1.

**Table 1.** Degree of expression of antigens and cytokines (molecule) in and/or on cholangiocytes and mononuclear cells

| Molecule | Cholangiocyte | Lymphocyte | Macrophage |
|---|---|---|---|
| MHC class I | +++ | + | + |
| CD3 | - | +++ | - |
| IFN-γ | - | +++ | - |
| CD4 | - | +++ | - |
| CD8 | - | +++ | - |
| FAS | +++ | + | - |
| FASL | ++ | + | - |
| TNF-α | - | +++ | +++ |

-: no; +: weak; ++: moderate; +++: intense.

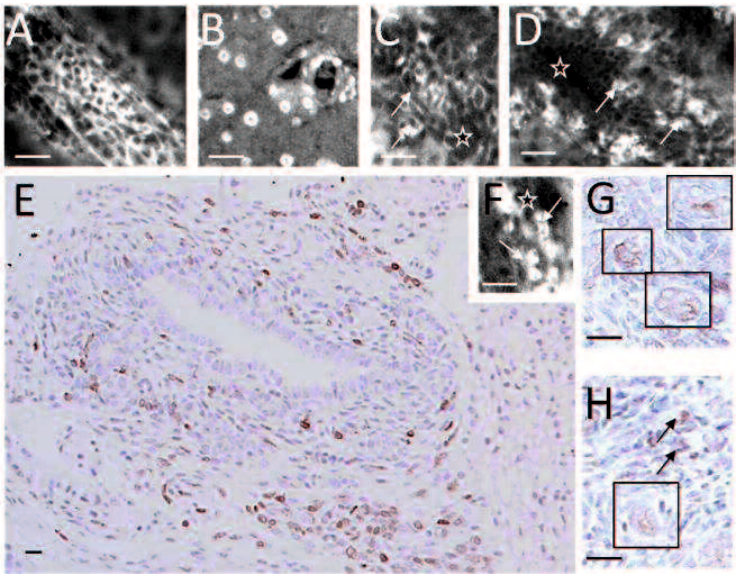


**Fig. 5**: Reactivity of autoantibodies (**A**, **B**) to normal cells, and expression of proteins in cholangiocyte and infiltrated cells (**C**-**H**). High titers of sera from infected mice, which do not react with nucleus at this dilution, recognized cytoplasmic antigens of cholangiocyte but not of hepatocytes in uninfected mice (**A**). Low titers of sera from infected mice recognized nuclei of pancreatic ducts and acini, but not their cytoplasm, of uninfected mice (**B**). Intense MHC-class I expression on destructed cholangiocytes (arrows in **C**) in infected mice is associated with infiltration of macrophages (arrows in **D**), where $CD3^+$ (**E**) and IFN-$\gamma^+$ (arrows in **F**) lymphocytes are visible. Intense $FAS^+$ cholangiocytes (rectangles in **G**) with $FASL^+$ lymphocytes (arrows in **H**) and $FASL^+$ cholangiocytes (a rectangle in **H**) are seen. 12 dpi. **C**, **D**, **F** (the white star): bile ductal lumen. **A**-**D**, **F**: IF; **E**, **G**, **H**: IHC (positive cells: brown color, counterstained by Mayer's hematoxylin). **A**-**D**, **F**-**H**: x750; **e**: x350 (original magnification). Bar=50 μm.

### $Foxp3^+$ cells in bile duct lesions, regional lymph nodes and thymi

The number of $Foxp3^+$ cells in inflamed ductal lesions of the infected group (Fig. 6A) was similar to that of the control group (Fig. 6B). The number of $Foxp3^+$ cells decreased in regional lymph nodes at 5 dpi, but not at 10 dpi, and in thymi at 10 dpi, but not at 5 dpi, in the infected group (Fig. 6C-L).

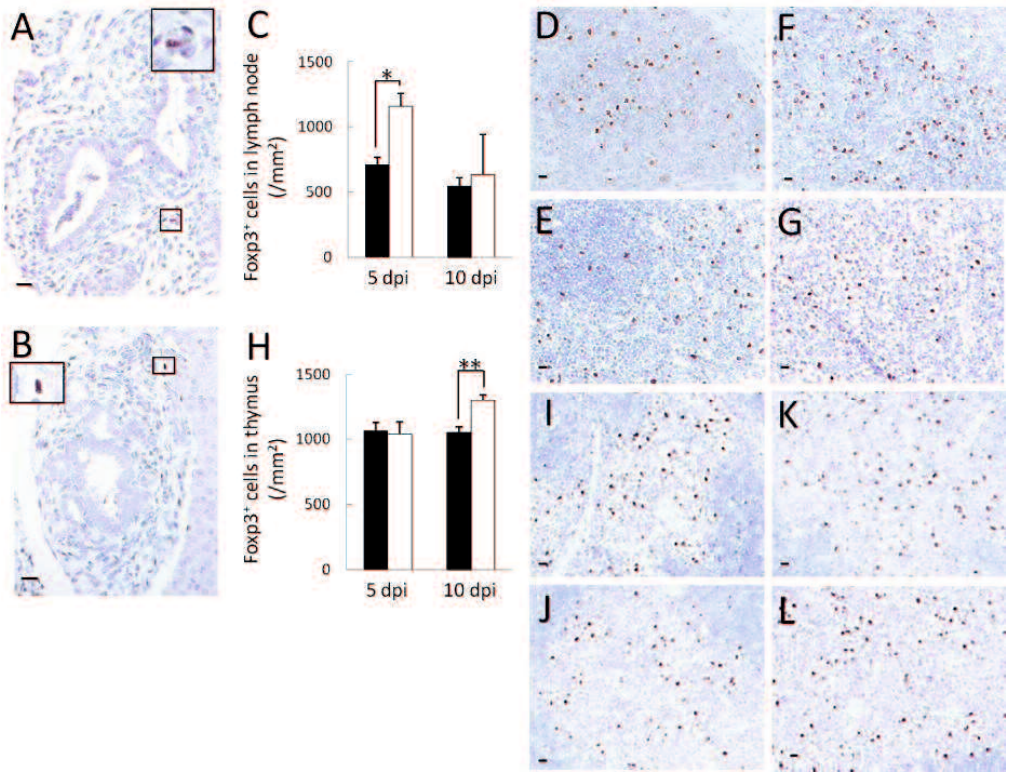


**Fig. 6**: Foxp3$^+$ cells in bile ducts (**A**, **B**), lymph nodes(**C**, **D**, **E**, **F**, **G**) and thymi (**H**, **I**, **J**, **K**, **L**). No increase of Foxp3$^+$ cells in bile ducts of the infected mice (**A** and enlargement of rectangle in **A**) compared with the control mice (**B** and enlargement of rectangles in **B**). Numbers of Foxp3$^+$ cells decreased in regional lymph nodes at 5 dpi, but not at 10 dpi, in the infected mice (**C**, **D**, **E**), compared with the control (**C**, **F**, **G**). Decreased numbers of Foxp3$^+$ cells in the infected mice at 10 dpi, but not at 5 dpi, in thymi (**H**, **I**, **J**), compared with the control (**H**, **K**, **L**). **A**, **B**, **D**-**G**, **I**-**L**: IHC (Foxp3$^+$ cells: brown color, counterstained by Mayer's hematoxylin). **D**,**E**,**I**, **J**: 5 dpi, and **F**, **G**, **K**, **L**: 10 dpi. **A**, **B**: x400; **D**-**G**, **I**-**L**: x200; inserts of **A**, **B**: x600 (original magnification). Bar=50 μm. **C**, **H** (the black columns: Reo-2 infected mice; the white columns: control mice), mean ± SEM. **P*<0.05, ***P*<0.01.

## Discussion

We demonstrated here Reo-2-mediated biliary destruction and propose two different mechanisms that may explain Reo-2-induced epithelial destruction. First, viral replication occurs shortly after infection (initiation phase), leading to duct destruction. Second, an autoimmune-mediated process (effector phase) develops in the destruction of duct.

During initiation phase, two types of duct destruction such as necrosis and apoptosis may be induced by Reo-2. Wilson *et al.* [1994] demonstrated that the Reo-3 *S1* gene is important for the determination of viral tropism in cholangiocytes. Attachment of reovirus to target cells is mediated through the filamentous, trimer reovirus signa1 protein, which is a serotype-independent receptor [Guglielmi *et al.* 2006]. Thus, the same mechanism may operate in Reo-2 infection, resulting in cell necrosis. Moreover, reovirus-induced apoptosis will be induced by the release of TNF-related apoptosis-inducing ligand (TRAIL) from infected cells and the activation of TRAIL-associated death receptors (DRs), DR4 and DR5, leading to apoptosis [Clarke & Tyler 2003]. It may operate in the present study, since apoptosis was observed.

The initial damage to cholangiocytes by Reo-2 may result in release of cholangiocytes-specific antigens, which facilitate immune responses during effector phase that ultimately exacerbate ductal damage. There are several possibilities supporting this idea as follows. There is specific autoantibodies production against the cytoplasm of cholangiocytes, suggesting that biliary duct destruction may be due to duct-specific immune-mediated mechanisms. Thus, induction of biliary pathology may occur still despite the absence of virus, underscoring a cholangiocyte antigen-mediated destruction pathway. The penetration of mononuclear cells into cholangiocytes

(epitheliotropism) is considered a key process for autoimmune-mediated destruction of biliary epithelium, which is typically followed by apoptosis and necrosis of epithelia [Nakamura *et al.* 2001]. $CD8^+$ T cells, which are responsible for apoptosis of the biliary epithelium [Shivakumar *et al.* 2007], respond to robust increases to MHC-coupled epithelial antigens. In addition, $FASL^+$ T cells respond to overexpressed FAS in ductal cells, which are caused by IFN-γ signaling from Th1 cells [Mack *et al.* 2005], leading to the destruction of biliary epithelia [Nakamura *et al.* 2001]. $FASL^+$ cholangiocytes suggest that the FASL upregulation may result in apoptotic fratricide of cholangiocytes other than $FASL^+$ lymphocytes injury to $FAS^+$ epithelia [Sokol & Mack 2001]. In addition, apoptosis of lymphocytes was often observed, which was likely associated with activated T-cell expression of FAS and FASL, since FASL is not normally expressed on cholangiocytes, but those cells of all biliary atresia patients expressed FASL [Sokol & Mack 2001].

Increase in systemic production of IFN-γ, including infiltration of $IFN\text{-}\gamma^+$ lymphocytes, suggest a Th1 response [Nakamura *et al.* 2001], which may result from a host response to cholangiocytes antigens. Moreover, higher IFN-γ mRNA expression from splenic cells was detected at effector phase than at viral multiplication phase in the same experimental protocol of our previous report [Onodera & Hayashi 2013]. Notably, these findings were associated with IFN-γ production in infants with biliary atresia. Bezzerra *et al.* [2002] discussed the recent support of the working hypothesis that pro-inflammatory signaling of lymphocytes is an important effector of epithelial injury in biliary atresia. Moreover, Orth *et al.* [2000] reported a marked increase in IFN-γ production in a cholangitis rat model and suggested that IFN-γ may facilitate secretion of pro-inflammatory cytokines by macrophages. Alternatively, a lack of IL-4 production

in Reo-2-infected mice may result from of mutually antagonistic effects by IFN-γ (one of representative Th1 cytokines) [Onodera & Hayashi 2013]. Moreover, production of reactive oxygen species from infiltrated macrophages may contribute to apoptosis and necrosis of cholangiocytes [Laskin & Pendino 1995].

Foxp3$^{+}$ Tregs produce immunosuppressive cytokines, such as TGF-β, IL-10 and IL-35, and maintain peripheral auto-tolerance [Sakaguch *et al.* 1996; Gravano & Vignali 2012]. Decreased TGF-β production may be, at least in part, due to decreased number of Tregs. Lack of inducible (i) Tregs (iTregs) in ductal lesions with less accumulation of iTregs in lymph nodes and naturally occurring (n) Tregs (nTregs) in thymi may permit the development of autoimmune cholangitis. Regarding nTregs in thymi, it has been recently shown that the transfer of i*n vitro*-generated nTregs, but not *in vitro*- generated iTregs, into Foxp3-deficient mice increase survival [Haribhai *et al.* 2011], suggesting there may be the functional difference between nTregs and iTregs. Alternatively, DCs were recognized in inflamed ducts. DCs, which are the professional antigen-presenting cells that present antigen to naïve T cells, may also play a role in suppressing of function of Tregs [Yamazaki *et al.* 2003; Cronin & Penninger 2007]. Further study is needed to clarify the interaction between Tregs and DCs in the development of autoimmune cholangitis.

Obstruction of bile ducts by fibrosis developed in weanling mice, but the disease was subclinical, and most mice recovered within three weeks after infection. This is different from human infantile biliary atresia with progressive biliary ductal lesions. However, immune-mediated damage of bile ducts may provide insights to the biliary pathology associated with human infantile biliary atresia. It has been proposed that biliary atresia may be the result of “a multiple-hit phenomenon”, which combine the

actions of several insult factors [Sokol & Mack 2001]. For example, macrophages release cytokines, especially TGF-β, that can stimulate hepatic stellate cells to synthesize and secrete collagen, resulting in the development of portal fibrosis and cirrhosis, which are detected in ductal lesions [Kisseleva & Brenner 2007]. In addition, it has been reported that bacterial components (e.g., intestinal lipopolysaccharides: LPS) may stimulate macrophages to produce enough TGF-β from those cells, resulting in induction of severe fibrosis [Bowen *et al.* 2013]. It seems likely, because biliary epithelial cells constantly express at least Toll-like receptor (TLR) 2-5 and can respond to the TLR ligands (LPS) derived from the duodenum [Harada *et al.* 2003]. In addition, it has been pointed out that IL-17A promotes the development of several autoimmune diseases as one of the factors [Stockinger & Veldhoen 2007]. However, production of IL-17A was not observed in infected mice. Taken together, these may be reasons why infected mice did not harbor persistent biliary lesions.

Reo-2 infection also causes autoimmune insulitis with IGT by targeting glutamic acid decarboxylase (GAD) (our unpublished observation). One might expect that Reo-2-induced cholangitis may be non-organ-specific process. However, similar outcomes were reported in rotavirus-induced biliary atresia. In these cases, the appearance of diabetes-associated autoantibodies against GAD and IA-2 indicated that β cell cells were targeted, instead of ductal cells [Honeyman *et al.* 2000].

In conclusion, Reo-2 infection in mice confers many similar outcomes to the human infections, with the notable exception that fibrotic lesions are less severe in mice. Further work is required to confirm that environmental factors contribute to progressive biliary atresia or whether the Reo-2 virus can trigger infantile biliary atresia in humans.

## Summary

Reovirus is a proposed cause of infantile biliary atresia. However, mechanistic insight regarding Reo-2 as a potential cholangiotropic virus is lacking. Furthermore, it is unknown whether Reo-2 infection can induce autoimmune-mediated bile duct injury. Lesions of bile ducts in newborn DBA/1J mice infected with Reo-2 were analyzed immunopathologically. Damage to biliary epithelia occurs after Reo-2 infection. In addition, nonsuppurative cholangitis with fibrosis in extrahepatic (especially septal) bile ducts developed following complete viral clearance from the liver. At the inflamed ducts, major histocompatibility complex class I expressing$^{(+)}$ and FAS$^{+}$ cholangiocytes were associated with FAS ligand$^{+}$ lymphocytes and tumor necrosis factor-α$^{+}$ mononuclear cells (macrophages and lymphocytes). These cholangiocytes were apoptotic and necrotic. Moreover, affected ducts were infiltrated by CD3$^{+}$, CD4$^{+}$, CD8$^{+}$, IFN-γ$^{+}$ and FAS$^{+}$ lymphocytes. Analysis of blood from Reo-2 infected mice revealed that they developed anti-cholangiocyte cytoplasm antibodies and had high serum IFN-γ concentration. Notably, there was no increase in Foxp3$^{+}$ lymphocytes at inflamed ducts, lymph nodes and thymi. Reo-2 infection induced T-helper cell type 1-dependent injury to bile ducts in weanling mice. The lesions observed in mice may be analogous to those associated with human infantile biliary atresia, which are caused by an autoimmune-mediated process.

# 4. Chapter 3.

## Reovirus type-2 infection in newborn DBA/1J mice reduces the development of late allergic asthma

## Introduction

There are several factors, including genetic predispositions and environmental factors, which affect the development of allergic airway inflammation. Airway allergy in human and animal models is mediated by Th 2 immune response to inhaled environmental allergens in sensitized individuals. This involves a two-phase allergic reaction: early and/or late phases [Skad *et al.* 1999; Hayashi 2011, 2012a]. In the early phase, IgE-sensitized mast cells degranulate and release mediators such as histamine and leukotriene, whereas the late phase of the allergic response mainly involves infiltration of eosinophils and Th2 type lymphocytes producing IL-4, IL-5 and IL-13 including IL-17 [Cosmi *et al.* 2011] and TNF-α [Babu *et al.* 2011] without participation of mast cells and IgE.

It has been hypothesized that the increased prevalence of allergic diseases in developed countries may be associated with the decline in some infections shifting the relative predominance between Th2 and Th1 responses [Strachan 1989; Von Hertzen & Haahtela 2004]. In addition, the lower prevalence of asthma, hay fever and eczema symptoms in autoimmune diseases such as type 1 diabetes (T1D) patients compared with age-matched controls has been reported [Meerwaldt *et al.* 2002], whereas pre-existing asthma seems to protect against the development of autoimmune disorders to varying degrees in men and women [Tirosh *et al.* 2006]. This suggests that these may be induction of mutual Th1/Th2 inhibitory effects [Mossmann & Coffman 1989].

Reovirus (Reo; serotypes 1, 2 and 3) is an RNA virus classified in the *Reoviridae* and included in the genus *Orthoreovirus*. All mammals serve as hosts for Reo infection, but disease is limited to very young people and manifests as a mild gastroenteritis [Onodera *et al.* 1990; Tyler *et al.* 1995; Danthi *et al.* 2006]. However, Reo-2 can induce transient

impaired glucose tolerance with mild insulitis peaked at approximately 10 days after infection. In this model the virus was inoculated into one day old newborn genetically autoimmune sensitive DBA/1J mice ($H2^q$ haplotype: first chromosome *VAS1* gene is responsible for autoimmunity [Holmdahl *et al.* 1990]). Most mice recovered from the disease within three weeks after infection [Onodera *et al.* 1990; Hayashi *et al.* 1998, 2001]. This may be due to the fact that a sufficient number of β cells are left intact after the destruction, and proliferation accompanied by disappearance of infiltrated cells may occur [Onodera *et al.* 1990].

We have reported previously that Reo-2 infection can induce transient expression of IFN-γ mRNA, but not IL-4 mRNA, from splenic cells shortly after the infection and during the developmental phase of insulitis when there has been elimination of virus from the mice [Hayashi *et al.* 1998, 2001]. This suggests that infected mice may develop two different types of Th1 responses. In the virus multiplication phase, it has been reported that reoviruses induce high IFN-α/β [Steele & Hauser 2005; Errington *et al.* 2008]. Also Toll-like receptor-3 on dendritic cells stimulated with reoviruses may induce IFN-α/β, leading to Th1 responses [Errington *et al.* 2008]. Later, in addition, Th1 cells will be induced as a consequence of the development of autoimmune insulitis [Hayashi *et al.* 1998, 2001].

At present the cumulative effects of virus infection and the following autoimmune T1D on the development of airway allergy are not known. To clarify this point, the effects of Reo-2 infection on the development of late allergic asthma were examined during the recovery phase of Reo-2-triggered insulitis.

## Materials and methods

### Animals

One-day-old DBA/1J newborn mice of either sex (Japan Charles River Co.) were used (total number used, *n*=58) as described previously [Hayashi *et al.* 1998, 2001]. They were kept at 25 ± 2 °C room temperature, 55 ± 10% humidity, and at 12-h light/dark cycle (lightening time 08:00-20:00) in metal cages sterilized by dry heating (180 °C, 30 min), and animals were given autoclaved (120 °C, 30 min) pellets (CA-1, CLEA Japan) and water freely. The number of mice used in each experimental group is given in parenthesis of experimental protocol. The animal experiments were approved by the Research Ethics Board of the Faculty of the Agriculture, Yamaguchi University.

### Virus

The BN-77 strain of Reo-2 was isolated from a cow with diarrhoea and passaged several times in primary bovine kidney cell culture [Kurogi *et al.* 1980], and grown on the HmLu-1 (Hamster lung fibroblast recloned in our laboratory) cell line as described previously [Onodera *et al.* 1990; Hayashi *et al.* 1998, 2001].

### Experimental protocols and sampling

As shown in Fig. 1, mice were divided into four groups as follows: Reo-2- infected mice were sensitized and challenged with ovalbumin (OVA) (group 1; *n*=12), uninfected-mice were sensitized and challenged with OVA (group 2; *n*=11), Reo-2-infected mice were not sensitized and challenged with OVA (group 3, *n*=10), and uninfected mice were neither sensitized nor challenged with OVA (group 4, *n*=9). One day old mice (body weight: approximately 1 g) were infected i.p. with $5.5 \times 10^5$ pfu. of Reo-2 in 0.05 ml of Eagle's MEM (Nissui) on what was designated 'day -28' (groups 1 and 3). The sensitization and challenge procedures were performed by the methods

described previously [Hayashi *et al.* 2003a]. Mice (groups 1 and 2) were sensitized i.p. with 10 µg of OVA (Grade V; Sigma-Aldrich Co.) in 1.2 mg aluminum hydroxide gel (Alum; SERVA) adjuvant (OVA/Alum), which was suspended in phosphate-buffered saline (PBS; pH 7.4), on day 0 and boosted on day 10. Four days after the second sensitization, the mice were challenged i.n. with 200 µg of OVA in 50 µl of PBS (both right and left nasal cavities by a micropipette alternately) under anesthesia by injection with 0.5 ml mixture of ketamin and xylazine i.p. Control groups (groups 2-4) were administration with PBS instead of either OVA or Reo-2. Four days after the challenge, blood, left lungs, pancreases and spleens were obtained from all groups. Pancreases were also sampled on day -18 to examine the presence of insulitis.

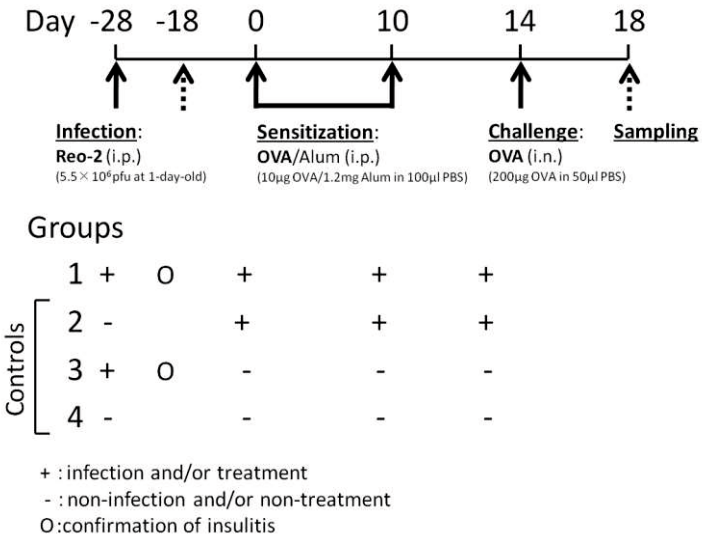


Fig. 1: Experimental protocol in Reo-2 infection and induction of late allergic asthma.

## Leukocyte number in blood

The absolute number of leukocytes/µl was counted on day 0 and 18 (*n*=8-14 in each group). The percentage of eosinophils, neutrophils, lymphocytes and monocytes was calculated from a blood smear stained with May-Grünwald-Giemsa and the total

number of each leukocyte was determined.

### Histological evaluation of pancreas

Pancreatic tissues on day -18 and on day 18 (*n*=4 in each group) were fixed in 10% of neutral-buffered formalin (pH 7.0) and embedded in paraffin wax. Sections 4 µm-thickness were stained with haematoxylin and eosin (H&E). For each mouse, the incidence (%) of insulitis (inflammatory cell infiltration into pancreatic islets) including peri-insulitis in the islets was evaluated, and an 'islet score index' was calculated by a method described previously [Hayashi *et al.* 1998]. The severity of the cellular infiltration was evaluated by light microscopy, and an insulitis score was given to each islet on a 0-4 scale (0 = no insulitis or peri-insulitis; 1 = insulitis < 25% of islet area; 2 = insulitis 25-50% of islet area; 3 = insulitis > 50% of islet area). The grade of insulitis/mouse was expressed as the average score [S.I. = total score/number of islets]. An average of 10 different pancreatic islets was examined.

### Histological evaluation of lung lesion

Left lung samples were fixed in 10% of neutral-buffered formalin (pH 7.0), and embedded in paraffin wax (*n*=8-12 in each group). Sections of 4 µm-thickness were stained with H&E, Periodic Acid Schiff's (PAS), alcian blue (pH 2.5) for goblet cells and/or connective tissue type mast cell, and methylen blue for mucosal type mast cell [Bui *et al.* 2010]. The severity of lesions in each transversely sectioned bronchus-bronchiole was evaluated by light microscopy and scored as follows [Hayashi *et al.* 2003a]: no lesions, 0; mucus or desquamated epithelial cells in the lumen, 1; a few goblet cells in the epithelial layer, 1; many such cells, 2; thickened basement membrane, 1; mild infiltration of eosinophils and lymphocytes in mucosa, 1; severe infiltration of those cells in the mucosa, 2; hypertrophy of smooth muscle cells in mucosa, 1. In each mouse, the S.I.

was calculated by dividing the total number of bronchi-bronchioles examined. The average of S.I. was then determined for each group. The number of eosinophils, lymphocytes, macrophages, plasma cells and mast cells in the bronchial-bronchiolar mucosa was determined by eyepiece micrometer on five different bronchi-bronchioles at random in each left lung. Each result was averaged and totaled in each mouse, and thereafter the mean ± SEM of each experiment was calculated.

IHC

Deparaffinized sections of lung from all groups (*n*=5 in each group) were treated with microwave oven (500 W for five min) in 10 mM citrate buffer (pH 6.0). Endogenous peroxidase activity was inactivated in 3% hydrogen peroxide in methanol for 10 min. Sections were treated with 5% bovine serum albumin (BSA; Sigma-Aldrich) in PBS and normal goat serum for 30 min to block non-specific binding of antibody. Additionally, sections were treated with avidin/biotin blocking kit (Vector Laboratories, Burlingame, CA, USA). Sections were treated with primary antibodies as follows: rat anti-mouse IL-4 mAb (Pharmingen, San Diego, CA, USA) diluted in 1/10; rat anti-mouse IL-5 mAb (Southern Biotechnology, Birmingham, AL, USA) diluted in 1/10; goat anti-mouse IL-13 pAb (R&D system, Inc., Minneapolis, MN,USA) diluted in 1/20; rat anti-mouse IFN-γ mAb (Upstate Biotechnology) diluted in 1/20; rat anti-mouse VLA-4 mAb (Antigenix, Franklin Square, NY, USA) diluted in 1/5; rat anti-mouse VCAM-1 mAb (Antigenix, Huntington Station, NY, USA) diluted in 1/5 and goat anti-eotaxin-2 pAb (Santa Cruz Biotechnology Inc.) diluted in 1/50. Thereafter, sections were treated with secondary antibodies, biotinylated rabbit anti-rat IgG (Vector Laboratories) or biotinylated rabbit anti-goat IgG (DakoCytomation, Carpinteria, CA, USA) depending on the immunized animals of primary antibodies for one h. Sections were treated with

peroxidase-labeled streptavidin (Invitrogen Co., Camarillo, CA, USA) for 10 min and incubated with 3,3-diaminobenzidine substrate (Roch Diagnostic) for 10 min. Sections were counterstained with methyl green for 5 min. Incubations were done at room temperature except for primary antibodies (4 °C), and sections were washed three times with PBS between each step. The reaction without primary antibody served as negative control.

### Isolation of splenocytes

Spleens (*n*=5 in each group) were removed aseptically and placed in PBBS (pH 7.4). Single cell suspensions were made by teasing spleens apart with scissors and passing through a disposable syringe with a 21G needle (Terumo Co.). Cell suspensions were collected in sterile conical tubes (Fisher Sci.), and thereafter, red blood cells were hemolysed by Tris-buffered $NH_4Cl$ solution, and the splenocytes were washed in PBBS followed by centrifugation at 800 *g* for 10 min at 4 °C. The total number of splenic cells was counted using a hemocytometer and diluted in MEM with kanamycin (100 μg/ml) to a density of $1x10^6$ cells/ml. Viability of cells was more than 98% by trypan blue dye exclusion test. Splenocytes ($2x10^5$/200 μl MEM with 5% heat-inactivated fetal calf serum (Gibco) were cultured for 48 h at 37 °C in 5% $CO_2$ in the presence of 5.5 μg/ml of concanavalin A (Con A; ICN Biomedical Inc.) in 96 well-plates (Coster) and supernatants were obtained and stored at -80 °C until use.

### IL-4, IL-5 and IFN-γ in supernatants from cultured splenic cells, and OVA-specific IgE, TNF-α and IFN-α in plasma by ELISA

Concentrations of IL-4 (Bender MedSystems GmbH), IL-5 (R&D system, Inc.) and IFN-γ (Bender MedSystems GmbH) in supernatants from cultured splenocytes, and values for OVA-specific IgE (DS pharmacia Biomedical Co., Ltd) ,TNF-α (R&D system, Inc.)

and IFN-α (PBL Interferon Source, Piscataway, NJ, USA) in plasma were measured by mouse ELISA kits according to the manufacturer's instructions. Detectable amounts of IL-4, IL-5 IFN-γ, OVA-specific IgE, TNF-α and IFN-α are 2.0 pg/ml, 3.3 pg/ml, 5.3 pg/ml, 2.7 ng/ml, 5.1 pg/ml or 12.5 pg/ml respectively. In case of cytokines could not be detected, their concentration was estimated as 0.

### Statistical analysis

The means ± SEM were calculated and analyzed by one-way ANOVA test and then by Student's *t*-test (two-tailed). The accepted level of significance was $P<0.05$. The data are expressed as the mean of sample examined mice ± SEM.

## Results

### Number of leukocytes in blood

As shown in Fig. 2, on day 18, but not on day 0, there was a significant increase in the number of total leukocytes (**A**), eosinophils (**B**), lymphocytes (**C**) and monocytes (**E**) ($P<0.05$ or $P<0.01$) in group 2 compared with the other three groups. Although the number of neutrophils (**D**) in the groups 1 and 2 increased compared with the groups 3 and 4 ($P<0.01$), there was no significant difference in the number of neutrophils between the group 1 and the group 2.

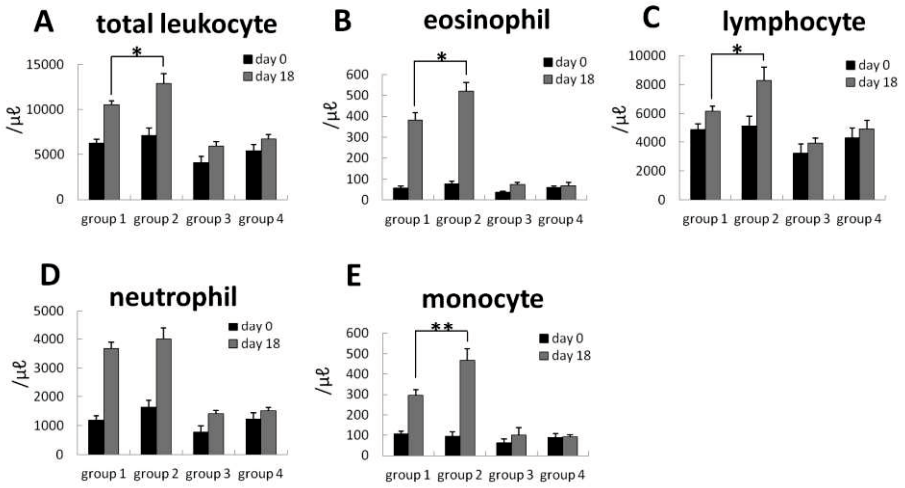


Fig. 2: Number of each leukocyte (A-E) in blood (/μl) in each group on days 0 and 18. Each value represents the mean ± SEM. **P*<0.05, ***P*<0.01.

## Pancreatic islet lesions

As shown in Fig. 3, there was mild cellular infiltration in and/or around pancreatic islets showing cell destruction, although those changes varied among islets and mice 10 days after Reo-2 infection on day -18 in the groups 1 and 3. Some animals developed severe insulitis (A and B). Reacting cells consisted of mostly lymphocytes mixed with some neutrophils, eosinophils, macrophages and plasma cells. Cellular infiltration with edema and hyperaemia in the interstitial connective tissue, and necrosis of some exocrine pancreatic tissues were also seen. S.I. and % were 1.03 and 63.3% in the group 1 and those were 1.00 and 53.4% in the group 3, 10 days after infection (on day -18), whereas those were not seen in both groups on day 18 (C and D). On the other hand, there was no insulitis in the groups 2 and 4 (E and F) on day -18 and on day 18 (data not shown).

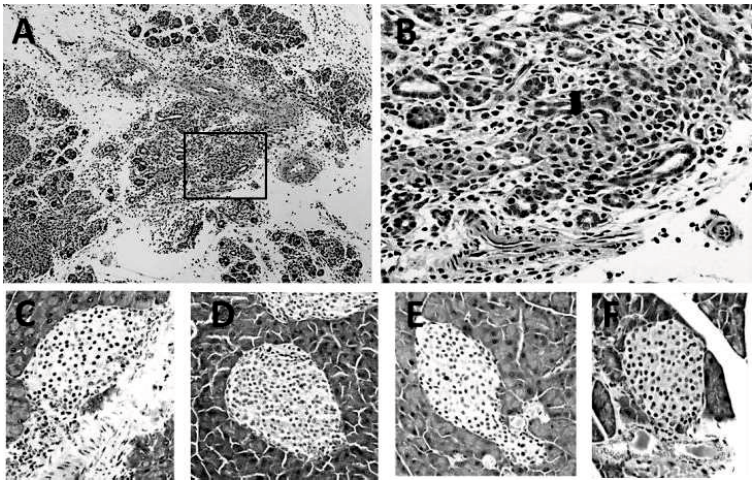


Fig. 3: Histopathology of pancreases. On day -18, severe cellular infiltration in and around pancreatic islets (rectangle in A, and an arrow in B, which is enlargement of rectangle of A, indicates one islet) with edema in the interstitial connective tissue is shown in the group 1. On day 18, pancreases including islets showing normal appearance and there are no infiltration of inflammatory cells at pancreatic islets in the groups 1 (C) and 3 (D). There is no insulitis in the groups 2 (E) and 4 (F) on day 18. A-F: H&E. A: ×100, B: ×400, C-F: ×200.

## Bronchial-bronchiolar lesions

As shown in Fig. 4, bronchial-bronchiolar lesions in the group 1 were less severe (A and B) compared with the group 2 (C and D). In the group 2 there was goblet cell metaplasia and/or hyperplasia with mucous hypersecretion (F), whereas those changes were minor in the group 1 in general (E). There was severe infiltration of lymphocytes and eosinophils with degranulation, and the mucous membrane was edematous in the inflamed bronchi-bronchioles. In those lesions, destroyed and desquamated epithelial cells in the bronchial-bronchiolar lumen and hypertrophic smooth muscle cells were observed in some cases (D) in the group 2.

A number of infiltrating eosinophils and lymphocytes were identified in and/or around blood vessels in the groups 1 and 2. There were a few mucosal type, but not connective tissue type, mast cells in the bronchial wall in the group 1 (G) and in the group 2 (H). There were no bronchial-bronchiolar lesions with eosinophilic infiltration in the groups 3 and 4 (data not shown).

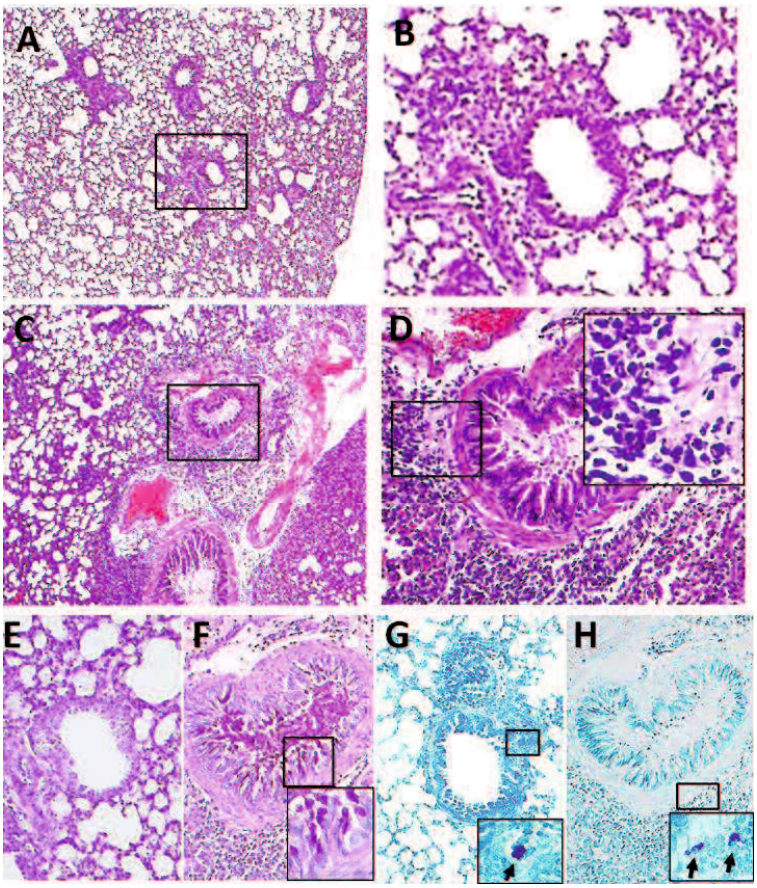


**Fig. 4**: Representative histopathology of bronchial-bronchiolar lesions is shown. Mild bronchitis-bronchiolitis with some eosinophils and lymphocytes is visible (**A**, and **B**; enlargement of rectangle in **A**). On the other hand, severe bronchiolitis with desquamated epithelial cells in bronchial lumen and hypertrophic smooth muscle cells are seen (**C**, and **D**; enlargement of rectangle in **C**). There are a few eosinophils and lymphocytes (**B**) and densely infiltrated those cells (**D**, and insert; enlargement of rectangle in **D**). Mucin production is not visible in the group 1 (**E**), whereas metaplasia and hyperplasia of goblet cell (insert; enlargement of rectangle in **F**) with mucous hypersecretion are observed in the group 2. A few mast cells are shown in **G** (an arrow in insert; enlargement of rectangle in **G**) and in **H** (arrows in insert; enlargement of rectangle in **H**). Group 1 (**A**, **B**, **E** and **G**), and group 2 (**C**, **D**, **F** and **H**). **A**-**D**: H&E; **E** and **F**: periodic acid-Schiff's (PAS); **G** and **H**: methylen blue. **A** and **C**: ×40; **B** and **D**-**H**: ×200; and inserts of **D** and **F**-**H**: ×400.

## S.I. (severity of lesions) of bronchial lesions and characterization of inflammatory cell

As shown in Fig. 5, the S.I. of bronchial-bronchiolar lesions in the group 2 increased (S.I.; 1.9 ± 0.5), whereas bronchial-bronchiolar lesions were mild in the group 1 (S.I.; 0.8 ± 0.1) ($P$<0.05) (**A**). There was a slight infiltration of lymphocytes, neutrophils and macrophages within the normal range in bronchial-bronchiolar lesions

in the groups 3 and 4.

The numbers of eosinophils, but not lymphocytes, infiltrating at the bronchi-bronchioles increased significantly in the group 2 compared with the group 1 ($P$<0.01) (**B**). There were no significant increase in the number of neutrophils, plasma cells, macrophages and mast cells in all groups.

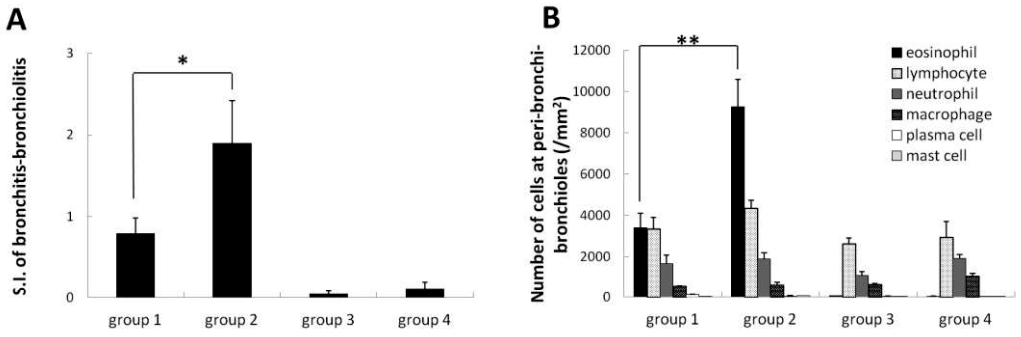


**Fig. 5**: S.I. of bronchial-bronchiolar lesions (**A**). Number of inflammatory cells at the site of bronchi-bronchioles (/mm$^2$) (**B**). Each value represents the mean ± SEM. *$P$<0.05, **$P$<0.01.

## IHC of bronchi-bronchioles

As shown in Fig. 6, a small number of IL-4$^+$ (**A**), IL-5$^+$ and IL-13$^+$ lymphocytes and some IFN-γ$^+$ lymphocytes were found at the bronchi-bronchiolar mucosa in the group 1. On the other hand, many IL-4$^+$ (**B**), IL-5$^+$ and IL-13$^+$ lymphocytes were observed at the bronchial-bronchiolar mucosa with some IFN-γ$^+$ lymphocytes in the group 2. Bronchial mucosal epithelium, endothelial cells and eosinophils in the bronchial-bronchiolar walls including pulmonary interstitial tissues strongly expressed eotaxin-2 (**E**) in the group 2. Those cells were fewer in number and weakly expressed eotaxin-2 in the group 1 (**D**). In addition, lymphocytes and eosinophils were positive for VLA-4 (**H**), and vascular endothelial cells were positive for VCAM-1 (**K**), but expression was weak (**G** and **J**) in the group1. There was no expression of IL-4, IL-5, IL-13, IFN-γ, VLA-4, VCAM-1 and

eotaxin-2 in lungs of the groups 3 (**C**, **F**, **I** and **L**) and 4 (data not shown).

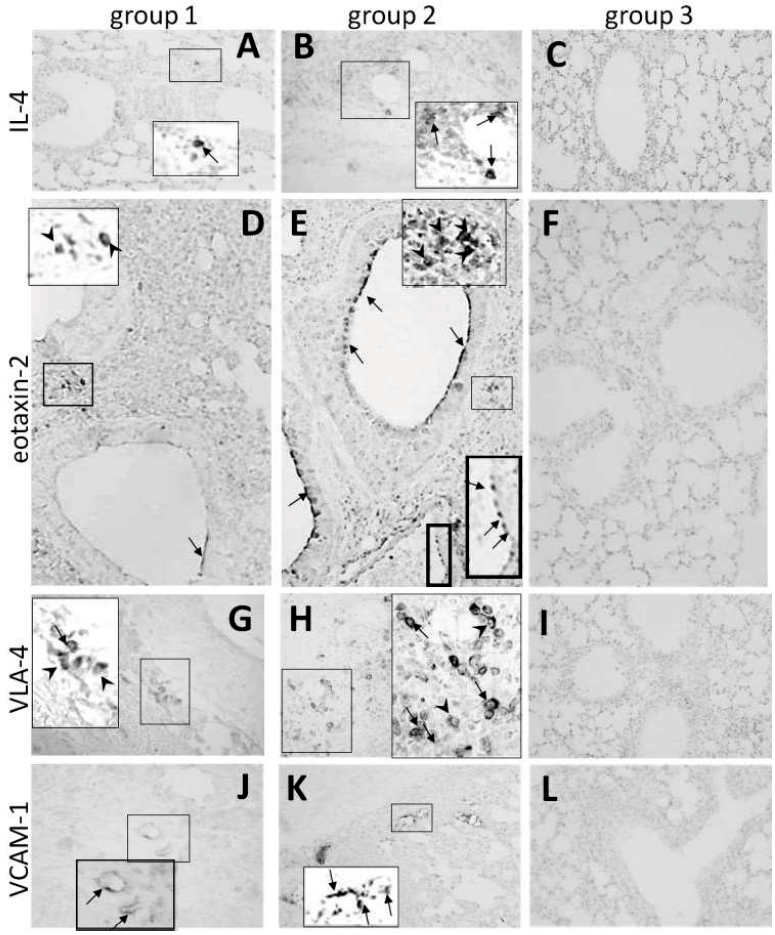


**Fig. 6**: IHC of bronchial-bronchiolar lesions. Arrows in inserts indicate IL-4$^+$ (enlargement of rectangle in **A** and **B**) lymphocytes. Arrowheads in insert (enlargement of thin rectangle in **D** and **E**) show eotaxin-2$^+$ eosinophils. Arrows in **E** indicate eotaxin-2$^+$ bronchial mucosal epithelium, and arrows in insert of **E** (enlargement of bold rectangle of **E**) show eotaxin-2$^+$ vascular endothelial cells. Arrow of insert in **G** and **H** (enlargement of rectangle in **G** and **H** respectively) show VLA-4$^+$ lymphocytes and arrowheads show eosinophils (rectangle in **G** and **H**). Arrows of insert (enlargement of rectangle in **J**) show weak expression of VCAM-1 on endothelium, whereas intense expression of VCAM-1 (arrows of rectangle in **K**) is visible. Groups 1 (**A**, **D**, **G** and **J**), 2 (**B**, **E**, **H** and **K**), and 3 (**C**, **F**, **I** and **L**). **A**-**C**: IL-4; **D**-**F**: eotaxin-2; **G**-**I**: VLA-4; **J**-**L**: VCAM-1. **A**-**L**: ×200; insert of **A**, **B**, **D**, **E**, **G**, **H**, **J** and **K**: ×400.

## Production of IL-4, IL-5 and IFN-γ in supernatants from cultured splenocytes stimulated with Con A including values of OVA-specific IgE, IFN-α and TNF-α in plasma

As shown in Fig. 7, IL-4 (**A**) and IL-5 (**B**) values in the group 1 decreased compared with the group 2 ($P$<0.05). In contrast, there was a marked increase in IFN-γ values in the group 1 (**C**) compared with the group 2. In addition, IFN-γ values in the control group 3 increased compared with the control group 4 ($P$<0.05), and there was no difference in IFN-γ values between the group 1 and the group 3 (**C**). In the groups 1 and 2 compared with the groups 3 and 4, OVA-specific IgE (**D**) and TNF-α (**E**) values increased. In addition, each value in the group 1 was significantly lower than that in the group 2 ($P$<0.05). There was no significant increase in IFN-α value in the group 1 compared with the controls (**F**).

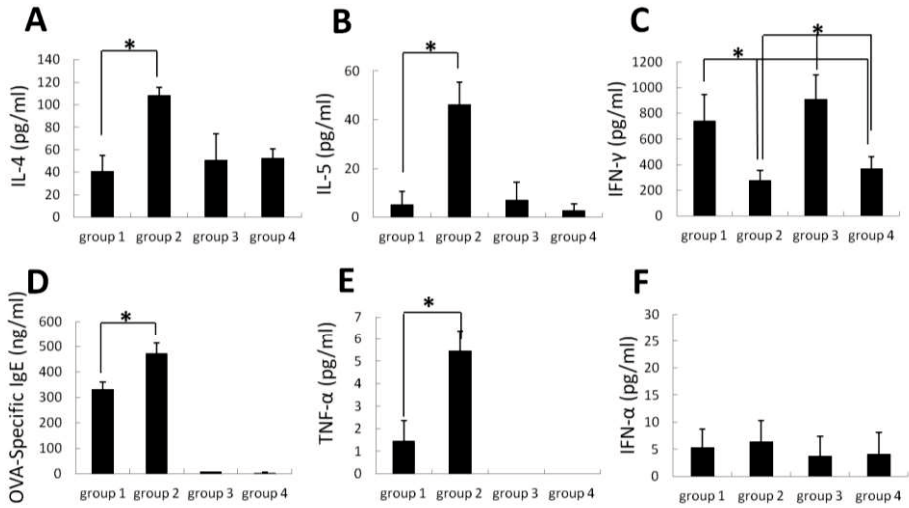


**Fig. 7**: Values of IL-4 (**A**), IL-5 (**B**) and IFN-γ (**C**) in supernatants of cultured splenic cells stimulated with Con A, and OVA-specific IgE (**D**), TNF-α (**E**) and IFN-α (**F**) in plasma. Note the significantly decreased IL-4, IL-5, OVA-specific IgE and TNF-α values, while IFN-γ values were increased (the group 1 *vs.* group 2, and the group 3 *vs.* the group 4 respectively). There was no increased IFN-α production in four groups. Each value represents the mean ± SEM. *$P$<0.05.

## Discussion

The present study demonstrated the reduction in the severity of Th2 type late allergic asthma, characterized by the infiltration of lymphocytes and eosinophils, in DBA/1J mice infected with Reo-2 at birth. It is possible that this is because systemic OVA-specific IgE, IL-4 and IL-5 values were low, whereas systemic IFN-γ values were high in the Reo-2 infected group (group 1) compared with the control groups. The mechanisms of the reduced late allergic asthma reaction with low eosinophilic reaction may be induced by mutual Th1/Th2 inhibitory effects [Mosmann & Coffman 1989]. Interestingly, high IFN-γ production from cultured splenic cells stimulated with Con A was observed not only in the group 1 but also in the group 3, suggesting that the existence of an antigen-unrelated memory pool of Th1 cells and/or increased Th1 dominant cell population among Th cells, including a balance shift from Th2 cells, to Th1 cells, may be induced in the Reo-2-infected group. Allergen non-specific suppressive effects by Th1 cells in Reo-2-infected mice seems likely, because treatment with environmental factors (such as bacterial DNA and certain olygodeoxynucleotides containing CpG motifs, a 6-base DNA motifs consisting of an unmethylated CpG dinucleotide flanked by two 5' purines and two 3'pyrimidines) can have stimulatory effects on dendritic cells via Toll-like receptors, resulting in production of IFN-α. This stimulates production of IFN-γ from Th1 cells, and thus Reo-2-infected mice develop more severe insulitis compared with that seen in Reo-2-infected mice that had only been treated with virus [Hayashi *et al.* 2002b]. Moreover, it has been shown that viruses can lead to activation of non-specific memory T cells [Seline *et al.* 1994]. Further study is needed to clarify this point. Alternatively Reo-2 infected mice with late asthma (group 1) which also develop Th1 responses, did not show increased IFN-α

production [Errington *et al.* 2008], compared with the controls. Thus the explanation for suppressive effects of Reo-2 infection on asthma, may not be related to IFN-α at the effector phase inducing increased may not be related to IFN-γ production directly.

Based upon the present immunological and immunohistochemical results, a possible explanation for the inhibitory effects of Reo-2 infection could be as follows. In the initiation phase, Th2 cell dominant reactions occur after interaction between antigen presenting cells and Th0 cells [Hayashi 2011, 2012a]. Thereafter, IL-5 production from OVA-sensitized Th2 cells interacting with OVA may induce eosinopoiesis in bone marrow [Durham *et al.* 1992], leading to blood eosinophilia in the effector phase. Alternatively, some studies on asthmatic patients have revealed an increased TNF-α production in bronchoalveolar lavage fluid [Keating *et al.* 1997; Yao T. *et al.* 2009]. TNF-α, which may be produced by Th2 cells being responsible for the development of airway allergy [Ito *et al.* 2005; Babu *et al.* 2011], may be reduced by Th1 cytokines especially IFN-γ. TNF-α and also Th2 cytokines (e.g. IL-4 and IL-13) are able to induce expression of adhesion molecules such as VCAM-1 on pulmonary vascular endothelium [Lassalle *et al.* 1993; Yamamoto *et al.* 1998; Wills-Karp & Karp 2004; Hayashi & Fujii 2008]. This may lead to attachment of lymphocytes and eosinophils expressing the β1-integrin VLA-4, a ligand for VCAM-1 [Okigami *et al.* 2007]. Eotaxin-2 may also play an important role in the accumulation of eosinophils and infiltration of those cells at the site of bronchi-bronchioles [Yao T. *et al.* 2009]. As demonstrated here in the group 2, pulmonary vascular endothelial cells and bronchi-bronchioles epithelial cells expressed eotaxin-2 intensely, which may be induced by IL-4 [Zimmermann *et al.* 2000] and IL-13 [Li *et al.* 1999], and eotaxin-2 may act as chemoattractants for eosinophils, but not for lymphocytes [Ponath et al. 1996]. Thereafter IL-4 from Th2 may activates again

eosinophils and lead to the production of eotaxin-2 and IL-13 from Th2 cells, leading to hyperplasia/metaplasia of goblet cells [Miyahara *et al.* 2006; Hayashi 2011, 2012a]. Finally, harmful substances (e.g. major basic protein, reactive oxygen species) from activated eosinophils may damage epithelial cells [Tagari *et al.* 1992; Honda & Chihara 1999]. This seems likely because degranulation of eosinophils was often observed. In these processes mast cells may not contribute to the development of lesions. These steps may be impaired by systemic, but not local, Reo-2 infection, leading to the reduction in the development of asthma.

It has been reported recently that Reo-1 that prohibited the development of allergy induced by peanut antigens in young mice [Fecek *et al.* 2010]. Similarly, Reo-2 infection during early life may ameliorate the development of asthma at a later age by dual effects of Th1 cells even after the stage of no viral footprints and the recovery from the disease (insulitis). Reoviruses are widely distributed in human (more than 60%) and in general reovirus is non-pathogenetic [Onodera *et al.* 1990; Selb & Webr 1994; Zurney *et al.* 2009]. However, whether these viruses play a similar role in human asthma remains to be established.

## Summary

The aim of the present study was to determine whether or not the development of a helper T (Th) 1 response induced by Reovirus type-2 (Reo-2) infection would protect against the development of Th2-mediated late allergic asthma. This hypothesis was examined by infecting one day old neonatal DBA/1J mice with Reo-2 in an ovalbumin (OVA)-induced late asthma model. Compared with the controls (either infected or uninfected mice with or without OVA sensitization and/or OVA challenge), Reo-2 infection lessened the magnitude of the subsequent allergic Th2-mediated late asthma. In infected mice with allergic late asthma, there was decreased infiltration of interleukin (IL)-$4^+$, IL-$5^+$, IL-$13^+$, and very late antigen (VLA)-$4^+$ lymphocytes, and eotaxin-$2^+$ and VLA-$4^+$ eosinophils, in both bronchial and bronchiolar lesions. Also the expression of vascular cell adhesion molecule (VCAM)-1 and eotaxin-2 on vascular endothelial cells was reduced. Moreover, the systemic production of IL-4, IL-5, tumor necrosis factor-α and OVA-specific IgE was reduced, whereas systemic IFN–γ production was increased. In addition, there was no increase in IFN-α production. Thus the present study suggests that systemic Reo-2 infection at birth may reduce the development of subsequent late allergic asthma by the induction of a Th1 response. Therefore the potential suppressive mechanism(s) that might be induced by Reo-2 infection in newborn mice and their effects on the development of late allergic asthma are discussed.

# 5. General conclusion

1) In this PhD thesis special attention is paid to underlying molecular mechanisms in the development of allergic asthma, biliary atresia and T1D by modulation of microbes from the point of view of a concept of Th1/Th2 balance shift. Also informative reports of other allergic diseases related with modulation by pathogens are included. Moreover, the mechanisms in the development of both autoimmune and allergic airway diseases related with the function of Tregs will be included [Sakaguchi *et al.* 1995, 1996, 2006; Kearley *et al.* 2005; Robinson 2009], since the hygiene hypothesis has been implicated in the increasing incidence of both disorders [Okada *et al*. 2010].

2) Simple, effective, easy and safe methods with fewer side effects in vivo may be required for preventive intervention. The major activity of IL-18 is the induction of Th1 cells in the presence of IL-12, and IL-12 without IL-18 has an independent pathway to induce Th1 response [Hayashi *et al.* 2001], suggesting complexity of targeting those cytokines. Blocking of co-stimulation in antigen presenting process and elimination of B cells including IL-6 are effective, but those therapies may severely compromise immune responsiveness in general.

3) van Raalte *et al.* [2009] have reported that despite excellent efficacy in terms of immunosuppression, glucocorticoid (GC) therapy is hampered by their notorious metabolic side effect profile. Thus, current trials to segregate GC's anti-inflammatory and metabolic actions are currently being developed. On the other hand, compared to glucocorticoids, cytokine targeted therapy has some merit, since side effects such as increased metabolic action may be less in cytokine therapy. Combination of the use of

immunosuppressants and cytokine targeted therapy also seems likely.

4) Balance shift from immunogenic to tolerogenic DCs by targeting IFN-α/β together with normalization of Treg cell function in individuals has the potential to lead to remission of immune disease. However, there are a little information about the IFN-α/β therapy and complicated interaction of DCs and Treg cells for balance shift [Kang *et al.* 2007]. Moreover, the information of side effects is totally lacking. Thus, further studies are needed to accumulate the information for therapy.

5) In this PhD thesis, I analyzed the pathology of immune diseases from the point of view of Th1/Th2 unbalanced diseases, and clarified that the environmental factors exacerbate or inhibit the development of immune diseases. In chapter 1, it was suggested that Tregs may regulate the development of late allergic asthma (Th2 predominant diseases) by cell-cell contact and immunosuppressive cytokine productions. In chapter 2, Reo-2 infection induced Th1-dependent injury to bile ducts by an autoimmune-mediated process following to viral proliferation in weanling mice, and the lesions observed in mice may be analogous to those of human infantile biliary atresia. In chapter 3, systemic Reo-2 infection at birth may reduce the development of subsequent late allergic asthma by Th1/Th2 balance shift toward Th1 response even after elimination of virus.

6) The PhD thesis has been done by the purpose of therapy by Th1/Th2 balance shift for clinical use. For that the PhD thesis may give useful and valuable information.

# 6. Acknowledgements

Completion of this doctoral thesis was possible with the support of several people. I would like to express my sincere gratitude to all of them. First of all, I am extremely grateful to my research guide, Dr. Toshiharu Hayashi, DVM, PhD, and Professor, Laboratory of Veterinary Pathology, The United Graduate School of Veterinary Science, Yamaguchi University, for his valuable guidance, scholarly inputs and consistent encouragement I received throughout the research work. My doctoral thesis was possible only because of the unconditional support provided by him despite his busy schedules. Thank you for all your help and support.

I thank Dr. Takuya Mizuno, DVM, PhD and Professor, Laboratory of Veterinary Clinical Pathology, The United Graduate School of Veterinary Science, Yamaguchi University, for the academic supports and his grateful contributions on the research papers of this thesis.

Dr. Ken Maeda, DVM, PhD and Professor, Laboratory of Veterinary Microbiology and Dr. Hiroshi Sato, DVM, PhD and Professor, Laboratory of Veterinary Parasitology, The United Graduate School of Veterinary Science, Yamaguchi University, Dr. Takehito Morita, DVM, PhD and Professor, Laboratory of Veterinary Pathology, Joint Department of Veterinary Medicine, Faculty of Agriculture, Tottori University and Dr. Akinori Shimada, DVM, PhD and Professor, Faculty of Life and Environmental Science, Laboratory of Pathology, Azabu University, have extended their valuable comments on some researches and I express my gratitude to them.

The member of Laboratory of Veterinary Pathology, Yamaguchi University, have been very kind enough to extend their help at various phase of the research studies, whenever I approached them, and I do hereby acknowledge all of them.

The thesis would not have come to a successful completion, without the helping and encouraging I received from all of my friends.

Finally, I am especially grateful to my family for all their love and encouragement. I owe a lot to my parents, who helped me at every stage of my personal and academic life, and longed to see this achievement come true. Thank you.

Tomomi Nakashima

March 2014

# 7. References


Aggarwal S, Ghilardi N, Xie MH, de Sauvage FJ, Gurney AL. Interleukin-23 promotes a distinct CD4 T cell activation state characterized by the production of interleukin-17. *J. Biol. Chem.* 2003;278:1910-1914.

Aikawa T, Shimura S, Sasaki H, Ebina M, Takishima T. Marked goblet cell hyperplasia with mucus accumulation in the airways of patients who died of severe acute asthma attack. *Chest* 1992;101:916-921.

Akdis CA, Blesken T, Akdis M, Wüthrich B, Blaser K. Role of IL-10 in specific immunotherapy. *J. Clin. Invest.* 1998;102:98-106.

Akdis M, Verhagen J, Taylor A, *et al.* Immune responses in healthy and allergic individuals are characterized by a fine balance between allergen-specific T regulatory 1 and T helper 2 cells. *J. Exp. Med.* 2004;199:1567-1575.

Alarcón-Segovia D, Tumlin JA, Furie RA, *et al.* LJP 394 for the prevention of renal flare in patients with systemic lupus erythematosus: results from a randomized, double-blind, placebo-controlled study. *Arthritis Rheum.* 2003;48:442–454.

Amoura Z, Haroche J, Piette JC. Systemic lupus erythematosus: future therapeutic avenues. *Rev. Med. Interne.* 2008;29:718–724.

Babu SK, Puddicombe SM, Arshad HH, *et al.* Tumor necrosis factor alpha (TNF-α) autoregulates its expression and induces adhesion molecule expression in asthma. *Clin. Immunol.* 2011;140:18-25.

Bach JF. The effect of infections on susceptibility to autoimmune and allergic diseases. *N. Engl. J. Med.* 2002;347:911-920.

Bachert C. Immediate and late phases of allergic rhinitis. *Immun. Infekt.* 1990;18:164-168.

Bangaru B, Rachel M, Glaser JH, *et al.* Comparative studies of biliary atresia in the human newborn and reovirus-induced cholangitis in weanling mice. *Lab. Invest*. 1980;43:456-462.

Bauer E, Williams BA, Smidt H, Verstegen MW, Mosenthin R. Influence of the gastrointestinal microbiota on development of the immune system in young animals. *Curr. Issues Intest. Microbiol.* 2006;7:35-51

Bellmann K, Kolb H, Hartmann B, *et al.* Intervention in autoimmune diabetes by targeting the gut immune system. *Int. J. Immunopharmacol.* 1997;19:573-577.

Berry MA, Hargadon B, Shelley M, *et al.* Evidence of a role of tumor necrosis factor alpha in refractory asthma. *N. Engl. J. Med.* 2006;354:697-708.

Bezerra JA. Biliary atresia-translational research on key molecular processes regulating biliary injury and obstruction. *Chang Gung Med. J.* 2006;29:222-230.

Bezerra JA, Tiao G, Ryckman FC, *et al.* Genetic induction of proinflammatory immunity in children with biliary atresia. *Lancet* 2002;360:1563-1659.

Bopp T, Becker C, Klein M, *et al.* Cyclic adenosine monophosphate is a key component of regulatory T cell-mediated suppression. *J. Exp. Med*. 2007;204:1303-1310.

Borish L, Aarons A, Rumbyrt J, *et al.* Interleukin-10 regulation in normal subjects and patients with asthma. *J. Allergy Clin. Immunol.* 1996;97:1288-1296.

Bowen T, Jenkins RH, Fraser DJ. MicroRNAs, Transforming Growth Factor Beta-1, and Tissue Fibrosis. *J. Pathol.* 2013;229:274-285.

Braga M, Quecchia C, Cavallucci E, *et al.* T regulatory cells in allergy. *Int. J. Immunopathol. Pharmacol.* 2011;24:55S-64S.

Broide DH. Allergic rhinitis: Pathophysiology. *Allergy Asthma Proc.* 2010;31:370-374.

Brusko TM, Wasserfall CH, Clare-Salzler MJ, Schatz DA, Atkinson MA. Functional defects

and the influence of age on the frequency of $CD4^+$ $CD25^+$ T-cells in type 1 diabetes. *Diabetes* 2005;54:1407-1414.

Bui LK, Hayashi T, Nakashima T, Horii Y. Eosinophilic venulitis in the small intestines in a mouse model of late asthma. *Inflammation* 2011;34:499-508.

Caramalho I, Lopes-Carvalho T, Ostler D, *et al.* Regulatory T cells selectively express toll-like receptors and are activated by lipopolysaccharide. *J. Exp. Med.* 2003;197:403-411.

Cardwell CR, Shields MD, Carson DJ, Patterson CC. A meta-analysis of the association between childhood type 1 diabetes and atopic disease. *Diabetes Care* 2003;26:2568-2574.

Cardwell CR, Carson DJ, Yarnell J, Shields, MD, Patterson CC. Atopy, home environment and the risk of childhood-onset type 1diabetes: a population-based case-control study. *Pediatr. Diabetes* 2008;9:191-196.

Chen W, Jin W, Hardegen N, *et al.* Conversion of peripheral $CD4^+CD25^-$ naive T cells to $CD4^+CD25^+$ regulatory T cells by TGF-beta induction of transcription factor Foxp3. *J. Exp. Med.* 2003;198:1875-1886.

Chen Z, Herman AE, Matos M, Mathis D, Benoist C. Where $CD4^+CD25^+$ Treg cells impinge on autoimmune diabetes. *J Exp Med.* 2005;202:1387-1397.

Clarke P, Tyler KL. Reovirus-induced apoptosis: A minireview. *Apoptosis* 2003;8:141-150.

Clarke P, Richardson-Burns SM, DeBiasi RL, *et al.* Mechanisms of apoptosis during reovirus infection. *Curr. Top. Microbiol. Immunol.* 2005;289:1-24.

Cookson W. Genetics and genomics of asthma and allergic diseases. *Immunol. Rev.* 2002;190:195-206.

Cosmi L, Liotta F, Maggi E, Romagnani S, Annuziato F. Th17 cells: new players in asthma

pathogenesis. *Allergy* 2011;66:989-998.

Criscione LG, Pisetsky DS. B lymphocytes and systemic lupus erythematosus. Curr. Rheumatol. Rep. 2003;5:264–269.

Cronin SJ, Penninger JM. From T-cell activation signals to signaling control of anti-cancer immunity. *Immunol. Rev.* 2007;220:151-168.

Curiel TJ, Coukos G, Zou L, *et al.* Specific recruitment of regulatory T cells in ovarian carcinoma fosters immune privilege and predicts reduced survival. *Nat. Med.* 2004;10:942-949.

Danthi P, Hansberger MW, Campbell JA, Forrest JC, Dermody TS. JAM-A-independent, antibody-mediated uptake of reovirus into cells leads to apoptosis. *J. Virol.* 2006;80:1261-1270.

Díaz-Jouanen E, Abud-Mendoza C, Garza-Elizondo MA, *et al.* Guidelines in RA treatment: concepts on safety and recommendations using anti-TNF-alpha inhibitors. Grupo de Estudio de Nuevas Terapias de Enfermedades reumáticas (GENTE). *Rev. Invest. Clin.* 2009;61:252-266.

Doria A, Briani C. Lupus: improving long-term prognosis. *Lupus* 2008;17:166–170.

Durham SR, Ying S, Varney VA, *et al.* Cytokine messenger RNA expression for IL-3, IL-4, IL-5, and granulocyte/macrophage-colony-stimulating factor in the nasal mucosa after local allergen prococation: relationship to tissue eosinophilia. *J. Immunol.* 1992;148:2390-2394.

Egawa M, Mukai K, Yoshikawa S, *et al*. Inflammatory monocytes recruited to allergic skin acquire an anti-inflammatory M2 phenotype via basophil-derived interleukin-4. *Immunity* 2013;38:570-580.

Elkord E. Novel therapeutic strategies by regulatory T cells in allergy. *Chem. Immunol.*

*Allergy* 2008;94:150-157.

Errington F, Steele L, Parestwich R, *et al.* Reovirus activates human dendritic cells to promote innate antitumor immunity. *J. Immunol.* 2008;180:6018-6026.

Fecek RJ, Marcondes Rezende M, Busch R, *et al.* Enteric reovirus infection stimulates peanut-specific IgG2a responses in a mouse food allergy model. *Immunobiology* 2010;215:941-948.

Finck BK, Chan B, Wofsy D. Interleukin 6 promotes murine lupus in NZB/NZW F1 mice. *J. Clin. Invest.* 1994;94:585–591.

Fontenot JD, Rasmussen JP, Williams LM, *et al.* Regulatory T cell lineage specification by the forkhead transcription factor foxp3. *Immunity* 2005;22:329-341.

Gambineri E, Torgerson TR, Ochs HD. Immune dysregulation, polyendocrinopathy, enteropathy, and X-linked inheritance (IPEX), a syndrome of systemic autoimmunity caused by mutations of FOXP3, a critical regulator of T-cell homeostasis. *Curr. Opin. Rheumatol.* 2003;15:430-435.

Gravano DM, Vignali DA. The battle against immunopathology: infectious tolerance mediated by regulatory T cells. *Cell. Mol. Life Sci.* 2012;69:1997-2008.

Grossman WJ, Verbsky JW, Barchet W, *et al.* Human T regulatory cells can use the perforin pathway to cause autologous target cell death. *Immunity* 2004;21:589-601.

Guglielmi KM, Johnson EM, Stehle T, *et al.* Attachment and cell entry of mammalian orthoreovirus. *Curr. Top. Microbiol. Immunol.* 2006;309:1-38.

Hamzaoui A, Ammar J, Hamzaou K. Regulatory T cells in induced sputum of asthmatic children: association with inflammatory cytokines. *Multidiscip. Respir. Med.* 2010;5:22-30.

Harada K, Oihara S, Isse K, *et al.* Lipopolysaccharide activates nuclear factor-kappaB

through toll-like receptors and related molecules in cultured biliary epithelial cells. *Lab. Invest.* 2003;83:1657-1667.

Haribhai D, Williams JB, Jia S, *et al.* A requisite role for induced regulatory T cells in tolerance based on expanding antigen receptor diversity. *Immunity* 2011;35:109-122

Hasegawa K, Hayashi T. Synthetic CpG oligodeoxynucleotides accelerate the development of lupus nephritis during preactive phase in NZB x NZWF1 mice. *Lupus* 2003;12:838-845.

Hattori K, Nishikawa M, Watcharanurak K, *et al.* Sustained exogenous expression of therapeutic levels of IFN-gamma ameliorates atopic dermatitis in NC/Nga mice via Th1 polarization. *J. Immunol.* 2010;184:2729-2735.

Hatzivlassiou M, Grainge C, Kehagia V, Lau L, Howarth PH. The allergen specificity of the late asthmatic reaction. *Allergy* 2010;65:355-358.

Hayashi T. Therapeutic strategies for SLE involving cytokines:mechanism-oriented Therapies especially IFN-γ targeting gene therapy. *J. Biomed. Biotechnol.* 2010;doi:10.1155/2010/461641

Hayashi T. Immunopathogenesis of distant manifestation in effector phase after local airway allergy. *Res. Trends.* 2011;12:67-76.

Hayashi T. Molecular mechanisms in allergic rhinitis: modulation by microbes. Chapter II. *In*: Berhardt LV, ed. *Advances in Medicine and Biology*, Vol. 40. New York: NOVA Sci. Pub, 2012a. ISBN: 9781621004219.

Hayashi T. Molecular mechanisms of metaplasia, differentiation and hyperplasia of goblet cell in allergic asthma. *J. Aller. Ther.* 2012b;3:1-10. Open access.

Hayashi T, Fujii T. Acute urticaria [corrected]-like lesions in allergen-unexposed cutaneous tissues in a mouse model of late allergic rhinitis. *Int. J. Exp. Pathol.*

2008;89:188-200.

Hayashi T, Morimoto M, Iwata H, Onodera T. Interferon-gamma plays a role in pancreatic islet-cell destruction of reovirus type 2-induced diabetes-like syndrome in DBA/1 suckling mice. *Int. J. Exp. Pathol.* 1998;79:313-320.

Hayashi T, Morimoto M, Iwata H, Onodera T. Possible involvement of IL-12 in Reovirus type-2-induced diabetes in newborn DBA/1 mice. *Scand. J. Immunol.* 2001;53:572-578.

Hayashi T, Maeda K, Hasegawa K, *et al.* Systemic administration of interferon-gamma-expressing plasmid reduces late allergic bronchitis in a mouse model of asthma. *Int. J. Exp. Pathol.* 2002a;83:81-86.

Hayashi T, Yoshinaka K, Hasegawa K, Maeda K, Onodera T. CpG oligodeoxynucleotides accelerate reovirus type 2-triggered insulitis in DBA/1 suckling mice. *Int. J. Exp. Pathol.* 2002b;83:217-223.

Hayashi T, Adachi Y, Hasegawa K, Morimoto M. Less sensitivity for late airway inflammation in males than females in BALB/c mice. *Scand. J. Immunol.* 2003a;57:562-567

Hayashi T, Yasutomi Y, Hasegawa K, *et al.* Interleukin-4-expressing plasmid DNA inhibits reovirus type-2-triggered autoimmune insulitis in DBA/1 J suckling mice. *Int. J. Exp. Pathol.* 2003b;84:101-106.

Hayashi T, Hasegawa K, Adachi C. Elimination of $CD4^{+}CD25^{+}$ T cell accelerates the development of glomerulonephritis during the preactive phase in autoimmune-prone female NZB x NZW F mice. *Int. J. Exp. Pathol.* 2005a;86:289-296.

Hayashi T, Hasegawa K, Ichinohe N. ICAM-1 expression on endothelium and systemic cytokine production in cutaneous neutrophilic leukocytoclastic vasculitis in

NZBxNZWF1 mice. *Histol. Histopathol.* 2005b;20:45–52.

Hayashi T, Hasegawa K, Sasaki Y, Onodera T. Elimination of $CD4^+$ $CD25^+$ regulatory T cells breaks down reovirus type 2-triggered and CpG ODN-induced prolonged mild autoimmune insulitis in DBA/1 mice. *Scand. J. Immunol.* 2006;63:116-124.

Hayashi T, Hasegawa K, Sasaki Y, *et al.* Systemic administration of interleukin-4 expressing plasmid DNA delays the development of glomerulonephritis and prolongs survival in lupus-prone female NZB x NZW F1 mice. *Nephrol. Dial. Transplant.* 2007;22:3131-3138.

Hayashi T, Hasegawa K, Sasaki Y. Systemic administration of olygodeoxynucleotides with CpG motifs at priming phase reduces local Th2 response and late allergic rhinitis in BALB/c mice. *Inflammation*. 2008a;31:47-56.

Hayashi T, Hayashi H, Fujii T, Adachi C, Hasegawa K. Ultrastructure of myoepithelial cells as a target cell in sialoadenitis of submandibular glands of lupus-prone female NZBxNZWF1 mice. *Virchows Arch.* 2008b;453:177–188.

Hayashi T, Adachi C, Hasegawa K. Systemic treatment of anti-$CD4^+CD25^+$ T cell monoclonal antibody exacerbates sialoadenitis in submandibular glands during the early life in lupus-prone female NZB x NZWF mice. *J. Oral Pathol. Med.* 2009;38:234-240.

Hellings PW, Vandenberghe P, Kasran A, *et al.* Blockade of CTLA-4 enhances allergic sensitization and eosinophilic airway inflammation in genetically predisposed mice. *Eur. J. Immunol.* 2002;32:585-594.

Holloway JW, Yang IA, Holgate ST. Genetics of allergic disease. *J. Allergy Clin. Immunol.* 2010;125:S81-94.

Holmdahl R, Andersson M, Goldschmidt TJ, *et al.* Type II collagen autoimmunity in

animals and provocations leading to arthritis. *Immunol. Rev.* 1990;118:193-232

Honda K, Chihara J. Eosinophil activation by eotaxin-eotaxin primes the production of reactive oxygen spiecies from eosinophils. *Allergy* 1999;54:1262-1269.

Honeyman MC, Coulson BS, Stone NL, *et al.* Association between rotavirus infection and pancreatic islet autoimmunity in children at risk of developing type 1 diabetes. *Diabetes* 2000;49:1319-1324.

Horwitz DA, Zheng SG, Wang J, Gray JD. Critical role of IL-2 and TGF-β in generation, function and stabilization of Foxp3$^+$ CD4$^+$ Treg. *Eur. J. Immunol.* 2008;38:912–915.

Iellem A, Mariani M, Lang R, *et al.* Unique chemotactic response profile and specific expression of chemokine receptors CCR4 and CCR8 by CD4$^+$CD25$^+$ regulatory T cells. *J. Exp. Med.* 2001;194:847-853.

Ito T, Wang YH, Duramad O, *et al.* TSLP-activated dendritic cells induce an inflammatory T helper 2 cell response through OX40 ligand. *J. Exp. Med.* 2005;202:1213-1223.

Jiang S, Lechler RI. CD4$^+$CD25$^+$ regulatory T-cell therapy for allergy, autoimmune disease and transplant rejection. Inflamm. *Allergy Drug Targets* 2006;5:239-242.

Jutel M, Akdis M, Budak F, *et al.* IL-10 and TGF-beta cooperate in the regulatory T cell response to mucosal allergens in normal immunity and specific immunotherapy. *Eur. J. Immunol.* 2003;33:1205-1214.

Kalunian KC, Davis JCJr, Merrill JT, *et al.* Treatment of systemic lupus erythematosus by inhibition of T cell costimulation with anti-CD154: a randomized, double-blind, placebo-controlled trial. *Arthritis Rheum.* 2002;46:3251–3258.

Kang HK, Liu M, Datta SK. Low-dose peptide tolerance therapy of lupus generates plasmacytoid dendritic cells that cause expansion of autoantigen-specific regulatory T cells and contraction of inflammatory Th17 cells. *J. Immunol.* 2007;178:7849-7858.

Karavanaki K, Tsoka E, Karayianni C, *et al.* Prevalence of allergic symptoms among children with diabetes mellitus type 1 of different socioeconomic status. *Pediatr. Diabetes* 2008;9:407-416.

Karni A, Koldzic DN, Bharanidharan P, Khoury SJ, Weiner HL. IL-18 is linked to raised IFN-gamma in multiple sclerosis and is induced by activated $CD4^+$ T cells via CD40-CD40 ligand interactions. *J. Neuroimmunol.* 2002;125:134-140.

Kay BA. Modulation of inflammation in allergic disease. *Allergy Clin. Immunol. Int.-J. World Allergy* 2004;16:206-210.

Kaur D, Brightling C. OX40/OX40 ligand interactions in T-cell regulation and asthma. *Chest* 2012;141:494-499.

Kearley J, Barker JE, Robinson DS, Lloyd CM. Resolution of airway inflammation and hyperreactivity after in vivo transfer of $CD4^+CD25^+$ regulatory T cells is interleukin 10 dependent. *J. Exp. Med.* 2005;202:1539-1547.

Keatings VM, O'Connor BJ, Wright LG, Huston DP, Corrigan CJ, Barnes PJ. Late response to allergen is associated with increased concentration of tumor necrosis factor-alpha and IL-5 in induced sputum. *J. Allergy Clin. Immunol.* 1997;99:693-698.

Kero J, Gissler M, Hemminki E, Isolauri E. Could TH1 and TH2 diseases coexist? Evaluation of asthma incidence in children with coeliac disease, type 1 diabetes, or rheumatoid arthritis: a register study. *J. Allergy Clin. Immunol.* 2001;108:781–783.

Kim HJ, Hwang SJ, Kim BK, Jung KC, Chung DH. NKT cells play critical roles in the induction of oral tolerance by inducing regulatory T cells producing IL-10 and transforming growth factor beta, and by clonally deleting antigen-specific T cells. *Immunology* 2006;118:101-111.

Kisseleva T, Brenner DA. Role of hepatic stellate cells in fibrogenesis and the reversal of

fibrosis. *J. Gastroenter. Hepatol.* 2007;22 Suppl 1:S73-78.

Klinman DM, Steinberg AD. Inquiry into murine and human lupus. *Immunol. Rev.* 1995;144:157–193.

Knol EF, Olszewski M. Basophils and mast cells: Underdog in immune regulation? *Immunol. Lett.* 2011;138:28-31.

Knosp CA, Schiering C, Spence S, *et al.* Regulation of Foxp3$^{+}$ inducible regulatory T cell stability by SOCS2. *J. Immunol.* 2013;190:3235-3245.

Koffler D. Immunopathogenesis of systemic lupus erythematosus. *Annu. Rev. Med.* 1974;25:149–164.

Koga K, Takaesu G, Yoshida R, *et al.* Cyclic adenosine monophosphate suppresses the transcription of proinflammatory cytokines via the phosphorylated c-Fos protein. *Immunity* 2009;30:372-383.

Koning H, Neijens HJ, Baert MR, Oranje AP, Savelkoul HF. T cells subsets and cytokines in allergic and non-allergic children. II. Analysis and IL-5 and IL-10 mRNA expression and protein production. *Cytokine* 1997;9:427-436.

Korn T, Bettelli E, Oukka M, Kuchroo VK. IL-17 and Th17 Cells. *Annu. Rev. Immunol.* 2009;27:485-517.

Kukreja A, Cost G, Marker J, *et al.* Multiple immuno-regulatory defects in type-1 diabetes. *J. Clin. Invest.* 2002;109:131-140.

Kunz M, Ibrahim SM. Cytokines and cytokine profiles in human autoimmune diseases and animal models of autoimmunity. *Mediators Inflamm.* 2009;2009: Article ID 979258.

Kurogi H, Inaba Y, Takahashi E, Sato K, Omori T. Serological relationship between Japanese strains of Reovirus of bovine origin and type 2 reovirus strains. *Nati. Inst.*

*Anim. Health. Q.* 1980;20:32-33.

Laskin DL, Pendino KJ. Macrophages and inflammatory mediators in tissue injury. *Annu. Rev. Pharmacol. Toxicol.* 1995;35:655-677.

Lassalle P, Gosset P, Delneste Y, *et al.* Modulation of adhesion molecule expression on endothelial cells during the late asthmatic reaction: role of macrophage-derived tumor necrosis factor-alpha. *Clin. Exp. Immunol.* 1993;94:105-110.

Li L, Xia Y, Nguyen A, *et al.* Effects of Th2 cytokines on chemokine expression in the lung: IL-13 potently induces eotaxin expression by airway epithelial cells. *J. Immunol.* 1999;162:2477-2487.

Liu YJ. Dendritic cell subsets and lineages, and their functions in innate and adaptive immunity. *Cell.* 2001;106:259-262.

Liu AH. Endotoxin exposure in allergy and asthma: reconciling a paradox. *J. Allergy Clin. Immunol.* 2002;109:379-392.

Llorente L, Richaud-Patin Y, García-Padilla C, *et al.* Clinical and biologic effects of anti-interleukin-10 monoclonal antibody administration in systemic lupus erythematosus. Arthritis Rheum. 2000;43:1790–1800.

Lowder TW, Kunz HE. Regulatory T Cells in Asthma and Airway Hyperresponsiveness. *J. Aller. Ther.* 2011. Open access.

Mack CL, Tucker RM, Lu BR, *et al.* Armed $CD4^+$ Th1 effector cells and activated macrophages participate in bile duct injury in murine biliary atresia. *Clin. Immunol.* 2005;115:200-209.

Mack CL. The pathogenesis of biliary atresia: evidence for a virus-induced autoimmune disease. *Semin. Liv. Dis.* 2007;27:233-242.

Maldonado RA, von Andrian UH. How tolerogenic dendritic cells induce regulatory T

cells. *Adv. Immunol.* 2010;108:111-165.

Mathian A, Weinberg A, Gallegos M, Banchereau J, Koutouzov S. IFN-α induces early lethal lupus in preautoimmune (New Zealand Black x New Zealand White)F1 but not in BALB/c mice. *J. Immunol.* 2005;174:2499–2506.

McGee HS, Agrawal DK. Naturally occurring and inducible T-regulatory cells modulating immune response in allergic asthma. *Am. J. Respir. Crit. Care Med.* 2009;180:211-225.

Meerwaldt R, Odink RJ, Landaeta R, *et al.* A lower prevalence of atopy symptoms in children with type 1 diabetes mellitus. *Clin. Exp. Allergy* 2002;32:254-255.

Melgert BN, Postma DS, Kuipers I, *et al.* Female mice are more susceptible to the development of allergic airway inflammation than male mice. *Clin. Exp. Allergy* 2005;35:1496-1503.

Meloni F, Solari N, Cavagna L, *et al.* Frequency of Th1, Th2 and Th17 producing T lymphocytes in bronchoalveolar lavage of patients with systemic sclerosis. *Clin. Exp. Rheumatol.* 2009;27:765-772.

Menon K, Wu Y, Haas J, *et al.* Diminished degradation of myelin basic protein by anti-sulfatide antibody and interferon-gamma in myelin from glia maturation factor-deficient mice. *Neurosci. Res.* 2007;58:156-163.

Minai-Fleminger Y, Levi-Schaffer F. Mast cells and eosinophils: the two key effector cells in allergic inflammation. *Inflamm. Res.* 2009;58:631-638.

Mitsias DI, Kapsogeorgou EK, Moutsopoulos HM. Sjögren's syndrome: why autoimmune epithelitis? *Oral Dis.* 2006;12:523-532.

Miyahara S, Miyahara N, Matsubara S, *et al.* IL-13 is essential to the late-phase response in allergic rhinitis. *J. Allergy Clin. Immunol.* 2006;118:1110–1116.

Miyake T, Inaba M, Fukui J, *et al.* Prevention of graft-versus-host disease by intrabone marrow injection of donor T cells: involvement of bone marrow stromal cells. *Clin. Exp. Immunol.* 2008;152:153-162.

Moniuszko M, Kowal K, Zukowski S, Dabrowska M, Bodzenta-Lukaszyk A. Frequencies of circulating $CD4^{+}CD25^{+}CD127^{low}$ cells in atopics are altered by bronchial allergen challenge. *Eur. J. Clin. Invest.* 2008;38:201-204.

Monneaux F, Muller S. Molecular therapies for systemic lupus erythematosus: clinical trials and future prospects. *Arthritis Res. Ther.* 2009;11:234.

Morecki R, Glaser JH, Johnson AB, *et al.* Detection of reovirus type 3 in the portal hepatis of an infant with extrahepatic biliary atresia: Ultrastructural and immunocytochemical study. *Hepatology* 1984;4:137-142.

Morimoto M, Ohji T, Iwata H, Hayashi T. Lactic dehydrogenase virus (LDV) infection inhibits allergic eosinophil reaction in the airway. *Res. Vet. Sci.* 2002;72:131-136.

Mosmann TR, Coffman R. TH1 and TH2 cells: different patterns of lymphokine secretion lead to different functional properties. *Annu. Rev. Immunol.* 1989;7:145–173.

Mu W, Ouyang X, Agarwal A, *et al.* IL-10 suppresses chemokines, inflammation, and fibrosis in a model of chronic renal disease. *J. Am. Soc. Nephrol.* 2005;16:3651-3660.

Nakamura K, Kitani A, Fuss I, *et al.* TGF-beta 1 plays an important role in the mechanism of $CD4^{+}CD25^{+}$ regulatory T cell activity in both humans and mice. *J. Immunol.* 2004;172:834-842.

Nakamura Y, Tsuneyama K, Harada K. Pathology and pathogenesis of intrahepatic bile duct loss. *J. Hepatobiliary Surg.* 2001;8:303-315.

Nakashima T, Hayashi T, Mizuno T. Reovirus type-2 infection in newborn DBA/1J mice reduces the development of late allergic asthma. *Int. J. Exp. Pathol.*

2012;93:234-242.

Nouri-Aria KT, Durham SR. Regulatory T cells and allergic disease. *Inflamm. Allergy Drug Targets* 2008;7:237-252.

Okada H, Kuhn C, Feillet H, Bach JF. The 'hygiene hypothesis' for autoimmune and allergic diseases: an update. *Clin. Exp. Immunol.* 2010;160:1-9.

Okigami H, Takeshita K, Tajima M, *et al.* Inhibitation of eosinophilia in vivo by a small molecule inhibitor of very late antigen (VLA)-4. *Eur. J. Pharmacol.* 2007;559:202-209.

Onodera T, Taniguchi T, Yoshihara K *et al.* Reovirus type 2-induced diabetes in mice prevented by immunosuppression and thymic hormone. *Diabetologia* 1990;33:192-196.

Onodera T, Hayashi T. Reovirus *In*: Taylor K, Hyöty H, Toniolo A, Zuckerman AA, eds. *Diabetes and Viruses*, New York, NY: Springer Science, 2013:71-80. ISBN: 9781461440505.

Oppmann B, Lesley R, Blom B, *et al.* Novel p19 protein engages IL-12p40 to form a cytokine, IL-23, with biological activities similar as well as distinct from IL-12. *Immunity* 2000;13:715-725.

Orth T, Neurath M, Schirmacher P, *et al.* A novel rat model of chronic fibrosing cholangitis induced by local administration of a hapten reagent into the dilated bile duct is associated with increased TNF-α production and autoantibodies. *J. Hepatol.* 2000;33:862-872.

Ott PA, Anderson MR, Tary-Lehmann M, Lehmann PV. $CD4^{+}CD25^{+}$ regulatory T cells control the progression from periinsulitis to destructive insulitis in murine autoimmune diabetes. *Cell Immunol.* 2005;235:1-11.

Papadimitriou JM. The biliary tract in acute murine reovirus 3 infection. Light and

electron microscopic study. *Am. J. Path.* 1968;52:595-611.

Peter M, Bode K, Lipford GB, *et al.* Characterization of suppressive oligodeoxynucleotides that inhibit Toll-like receptor-9-mediated activation of innate immunity. *Immunology* 2008;123:118-128.

Piccirillo CA, Tritt M, Sgouroudis E, *et al.* Control of type 1 autoimmune diabetes by naturally occurring $CD4^{+}CD25^{+}$ regulatory T lymphocytes in neonatal NOD mice. *Ann. N. Y. Acad. Sci.* 2005;1051:72-87.

Pizarro TT, Michie MH, Bentz M, *et al.* IL-18, a novel immunoregulatory cytokine, is up-regulated in Crohn's disease: expression and localization in intestinal mucosal cells. *J. Immunol.* 1999;162:6829-6835.

Ponath PD, Qin S, Ringler DJ, *et al.* Cloning of the human eosinophil chemoattractant, eotaxin. Expression, receptor binding, and functional properties suggest a mechanism for the selective recruitment of eosinophils. *J. Clin. Invest.* 1996;97:604-612.

Provoost S, Maes T, van Durme YM, *et al.* Decreased FOXP3 protein expression in patients with asthma. *Allergy* 2009;64:1539-1546.

Prud'homme GJ, Lawson BR, Theofilopoulos AN. Anticytokine gene therapy of autoimmune diseases. *Expert Opin. Biol. Ther.* 2001;1:359–373.

Robinson DS. Regulatory T cells and asthma. *Clin. Exp. Allergy* 2009;39:1314-1323.

Rosenbauer J, Herzig P, Giani G. Atopic eczema in early childhood could be protective against type 1 diabetes (T1D). *Diabetologia* 2003;46:784-788.

Rosenberg DP, Morecki R, Lollini LO, *et al.* Extrahepatic biliary atresia in a rhesus monkey (Macaca mulatta). *Hepatology* 1983;3:577-580.

Sakaguchi S, Sakaguchi N, Asano M, Itoh M, Toda M. Immunologic self-tolerance

maintained by activated T cells expressing IL-2 receptor alpha-chains (CD25). Breakdown of a single mechanism of self-tolerance causes various autoimmune diseases. *J. Immunol.* 1995;155:1151-1164.

Sakaguchi S, Toda M, Asano M, *et al.* T cell-mediated maintenance of natural self-tolerance: its breakdown as a possible cause of various autoimmune diseases. *J. Autoimmun.* 1996;9:211-220.

Sakaguchi S. Regulatory T cells: key controllers of immunologic self-tolerance. *Cell* 2000;101:455-458.

Sakaguchi S, Ono M, Setoguchi R, *et al.* $Foxp3^+$ $CD25^+$ $CD4^+$ natural regulatory T cells in dominant self-tolerance and autoimmune disease. *Immunol. Rev.* 2006;212:8-27.

Sakaguchi S, Wing K, Onishi Y, Prieto-Martin P, Yamaguchi T. Regulatory T cells: how do they suppress immune responses? *Int. Immunol.* 2009;21:1105-1111.

Salomon B, Lenschow DJ, Rhee L, *et al.* B7/CD28 costimulation is essential for the homeostasis of the $CD4^+CD25^+$ immunoregulatory T cells that control autoimmune diabetes. *Immunity* 2000;12:431-440.

Sasaki Y, Hayashi T, Hasegawa K. Lactate dehydrogenase-elevating virus infection at the sensitization and challenge phases reduces the development of delayed eosinophilic allergic rhinitis in BALB/c mice. *Scand. J. Immunol*. 2007;66:628-635.

Schiff LA, Nibert ML, Tyler KL. Orthoreoviruses and their replication. *In*: Knipe DM, Howley PM, eds. *Fields Virology,* 5th edn, Vol. 2. Philadelphia, PA: Lippincott Williams and Wilkins, 2007:1853-1915. ISBN: 9780781760607.

Selb B, Weber B. A study of human Reovirus IgG and IgA antibodies by ELISA and Western blot. *J. Virol. Methods.* 1994;47:15-26.

Seline LK, Nahill SR, Welsh RM. Cross-reactivities in memory cytotoxic T lymphocyte

recognition of heterologous viruses. *J. Exp. Med.* 1994;179:1933–1943.

Shevach EM. $CD4^+$ $CD25^+$ suppressor T cells: more questions than answers. *Nat. Rev. Immunol.* 2002;2:389-400.

Shevach EM. Mechanisms of $foxp3^+$ T regulatory cell-mediated suppression. *Immunity* 2009;30:636-645.

Shivakumar P, Campbell KM, Sabla GE, *et al.* Obstruction of extrahepatic bile ducts by lymphocytes is regulated by IFN-gamma in experimental biliary atresia. *J. Clin. Invest.* 2004;114:322-329.

Shivakumar P, Sabla G, Mohanty S, *et al.* Effector role of neonatal hepatic $CD8^+$ lymphocytes in epithelial injury and autoimmunity in experimental biliary atresia. *Gastroenterogy* 2007;133:268-277.

Skadhauge LR, Christensen K, Kyvik KO, Sigsgaard T. Genetic and environmental influence on asthma: a population-based study of 11,688 Danish twin pairs. *Eur. Respir. J.* 1999;13:8-14.

Smith DE. IL-33: a tissue derived cytokine pathway involved in allergic inflammation and asthma. *Clin. Exp. Allergy.* 2010;40:200-208.

Sokol RJ, Mack C. Etiopathogenesis of biliary atresia. *Semin. Liv. Dis.* 2001;21:517-24.

Steele TA, Hauser CC. The role of interferon-alpha in a successful murine tumor therapy. *Exp. Viol. Med. (Maywood)* 2005;230:487-493.

Stene LC, Nafstad P. Relation between occurrence of type 1 diabetes and asthma. *Lancet* 2001;357:607-608.

Sthoeger ZM, Sharabi A, Molad Y, *et al.* Treatment of lupus patients with a tolerogenic peptide, hCDR1 (Edratide): immunomodulation of gene expression. *J. Autoimmun.* 2009;33:77–82.

Stockinger B, Veldhoen M. Differentiation and function of Th17 T cells. *Curr. Opin. Immunol.* 2007;19:281-286.

Strachan DP. Hay fever, hygeine, and household size. *Br. Med. J.* 1989;299:1259-1260.

Strachan DP. Family size, infection and atopy: the first decade of the "hygeine hypothesis". *Thorax* 2000;55:S2-10.

Strickland DH, Holt PG. T regulatory cells in childhood asthma. *Trends Immunol.* 2011;32:420-427.

Suri-Payer E, Amar AZ, Thornton AM, Shevach EM. $CD4^+CD25^+$ T cells inhibit both the induction and effector function of autoreactive T cells and represent a unique lineage of immunoregulatory cells. *J. Immunol.* 1998;160:1212-1218.

Tagari P, Chee P, Chan C, *et al.* Quantitation of eosinophil Major Basic Protein cytotoxicity to rodent respiratory epithelium. *Agants Actions* 1992;37:171-173.

Takahashi T, Tagami T, Yamazaki S, *et al.* Immunologic self-tolerance maintained by $CD25^+CD4^+$ regulatory T cells constitutively expressing cytotoxic T lymphocyte-associated antigen 4. *J. Exp. Med.* 2000;192:303-310.

Tang Q, Henriksen KJ, Boden EK, *et al.* Cutting edge: CD28 controls peripheral homeostasis of CD4+CD25+ regulatory T cells. *J. Immunol.* 2003;171:3348-3352.

Tarbell KV, Yamazaki S, Olson K, Toy P, Steinman RM. $CD25^+$ $CD4^+$ T cells, expanded with dendritic cells presenting a single autoantigenic peptide, suppress autoimmune diabetes. *J. Exp. Med.* 2004;199:1467-1477.

Taylor A, Verhagen J, Akdis CA, Akdis M. T regulatory cells in allergy and health: a question of allergen specificity and balance. *Int Arch Allergy Immunol.* 2004;135:73-82.

Theofilopoulos AN, Koundouris S, Kono DH, Lawson BR. The role of IFN-gamma in systemic lupus erythematosus: a challenge to the Th1/Th2 paradigm in autoimmunity. *Arthritis Res.* 2001;3:136-141.

Tirosh A, Mandel D, Mimouni FB, *et al.* Autoimmune diseases in asthma. *Ann. Intern. Med.* 2006;144:877-883.

Toda A, Piccirillo CA. Development and function of naturally occurring $CD4^+CD25^+$ regulatory T cells. *J. Leukoc. Biol.* 2006;80:458-470.

Torres-Borrego J, Molina-Terán AB, Montes-Mendoza C. Prevalence and associated factors of allergic rhinitis and atopic dermatitis in children. *Allergol. Immunopathol.* 2008;36:90-100.

Tosca MA, Villa E, Silvestri M, *et al.* Discrepancy between sensitization to inhaled allergens and respiratory symptoms in pediatric patients with type 1 diabetes mellitus. *Pediatr. Allergy Immunol.* 2009;20:385-391.

Toubi E. The role of $CD4^+CD25^+$ T regulatory cells in autoimmune diseases. *Clin. Rev. Allergy Immunol.* 2008;34:338-344.

Tritt M, Sgouroudis E, d'Hennezel E, Albanese A, Piccirillo CA. Functional waning of naturally occurring $CD4^+$ regulatory T-cells contributes to the onset of autoimmune diabetes. *Diabetes* 2008;57:113-123.

Tyler KL, Squier MK, Rodgers SE, *et al.* Differences in the capacity of reovirus strains to induce apoptosis are determined by the viral attachment protein sigma 1. *J. Virol.* 1995;69:6972-6979.

Tyler KL, Sokol RJ, Oberhause SM, *et al.* Detection of reovirus RNA in hepatobiliary tissues from patients with extrahepatic biliary atresia and choledochal cysts. *Hepatology* 1998;27:1475-1482.

Vaarala O. Gut and the induction of immune tolerance in type 1 diabetes. *Diabetes Metab. Res. Rev.* 1999;15:353-361.

van Raalte DH, Ouwens DM, Diamant M. Novel insights into glucocorticoid-mediated diabetogenic effects: towards expansion of therapeutic options? *Eur. J. Clin. Invest.* 2009;39:81-93.

Von Hertzen LC, Haahtela T. Asthma and atopy-the price of affluence? *Allergy* 2004;59:124-137.

von Mutius E, Braun-Fahrländer C, Schierl R, *et al.* Exposure to endotoxin or other bacterial components might protect against the development of atopy. *Clin. Exp. Allergy.* 2000;30:1230-1234.

Weiner HL. Induction and mechanism of action of transforming growth factor-beta-secreting Th3 regulatory cells. *Immunol. Rev.* 2001;182:207-214.

Wen L, Ley RE, Volchkov PY, *et al.* Innate immunity and intestinal microbiota in the development of Type 1 diabetes. *Nature* 2008;455:1109-1113.

Wen Y, Gu J, Vandenhoff GE, Liu X, Nadler JL. Role of 12/15-lipoxygenase in the expression of MCP-1 in mouse macrophages. *Am. J. Physiol. Heart Circ. Physiol.* 2008;294:H1933-1938.

Westerholm-Ormio M, Vaarala O, Pihkala P, *et al.* Immunologic activity in the small intestinal mucosa of pediatric patients with type 1 diabetes. *Diabetes* 2003;52:2287-2295.

Wills-Karp M, Karp CL. Eosinophils in asthma: remodeling a tangled tale. *Science* 2004;305:1726-1729.

Wilson GA, Morrision LA, Fields BN. Association of the reovirus S1 gene with serotype 3-induced biliary atresia in mice. *J. Virol.* 1994;68:6458-6465.

Wong CK, Lit LCW, Tam LS, *et al.* Hyperproduction of IL-23 and IL-17 in patients with systemic lupus erythematosus: implications for Th17-mediated inflammation in auto-immunity. *Clin. Immunol.* 2008;127:385–393.

Wu K, Bi Y, Sun K, Wang C. IL-10-producing type 1 regulatory T cells and allergy. *Cell. Mol. Immunol.* 2007;4:269-275.

Xue K, Zhou Y, Xiong S, Xiong W, Tang T. Analysis of $CD4^+$ $CD25^+$ regulatory T cells and Foxp3 mRNA in the peripheral blood of patients with asthma. *J. Huazhong Univ. Sci. Technolog. Med. Sci.* 2007;27:31-33.

Yamamoto H, Sedgwick JB, Busse WW. Differential regulation of eosinophil adhesion and transmigration by pulmonary microvascular endothelial cells. *J. Immunol.* 1998;161:971-977.

Yamazaki S, Iyoda T, Tarbell K, *et al.* Direct expansion of functional CD25+ CD4+ regulatory T cells by antigen-processing dendritic cells. *J. Exp. Med.* 2003;198:235-247.

Yao T, Kojima Y, Koyanagi A, *et al.* Eotaxin-1, -2, and -3 immunoreactivity and protein concentration in the nasal polyps of eosinphilic chronic rhinosinusitis patients. *Laryngoscope* 2009;119:1053-1059.

Yao Y, Richman L, Higgs BW, *et al.* Neutralization of interferon-α/β-inducible genes and downstream effect in a phase I trial of an anti-interferon-α monoclonal antibody in systemic lupus erythematosus. *Arthritis Rheum.* 2009;60:1785–1796.

Zimmermann N, Hogan SP, Mishra A, *et al.* Murine eotaxin-2: a constitutive eosinophil chemokine induced by allergen challenge and IL-4 overexpression. *J. Immunol.* 2000;165:5839-5846.

Zurney J, Kobayashi T, Holm GH, Dermody TS, Sherry B. Reovirus mu2 protein inhibits

interferon signaling through a novel mechanism involving nuclear accumulation of interferon regulatory factor 9. *J. Virol.* 2009;83:2178-2187.